uOttawa

L'Université canadienne
Canada's university

FACULTÉ DES ÉTUDES SUPÉRIEURES ET POSTOCTORALES

uOttawa

L'Université canadienne
Canada's university

FACULTY OF GRADUATE AND POSDOCTORAL STUDIES

Arezu Jahani-asl

AUTEUR DE LA THÈSE / AUTHOR OF THESIS

M.Sc. (Cellular and Molecular Medicine)

GRADE / DEGREE

Department of Cellular and Molecular Medicine

FACULTÉ, ÉCOLE, DÉPARTEMENT / FACULTY, SCHOOL, DEPARTMENT

Influence of Phosphorylation on Caspase-3-Mediated akt1 Cleavage

TITRE DE LA THÈSE / TITLE OF THESIS

B .Tsang

DIRECTEUR (DIRECTRICE) DE LA THÈSE / THESIS SUPERVISOR

CO-DIRECTEUR (CO-DIRECTRICE) DE LA THÈSE / THESIS CO-SUPERVISOR

EXAMINATEURS (EXAMINATRICES) DE LA THÈSE / THESIS EXAMINERS

K. Turksen

B. Vanderhyden

Gary W. Slater

LE DOYEN DE LA FACULTÉ DES ÉTUDES SUPÉRIEURES ET POSTDOCTORALES /
DEAN OF THE FACULTY OF GRADUATE AND POSTDOCORAL STUDIES

Influence of Phosphorylation on Caspase-3-Mediated akt1 Cleavage

by

Arezu Jahani-asl

Thesis submitted to the
Faculty of Graduate and Postdoctoral Studies
in partial fulfillment of the requirements for the degree of
Master of Science

Department of Cellular and Molecular Medicine
Faculty of Medicine
University of Ottawa

Your file Votre référence
ISBN: 0-494-11300-6
Our file Notre référence
ISBN: 0-494-11300-6

1. ACKNOWLEDGEMENTS

I wish to express my gratitude and appreciation to my principal supervisor Dr. Benjamin K. Tsang for his guidance, patience, encouragement, enthusiasm, and financial support from his CIHR grant. Dr. Tsang always motivated me and provided a stimulating working environment for my professional development.

I wish to thank my co-supervisor Dr. Ajoy Basak for his input, technical support and his great contributions of the SELDI-M.S. analysis of the caspase-3-mediated Akt1 digests.

I wish to thank Dr. Barbara Vanderhyden and Dr. Gerard Cook, members of my Graduate Advisory Committee for their invaluable comments and counsel.

I wish to express my deepest gratitude to my parents Maliha Ayazi and Rahmat Jahani-asl, and my brother Dr. Mehran Jahani-asl for their never-ending emotional support and encouragement.

I wish to dedicate this thesis to my husband Dr. Vahab Soleimani, who has provided me with stimulating discussion and every kind of support throughout this project and at all times.

2. ABSTRACT

Caspase-3, an executioner of apoptosis, is negatively regulated by X-linked inhibitor of apoptosis protein (XIAP), a determinant of cisplatin resistance. XIAP down-regulation in ovarian cancer cells or treatment with cisplatin induces caspase-3-mediated AKT cleavage and apoptosis, while XIAP over-expression suppresses this cleavage and increases phospho-AKT content. The identity of the caspase-3 cleavage site(s) in Akt1 and the possible dependence of caspase-3-mediated cleavage on its phosphorylation status are unknown. The objectives of this thesis were to determine the caspase-3 cleavage site(s) in Akt1 and to examine the influence of phosphorylation on Akt1 cleavage in vitro. Our results suggested presence of three non-consensus ($EEEE^{117}$, $EEMD^{119}$, $DAKE^{398}$) and one consensus ($DQDD^{456}$) cleavage sites, and posphorylation of Akt1 influenced the pattern of cleavage in a site-specific manner: Whereas cleavage at site "$EEEE^{117}$" was facilitated by phosphorylation, that at sites "$EEMD^{119}$ and $DAKE^{398}$" were attenuated. The biological significance of these observations requires future investigation.

3. TABLE OF CONTENTS

4. LIST OF FIGURES

5. LIST OF TABLES

6. LIST OF ABBREVIATIONS

AA	Amino acid
Ala	Alanine
AIF	Apoptosis inducing factor
AMC	7-amino-4-methylcoumarin
Arg	Arginine
Asn	Asparagine
Asp	Aspartic acid
BAD	Bcl-X_L/Bcl-2 associated death factor
B.F.	Bovine Fetuin
BSA	Bovine serum albumin
C	Cysteine
CAPS	3-(cyclohexylamino)-1-propanesulfonic acid
CEF	Chicken embryo fibroblast
CHAPS	3-[(3-Cholamidopropyl) dimethylammonio]-1-propanesulfonate
CHCA	α-Cyano-4- hydroxycinnamic acid
cIAP-1	Human IAP-1
cIAP-2	Human IAP-2
Cys	Cysteine
D	Aspartic acid
DED	Death effector domain
DHB	2,3 hidroxy benzoic acid

DISC	Death inducing signalling complex
DTT	Dithiothreital
E	Glutamic acid
ECL	Enhanced Chemiluminescence
EGFR	Epidermal growth factor receptor
F	Phenylalanine
FADD	Fas-associated death domain protein
FKHR	Forkhead apoptotic regulator
FLICE	FADD-like interleukin-1–β-converting enzyme
Gln	Glutamine
Glu	Glutamic acid
Gly	Glycine
GSK3	Glycogen Synthase Kinase 3
H	Histidine
HEPES	(N-[2-hydroxyethyl] piperazine-N' -[2-ethane-sulfonic acid])
HRP	Horse Radish Peroxidase
I	Isoleucine
IAP	Inhibitor of Apoptosis Proteins
IκB	Inhibitor κB
IP3	Inositol trisphosphate
K	Lysine
L	Leucine
M	Methionine

MALDI-TOF	Matrix-Assisted Laser Desorption Ionization Time-of-Flight
MES	(2-[N-morpholine] ethane-sulfonic acid)
M.S.	Mass Spectrometry
MST2	STE-20-like kinase 2
N	Asparagine
NFκB	Nuclear factor κB
NO	Nitric Oxide
OSE	Ovarian surface epithelium
P	Proline
PCD	Programmed Cell Death
PDK	Phosphoinositide-dependent kinase
PH	Pleckstrin homology
Phospho-Akt1	Phosphorylated Akt1
PI3K	Phosphatidylinositol 3- Kinase
PIP2	Phosphatidylinositol 4, 5- bisphosphate
PIP3	Phosphatidylinositol 3, 4, 5- trisphosphate
PIPES	Piperazine-N,N'-bis(2-ethane-sulfonic acid)
PKB	Protein Kinase B
PVDF	Poly (vinylidene fluoride)
Q	Glutamine
R	Arginine
R_f	Ratio of fonts
RFU	Relative Fluorescence Unit

RTK	Receptor Tyrosine Kinase
Ser	Serine
SELDI-M.S.	Surface Enhanced Laser Desorption-Ionization Mass Spectrometry
Thr	Threonine
TNF	Tumor necrosis factor
TNFR1	Tumor Necrosis Factor Receptor 1
V	Valine
W	Tryptophan
XIAP	X-Linked Inhibitor of Apoptosis Protein
Y	Tyrosine

7. INTRODUCTION

Ovarian cancer causes more deaths than any other gynecological cancer in the world. Although the incidence of this disease is lower than other female-associated cancers, its mortality rate is very high, in that over one-half of all patients surrender to the disease (Harries et al, 2001). Cytoreductive surgery followed by adjuvant chemotherapy with paclitaxel and either cisplatin or carboplatin is the favored treatment modality, but chemoresistance abrasively limits successful therapy and most patients will have tumor recurrence within 3 years following treatment (Eltabbakh et al 2001). Increased resistance to apoptosis via deregulation of key pro- and anti-apoptotic factors has been proposed to play a central role in the onset and maintenance of chemoresistance (Mansouri et al, 2003; Hanahan and Weinberg, 2000; Thompson, 1995).

Apoptosis, or programmed cell death (PCD), is a genetically regulated cellular suicide mechanism that plays a critical role in a variety of biological systems, including normal cell turnover, the immune system, embryonic development, metamorphosis, hormone-dependent atrophy and chemical induced cell death (Arends et al, 1991; Elis et al, 1991; Cohen et al, 1992). The mechanism of apoptosis is evolutionarily conserved, and executed by a family of cysteine proteases called caspases (Alnemri et al, 1996). To date eleven human caspases have been identified (Yuan et al, 1993; Xue et al, 1995; Xue et al, 1996), many of which are specialized for apoptosis (caspase-3, -6, -7, -8, -9, and -10) (Earnshaw et al 1999). Caspases are highly regulated signaling molecules that target

structural components of the cytoskeleton and nucleus, as well as numerous proteins involved in survival signaling pathways (Kayalar et al, 1996; Mashima et al, 1997; Ku et al, 1997; Datta et al, 1997). In order to overcome chemoresistance via the manipulation of apoptotic pathways, a thorough understanding of the caspase systems and their regulation is essential.

Caspase activity is tightly regulated at several different levels. The intracellular anti-apoptotic proteins (IAPs) have been demonstrated to play a significant role in this regulation and modulating death-signaling pathways. They currently include X-linked IAP (XIAP), human IAP-1 and –2 (cIAP-1 and cIAP-2), neuronal apoptosis inhibitory protein (NAIP), survivin and livin (Ambrosini et al, 1997; Liston et al, 1996; Lin wt al, 2000). XIAP, cIAP-1 and -2 are direct inhibitors of caspase-3 and -7 and modulate the Bax/cytochrome c pathway by inhibiting caspase-9 (Roy et al, 1997; Deveraux et al, 1997; Takahash et al 1998; Deveraux et al, 1999), resulting in suppressed apoptosis. XIAP has been localized in human ovarian carcinomas, with levels being highest in proliferative but not apoptotic epithelial cells (Li et al, 2001).

In contrast to caspases, phosphatidylinositol 3- kinase (PI3K) and its downstream target protein kinase B (PKB/AKT) act in a survival signaling pathway to secure cell endurance and suppress apoptosis. Following activation of PI3K in response to growth factors or cytokines, AKT, an inactive cytosolic serine/threonine protein kinase, is recruited to the plasma membrane and activated by phosphorylation at threonine 308 and serine 473 (Allesi et al, 1996; Stokoe et al, 1997; Stephen et al, 1998). AKT performs its survival role

in multiple cell lineages (Brunet et al, 1999; Dudek et al, 1997; Kennedy et al, 1997) by phosphorylating and altering the activity of a number of pro-apoptotic mediators including caspase-9 (Datta et al, 1997; Wang et al, 1996; Brunet et al, 1999; Cardone et al, 1998; Del et al, 1997). Recently XIAP has been identified as a new downstream target of AKT and a potentially important mediator of the effect of AKT on cell survival (Dan et al, 2004).

The interaction between caspases and survival factors governs the life/death decision of the cell. Suppressed apoptosis as a result of over-expression of survival factors such as XIAP and AKT, leads to chemoresistance in human ovarian epithelial cancer (Cheng et al, 2002). In the process of investigating the PI3K/AKT biochemical pathways, our laboratory has demonstrated that AKT is a substrate for caspase-3 in ovarian cancer cells and that XIAP over-expression is associated with increased phospho-AKT content and decreased caspase-3-mediated AKT cleavage (Asselin et al, 2001). However the caspase-3 cleavage site(s) in AKT has not been defined and requires further analysis. Moreover, whether or not phosphorylation plays a role in this cleavage, remains to be investigated. The recognition of the cascade responsible for caspase-3-mediated processing of AKT and complications associated with this machinery may illustrate a possible mechanism through which chemoresistance may be conferred in human ovarian carcinoma.

In the present studies, we examined the caspase-3 consensus and non-consensus cleavage sites in Akt1 and the possibility of cleavage at these sites in vitro. We investigated specificities of these sites as well as their extent of cleavage in response to Akt1 phosphorylation/activation. These studies demonstrated for the first time that in addition to a

consensus DXXD site, there are at least three non-consensus caspase-3 motifs in Akt1. We showed that phosphorylation of Akt1 modulates its sensitivity to caspase-3-mediated cleavage in a site-specific manner.

8.0 LITERATURE REVIEW

8.1 Human Epithelial Ovarian Cancer

Ovarian cancer is among the 15 most commonly diagnosed cancers in women and the 12th leading cause of death for women in Canada. In 2004, about 2,300 new cases were identified and 1,550 deaths were reported in Canada alone (http://info.cancer.ca/CIS/E/CCE/HTML/35_954.html). The high mortality rate is associated with a late diagnosis. Only about 25% of patients are diagnosed when the disease is still confined to the ovary. At advanced stages (stages III and IV), when the disease has spread beyond the ovary, treatment becomes increasingly ineffective. About 90% of human ovarian carcinomas are thought to arise from the ovarian surface epithelium (OSE) cells (Feeley et al, 2001; Auersperg et al, 2001). It is estimated that only 5-10% of ovarian cancer cases have a hereditary origin (Eeles and Powles 2000).

According to the model proposed by Cramer and Welch (1983), tumorigenesis is initiated in epithelial inclusion cysts or invaginations which are formed in the process of ovulatory repair or changes in the ovarian structure with aging. OSE cells have mesenchymal and epithelial characteristics, but epithelial differentiation predominates in cells within inclusion cysts (Radisavljevic, 1977). Cyst formation results in the disruption of the connective tissues, exposing OSE cells further to proliferative cues from steroid-producing cells, follicular fluids and platelets. Excessive gonadotropin production, as

well as growth factors and cytokines within the ovary, have been implicated in the progression of OSE cancer (Cramer and Welch, 1983; Berchuck et al, 1993).

The lack of diagnostic tools for detection of ovarian cancer at an early stage hinders the ability to gain insights into the genes which cause this disease. To date, researchers have identified mutations in a vast number of genes associated with ovarian cancer (e.g. p53, BRCA1, EGFR, Ras and Myc). However, the majority of ovarian cancer specimens are from late stage cases and involve a multitude of genetic changes (Godwin et al, 1994), making it difficult to determine the initiating mutation and order of the mutations during the disease development.

Treatment of ovarian cancer mainly consists of cytoreductive surgery followed by adjuvant chemotherapy. Chemotherapy has developed swiftly during the last 15 years (Eltabbakh et al, 2001). Combination chemotherapy was superior to single-agent therapy and began to improve outcomes in women afflicted by this disease. By 1990, platinum compounds exhibited improved response rate, and platinum combined with alkylating agents became the new standard of care. The most current clinical trials have established combination therapy of cisplatin and paclitaxel as the first line chemotherapy due to its better toxicity profile (Muggia et al, 2000). Although this treatment course seems to be effective in a large percentage of cases, the development of chemoresistance is a major obstacle that significantly hinders successful treatment (Eltabbakh et al, 2001). Therefore, overcoming drug resistance is one important strategy to successful treatment of ovarian cancer.

8.2 Chemoresistance in Ovarian Cancer

Despite a clinical response at the completion of the primary chemotherapy, most patients have long-term disease or develop recurrent chemoresistant disease. The patient is considered to have clinically defined platinum-resistant disease if her tumor continues to grow during the platinum-based combination therapy or if her tumor does not regress following four to six cycles of chemotherapy (Markman et al, 1998). Most cancers are intrinsically resistant to chemotherapy or become resistant after an initial partial response (Harrison et al, 1995).

A number of explanations for chemoresistance have been put forward. They include: 1) Failure to modify the pro-drug to its active form; 2) Enhanced inactivation or detoxification of the drug; 3) Reduced retention of the drug within cells because of reduced inward transport or increased drug efflux; 4) Altered amount of activities of target proteins; 5) Enhanced capacity for DNA repair and 6) Increased resistance to apoptosis (Harrison et al, 1995). Increased resistance to apoptosis via deregulation of key pro- and anti-apoptotic pathways is proposed to be a key factor in the onset and maintenance of chemoresistance (Cheng et al, 2002). Recent evidence suggests that homeostasis of human OSE cells is maintained by a delicate balance in the expression and actions of cell survival factors versus death factors and that chemoresistance in ovarian cancer results in part from a defective apoptotic machinery in which survival factors such as XIAP, PI3K, and AKT are over-expressed (Cheng et al, 2002).

8.3 PI3K/AKT Pathway

8.3.1 Phosphatidylinositol 3-Kinase (PI3K)

Phosphatidylinositol 3-kinases (PI3Ks) are cytosolic enzymes which exist in multiple isoforms in mammalian cells. They are subdivided into three classes, referred to as I, II, and III (Roymans et al 2001; Vanhaesebroeck et al, 2001). The most studied of these enzymes are class I PI3Ks which are generally coupled to extracellular stimuli (Vivanco et al 2002). Class IA PI3K is a heterodimer composed of a p110 catalytic subunit (α, β, and γ) and a regulatory/adaptor subunit. There are at least seven adaptor proteins that are generated by expression and alternative splicing of three different genes (*p85, p50,* and *p55*). In contrast, class IB PI3K is comprised of a p110γ catalytic subunit and a p101 regulatory subunit, unrelated to p85 (Cantley et al, 2002; Inukai et al, 1997). Evidence suggests that PI3K class IA can be considered an oncogene because its aberrant function contributes to mitogenesis, cellular growth, and cellular transformation in a variety of neoplasias including ovarian cancer (Roymans et al, 2001; Varticovski et al, 1994; Hu et al, 1995). It has been demonstrated that inhibition of PI3K by LY294002 or wortmannin (two potent PI3K inhibitors), enhances apoptosis in human pancreatic cancer cells (Ng et al, 2000). In primary ovarian cancer cells and several ovarian epithelial cancer cell lines, the gene encoding the p110 α catalytic subunit of PI3K (PIK3CA) is present in increased copy number (Shayesteh et al, 1999). Moreover, LY294002 decreases growth of ovarian carcinoma and abolishes the decreased sensitivity to

paclitaxel caused by over-expression of an activated PI3K (Hu et al, 2000; Hu et al, 2002).

PI3KIA catalytic activity is strongly regulated in normal cells by diverse mechanisms. It is thought that an inactive p85-p110 complex is present in the cytoplasm of resting cells ready for activation by appropriate signals. Upon binding of tyrosine kinases to their receptors, p85-p110 complex is recruited to the receptors and becomes active presumably for two reasons: 1) the p110 catalytic subunit is now in close proximity to its lipid substrates in the cell membranes and 2) interaction of p85 with receptor tyrosine kinase (RTK) might relieve an inhibitory effect of p85 on p110 kinase activity (Yu et al, 1998). PI3K can also be activated by RTKs indirectly through RAS, which can bind and activate the p110 subunit (Kodaki et al, 1994). Once activated, PI3KIA converts the plasma membrane lipid phosphatidylinositol 4-phosphate and phosphatidylinositol 4, 5-bisphosphate (PIP2) to phosphatidylinositol 3, 4-bisphosphate and phosphatidylinositol 3, 4, 5-trisphosphate (PIP3), respectively. Pleckstrin homology domain-containing proteins, including AKT accumulate at sites of PI3K activation by directly binding to PIP2 and PIP3 (Kodaki et al, 1994).

The mechanisms by which the PI3K pathway contributes to cell survival include phosphorylation of the pro-apoptotic molecules BAD, caspase-3, glycogen synthase kinase 3 (GSK3), and cell cycle inhibitors p21 and p27 (Franke et al 1997). Several biological effects of PI3K are mediated through the activation of the downstream target AKT. For example, the oncogenic transforming activity of P3k proteins (oncoprotein v-

P3k of the avian retrovirus ASV 16 and ASV 8905, coding for the catalytic subunit of PI3K) is routed through Akt1, since dominant negative Akt1 is known to interfere with P3k induced-transformation (Aoki et al, 2000; Aoki et al, 1998; Cheng et al, 1997).

8.3.2 Protein Kinase B

Protein kinase B (PKB/AKT) is a member of the second-messenger regulated subfamily of serine/threonine protein kinases, which plays an essential role in an anti-apoptotic signaling pathway downstream of PI3K. AKT was initially identified as the mammalian homologue of the viral oncogene v-akt, known to be leukemogenic in mice. Three members, Akt/Akt1/PKBα, Akt2/PKBβ and Akt3/PKBγ have been identified in this family. The overall homology of these three isoforms is greater than 85% with human Akt1 having 81% and 83% amino acid identity with Akt2 and Akt3, respectively. All the isoforms of AKT share three distinct functional domains (Fig.1): an N-terminal PH domain which consists of about 100 amino acids mediating protein-protein and protein-lipid interactions, a serine/threonine-rich C-terminal catalytic domain, and a central kinase domain (Chan et al, 1999; Coffer et al, 1998; Fruman et al, 1998). All three isoforms share a caspase-3 classical motif (DXXD) in their C-terminal tail and a similar activation process appears to be operational for all three AKT isoforms.

Figure.1 Three isoforms of AKT share distinct functional domains

Akt1, Akt2, and Akt3 share distinct functional domains which include: an N-terminal pleckstrin homology (PH) domain of about 100 amino acids, mediating protein-protein and protein-lipid interactions, a serine/threonine-rich C-terminal catalytic domain, and a central kinase domain. Moreover, all three isoforms share a caspase-3 classical motif (DXXD) in their C-terminal tail and are activated by phosphorylation on two regulatory sites (threonine 308/309/305 and serine 473/474/472 for Akt1/2/3, respectively).

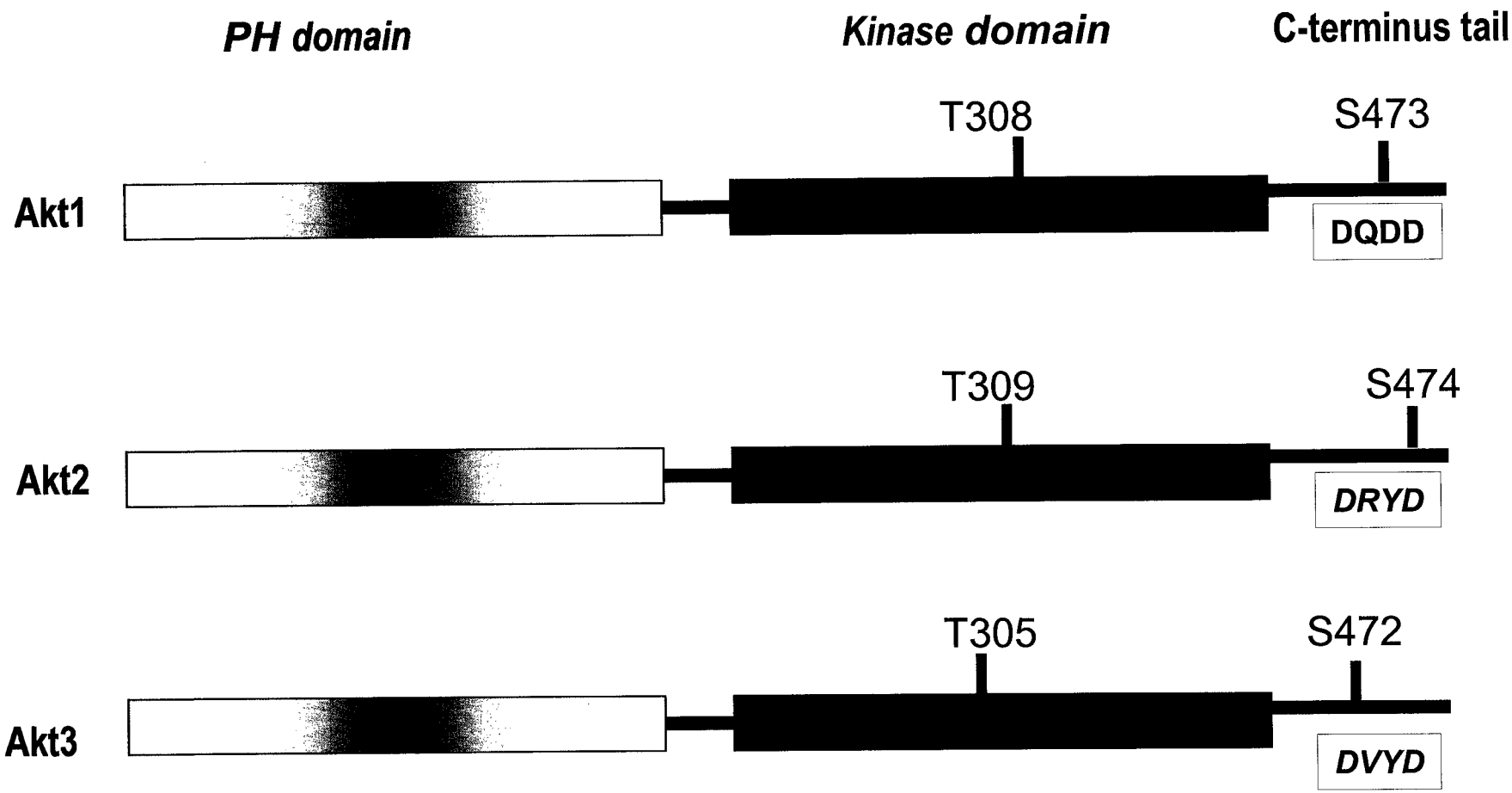
PH domain
Kinase domain
C-terminus tail
T308
S473
Akt1
DQDD
T309
S474
Akt2
DRYD
T305
S472
Akt3
DVYD

Fig. 1

8.3.2.1 AKT Activation

After the binding of growth factors to their cell surface receptors, AKT is translocated to the plasma membrane, secondary to the binding of the PH domain with products of phosphoinositide-3 kinase pathway: PIP2 and PIP3 (Fig. 2; Alesi et al, 1996; Stokoe et al, 1997; Stephen et al, 1998). The activation of AKT involves AKT phosphorylation on two regulatory sites: threonine 308/309/305 and serine 473/474/472 (Akt1/2/3, respectively), both of which are required for maximal kinase activity (Brodbeck et al, 1999). Phosphorylation of the threonine residue occurs through the activity of phosphoinositide-dependent kinase 1 (PDK1) (Chan et al, 1999; Coffer et al, 1998; Fruman et al, 1998). However, the identity of the kinase(s) putatively named PDK2, responsible for the phosphorylation of the serine residue remains unclear. AKT kinase activity has recently been shown to be required for serine phosphorylation to occur in vitro, suggesting that AKT auto-phosphorylation might play a role in the process (Toker et al, 2000). Following its activation, AKT must be released from the membrane in order to act on its downstream targets. It has been proposed that inositol triphosphate (IP3), presumably generated from PIP2 by phospholipase C-γ, could release PH domain-containing proteins from membranes (Hemmings et al, 1997). It is now clear that prolonged stimulation with growth factors results in phosphorylated AKT translocation to the nucleus. In fact some of its substrates, such as the forkhead family of transcription factors, are resident within this organelle (Meier et al, 1999).

Figure 2. PI3K/AKT Pathway: AKT activation

Activation of growth factor receptors leads to PI3K activation and conversion of PIP2 to PIP3. The binding of these phosphoinositides to the PH domain of Akt recruits Akt to the plasma membrane. Akt1 is phosphorylated on Thr 308 and Ser 473 by PDK1 and PDK2, respectively. Activated AKT phosphorylates substrates, resulting in a variety of biological effects including suppression of apoptosis.

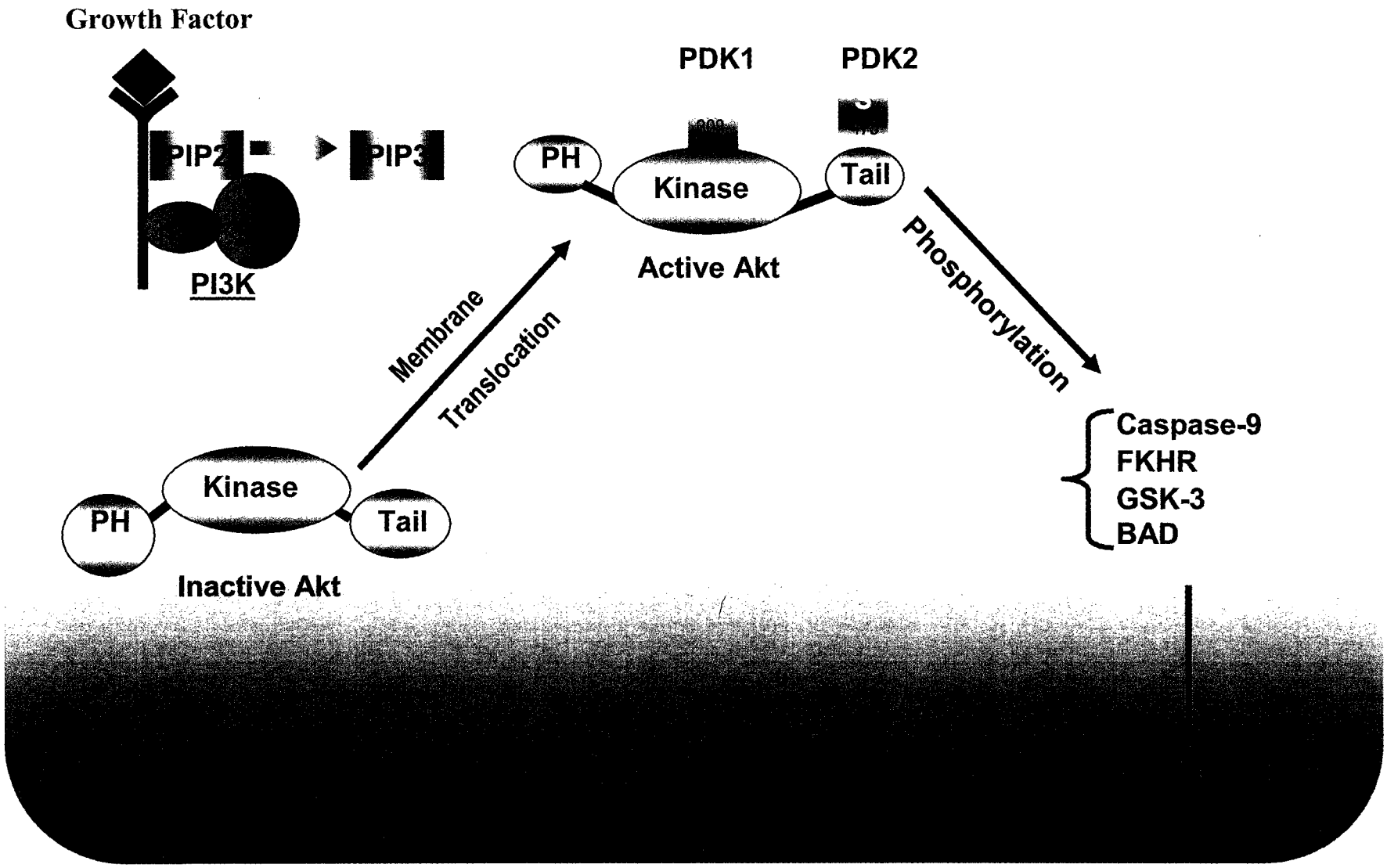
Growth Factor
PIP2
PIP3
PI3K
PDK1
PDK2
PH
Kinase
Tail
Active Akt
Membrane
Translocation
Phosphorylation
Caspase-9
FKHR
GSK-3
BAD
PH
Kinase
Tail
Inactive Akt

Fig. 2

8.3.2.2 AKT Cell Survival Mechanisms

The cell survival role of AKT has been demonstrated in multiple cell lineages (Brunet et al, 1999; Dudek et al, 1997; Kennedy et al, 1997). The mechanism by which AKT protects cells from death is likely multifactorial because AKT directly phosphorylates several components of apoptotic machinery such as the pro-apoptotic proteins BAD, caspase-9 and transcription factor FKHRL1 (Datta et al, 1997; Wang et al, 1996; Del et al, 1997; Cardone et al, 1998; Brunet et al, 1999) and can also influence cell survival by means of indirect effects on two central regulators of cell death: nuclear factor κB (NFκB) (Ramashkova et al, 1999; Kane et al, 1999) and p53 (Mayo et al, 2001; Zhou et al, 2001). BAD is a pro-apoptotic member of the Bcl-2 family that promotes cell death by binding the survival factor Bcl-X_L and inhibiting its action. AKT phosphorylates Bad at two sites (serine 112 and serine 136) and blocks this interaction by restoring anti-apoptotic function of Bcl-X_L (Datta et al, 1997; Wang et al, 1996). AKT inhibits caspase-9 protease activity and blocks FKHRL1 function, reducing Fas ligand transcription (Del et al, 1997; Cardone et al, 1998; Brunet et al, 1999). AKT can exert a positive effect on the function of the anti-apoptotic transcription factor NFκB by phosphorylating and inactivating IκB kinase (a kinase involved in degradation of NFκB inhibitor IκB) (Ramashkova et al, 1999). Furthermore, it inactivates p53, a key tumor suppressor, through phosphorylation and facilitates nuclear localization of MDM2 (a negative regulator of p53 function) and its consequent binding to p53 (Zhou et al, 2001).

8.3.2.3 Physiological Significance in Tumorigenesis: Akt1 versus Akt2 and Akt3

Although Akt1, Akt2, and Akt3 display high sequence homology and share similar upstream signal regulators and downstream targets, there are clear differences between the three isoforms in terms of biological and physiological functions. Akt1 expression is relatively uniform in various normal organs whereas high levels of Akt2 and Akt3 mRNA are detected in skeletal muscle, heart, placenta and brain (Cheng et al, 2002). The work that originally identified AKT as a potential human oncogene detected amplification of Akt1 in a single gastric carcinoma (Staal et al, 1987). *akt2* gene amplification has been found in ovarian, pancreatic, gastric, and breast tumors (Bellacosa et al, 1995; Cheng et al, 1996) and *akt3* gene encoding for Akt3 kinase (which shows a high degree of homology in their catalytic and PH domains to Akt1) is over-expressed in breast and prostate cancers (Bellacosa et al, 1995; Nakatani et al, 1999). Activation of the Akt3 protein has also been shown to promote cell survival and tumor development in 43 to 60% of non-familial melanomas (Stahl et al, 2004). However, a significant level of Akt3 is not detected in the ovary.

Akt1 has been implicated in a wide variety of cellular processes including adipocyte and muscle differentiation, glycogen synthesis, glucose uptake, apoptosis and cellular proliferation (Allesi et al, 1998; Coffer et al, 1998; Kohn et al, 1996; Jiang et al, 1999). Many researchers have reported an anti-apoptotic role for this AKT isoform in human and animal models. Constitutively activated and membrane targeted Akt1 causes focus

formation in chicken embryo fibroblasts (CEF) and hemangiosarcomas in chicken (Aoki et al, 1998). Akt1 is involved in the activation of NFκB1 by TNF and regulates the activity of FKHRL1, leading to the association of FKHRL1 with 14-3-3 proteins and its retention in the cytoplasm (Brunet et al, 1999). Moreover, Akt1 phosphorylates p27, impairs the nuclear import of p27 and opposes cytokine-mediated G1 arrest (Liang et al, 2002). It has been demonstrated that in the Akt1 null mouse model, the animals were viable but smaller than wild type littermates and their life span was shorter upon exposure to genotoxic stress. Over-expression of a constitutively active form of Akt1 in differentiated SH-SY5Y neuronal cells provided protection against apoptosis. Furthermore, transfection of SH-SY5Y cells with a plasmid encoding a kinase-deficient dominant negative Akt1 eliminated cytoprotection suggesting that activation of Akt1 is necessary and sufficient to inhibit apoptosis (Kang et al, 2003). In the same study, it was demonstrated that constitutively active Akt1 stably transfected into NIH3T3 cells resulted in a malignant phenotype.

The involvement of Akt2 as an anti-apoptotic factor is well-established in ovarian cancer. Amplification of Akt2 has been demonstrated in a number of human ovarian cancer cell lines, and an elevated level of the protein has been detected in about half of the primary ovarian carcinomas examined (Cheng et al, 1992; Yuan et al, 2000). Moreover, inhibition of PI3K/Akt2 by farnesyltransferase inhibitor-2777 has been demonstrated to induce apoptosis in ovarian cancer cells that over-express Akt2 (Jiang et al, 2000). It is reported that Akt2 activity promotes chemoresistance to cisplatin-induced apoptosis through the inhibition of the ASK1/JNK/P38 pathway (Yuan et al, 2003).

Despite the vast amount of research establishing an anti-apoptotic role for Akt1 and the recent discovery of increased Akt1 kinase activity in primary carcinomas of the ovary (Sun et al, 2001), a role for Akt1 in human ovarian epithelial carcinoma and cisplatin resistance has not been well-established and requires further investigation.

8.4 Apoptosis

Apoptosis is a normal physiological process of active cell death (Wyllie et al, 1980; Kerr et al, 1972). A fundamental feature of apoptosis is that it results from a decision by the cell based on information from its environment, its own internal metabolism, its development history and its genome (Williams et al, 1992). Unlike necrosis, cells entering apoptosis are often capable of survival but choose to die, presumably for the good of the whole organism and hence of their own genome (Kerr et al, 1972). Apoptosis serves as a major mechanism for the precise regulation of cell numbers and as a defense mechanism to remove unwanted and potentially dangerous cells, leading to regulation of development and homeostasis (Jacobson et al, 1997).

Morphologically, cells undergoing apoptosis demonstrate nuclear/cytoplasmic condensation and membrane protrusions. These initial changes are followed by fragmentation of the nuclear contents and subsequent encapsulation of these fragments into apoptotic bodies (Kerr et al, 1972). Biochemically, apoptotic cells are characterized by: 1) Reduction in the mitochondrial transmembrane potential; 2) Intracellular

acidification; 3) Production of reactive oxygen species; 4) Externalization of phosphatidylserine residues in membrane bilayers; 5) Degradation of DNA into high-molecular weight and oligonucleosomal fragments and 6) Selective cleavage of a subset of cellular proteins by a specialized family of cystein–dependent aspartate-directed proteases termed caspases (Wyllie et al, 1980; Lazbnik et al, 1994; Alnemri et al, 1996).

Apoptosis occurs in two phases: 1) a commitment to cell death, and 2) an execution phase characterized by a dramatic stereotypical morphological change in cell structure (Takahashi et al, 1996). Death receptor (extrinsic) pathway and mitochondrial (intrinsic) pathway are two major apoptotic pathways, both of which ultimately result in a proteolytic cascade involving caspases (Fig. 3) (Green et al, 2000; Salvesen et al, 1997; Song et al, 1999). In addition, a third apoptotic pathway involving the Apoptosis-Inducing Factor (AIF), appears to be functional exclusively in neurons.

Figure 3. Two Major Apoptotic Pathways

Death receptor (extrinsic) and mitochondrial (intrinsic) pathways are two major apoptotic pathways, both of which result in a proteolytic cascade involving caspases. In both pathways the ultimate goal is cell death via caspase-3-mediated proteolytic cleavage and activation of a number of pro-apoptotic proteins.

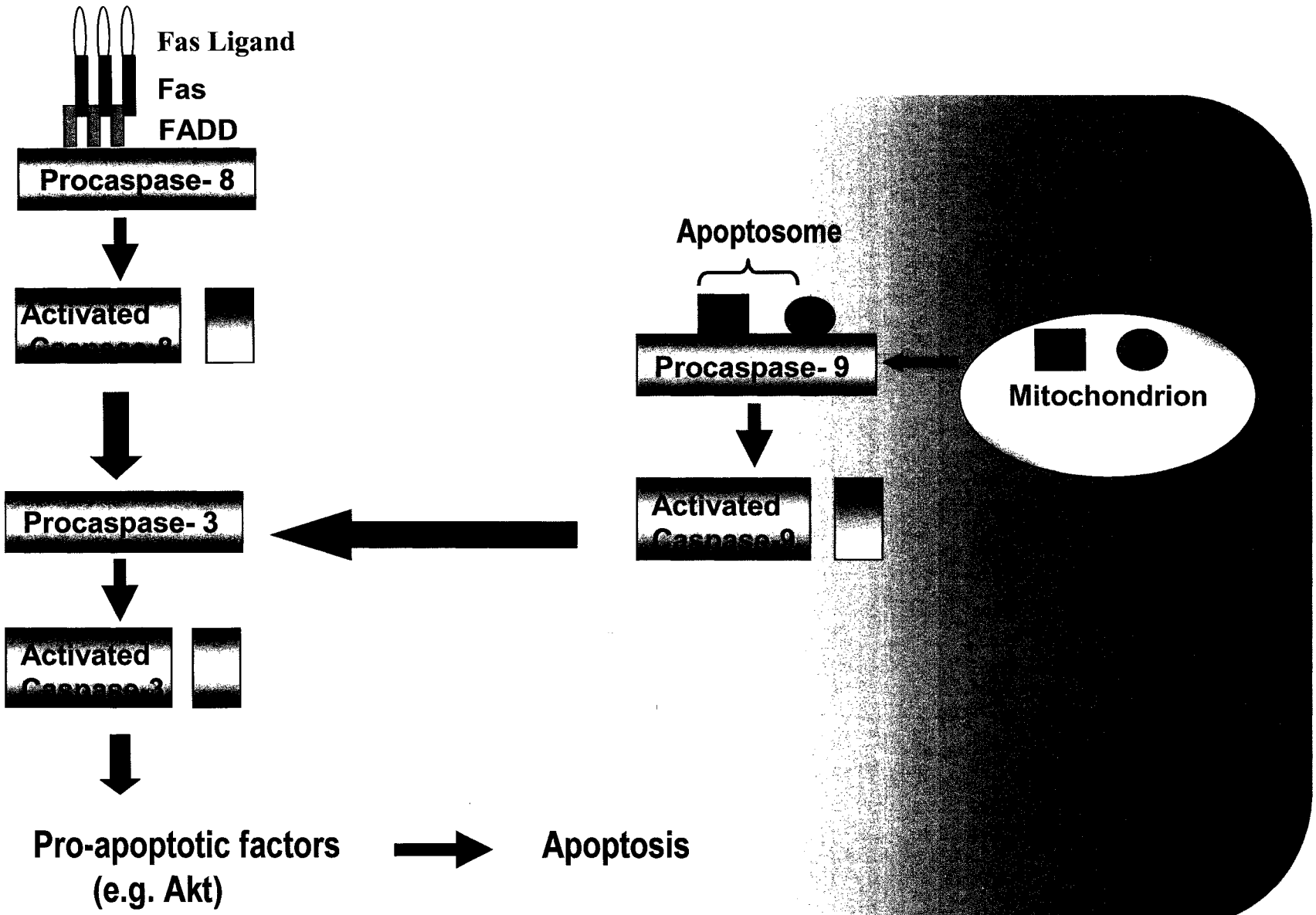
Fas Ligand
Fas
FADD
Procaspase- 8
Activated
Procaspase- 3
Activated
Pro-apoptotic factors
(e.g. Akt)
Apoptosis
Apoptosome
Procaspase- 9
Activated
Mitochondrion

Fig. 3

8.4.1 Extrinsic Pathway

One of the most extensively studied pathways of apoptosis results from ligation of transmembrane death receptors belonging to the tumor necrosis factor-R1 (TNF-R1) family. Upon the binding of specific ligands, these receptors transmit a lethal signal into the cell's interior that results in apoptotic cell death (Ashkenazi et al, 1998). The TNFR1/TNF pair presents a rather complex pathway with which to scrutinize apoptosis initiation, because this receptor/ligand pair can signal either apoptosis or an antagonistic NFκB-mediated survival pathway, depending on the cellular context. The TNF-R1 homologue Fas (CD95/Apo-1) has been the paradigm of choice, because addition of its cognate ligand, FasL, rapidly signals cell death (Nagata et al, 1995). As such, the Fas/FasL pair was used to isolate the components of the death-inducing signaling complex (DISC) that forms after Fas ligation (Muzio et al, 1998; Boldin et al 1996).

A seemingly simple DISC comprising Fas, the adaptor molecule FADD, and procaspase-8 was discovered by a combination of yeast two-hybrid and protein sequence analysis. Before this discovery, receptors were thought to signal either by phosphorylation status of key signaling molecules or by functioning as ion channels. The death receptor signaling by direct recruitment and activation of caspase-8, shed new light on the perplexing problem of how the first proteolytic event was generated during apoptosis (Fig. 3). It was demonstrated that once activated, caspase-8 activates caspase-3, which in turns leads to full implementation of the apoptotic program and the degradation phase of apoptosis (Slee et al, 1999).

8.4.2 Intrinsic Pathway

In the drug-induced (mitochondrial) apoptotic pathway, signals transmitted to the mitochondria (e.g. pro-apoptotic proteins from the Bcl-2 family such as Bax) trigger the release of cytochrome c, which associates with the scaffolding protein, Apaf-1 (Wang et al, 2001). Apaf-1 is a large, multi-domain protein composed of an N-terminal CARD domain, a CED4 homology domain, and a C-terminal WD40 repeat (Zou et al, 1997). It has been reported that in the presence of cytochrome C and dATP, Apaf-1 forms a large oligomeric complex of about 700 kDa termed the apoptosome, which recruits and activates procaspase-9 (Fig. 3) (Li et al, 1997; Zou et al 1999; Cain et al 2000). Caspase-9 results in the proteolytic cleavage and activation of downstream caspases including caspase-3, which in turns activates the caspase cascade and the degradation phase of apoptosis.

8.5 Caspases

In 1993, researchers discovered that the *Caenorhabditis elegans* (*C. elegans*) cell death gene *ced-3* had remarkable sequence similarity to interleukin-1β-converting enzyme (caspase-1), a mammalian proteinase responsible for proteolytic maturation of pro-interleukin-1β (Yuan et al, 1993; Cerretti et al, 1992; Thornberry et al, 1992). Subsequent studies identified over a dozen caspase family members (Xue et al, 1996; Yuan et al, 1993). Several lines of evidence indicated that caspases are important for

apoptosis. First, caspase activation was correlated with the onset of apoptosis (Tewari et al, 1995; Cohen et al, 197). Second, *C. elegans* mutants lacking the worm caspase CED-3 had a complete absence of developmental PCD (Ellis et al, 1986). Moreover, targeted deletion of caspase genes showed a definitive role for caspases in apoptosis, and animals deficient in caspase-3, caspase-8 and caspase-9 died prenatally because of profound defects in PCD (Green et al, 1998; Varfolomeev et al, 1998). Similarly, deletion of the gene for Drosophila caspase-1 caused larval lethality and also promoted melanotic tumor development (Song et al, 1997).

Phylogenic analysis reveals that, overall, there are two principal subfamilies of caspases. The caspase 1 subfamily (caspase 1, 4, 5, and 13) appears to be predominantly involved in the control of inflammation while caspase-3 subfamily (caspase-3, -6, -7, -8, -9, and -10) appears to be primarily specialized for apoptosis (Earnshaw et al, 1999).

8.5.1 Caspase Structure

Sequence analysis and x-ray crystallography data suggests that all caspases share a common structure containing: 1) an N-terminal prodomain, 2) a large subunit containing the active site cystein with a conserved QACXG motif, and 3) a C-terminal small subunit (Fig. 4; Wolf et al, 1999). An aspartate cleavage site separates the N-terminal prodomain from the large subunit and the large subunit from the C-terminal small subunit.

Figure. 4 All caspases share a common structure

All caspases share a common structure containing: 1) an N-terminal prodomain, 2) a large subunit, and 3) a C-terminal small subunit. Caspases with large prodomain are called initiator caspases and are thought to be involved in the initiation of the apoptotic response (e.g. caspase-8, and -9) and those with short prodomains (e.g. caspase-3) are so-called effector caspases, apparently activated by the initiator caspases. Caspase prodomain ranges in length from 23 amino acids (aa) for caspase-6 and -7 to 219 amino acid for caspase-10. Two related motifs have been found in this region. The death effector domain (DED) is found in caspase-8 and -10 and appears to be involved in interactions with DEDs of signaling adaptor proteins such as FADD. The caspase-recruitment domain (CARD) is found in caspase-1, 2, 4, and 9 and appears to be important in promoting interactions of these caspases with one another and with a range of other regulatory and adapter proteins.

Figure was adopted and modified from Shi et al, 2000.

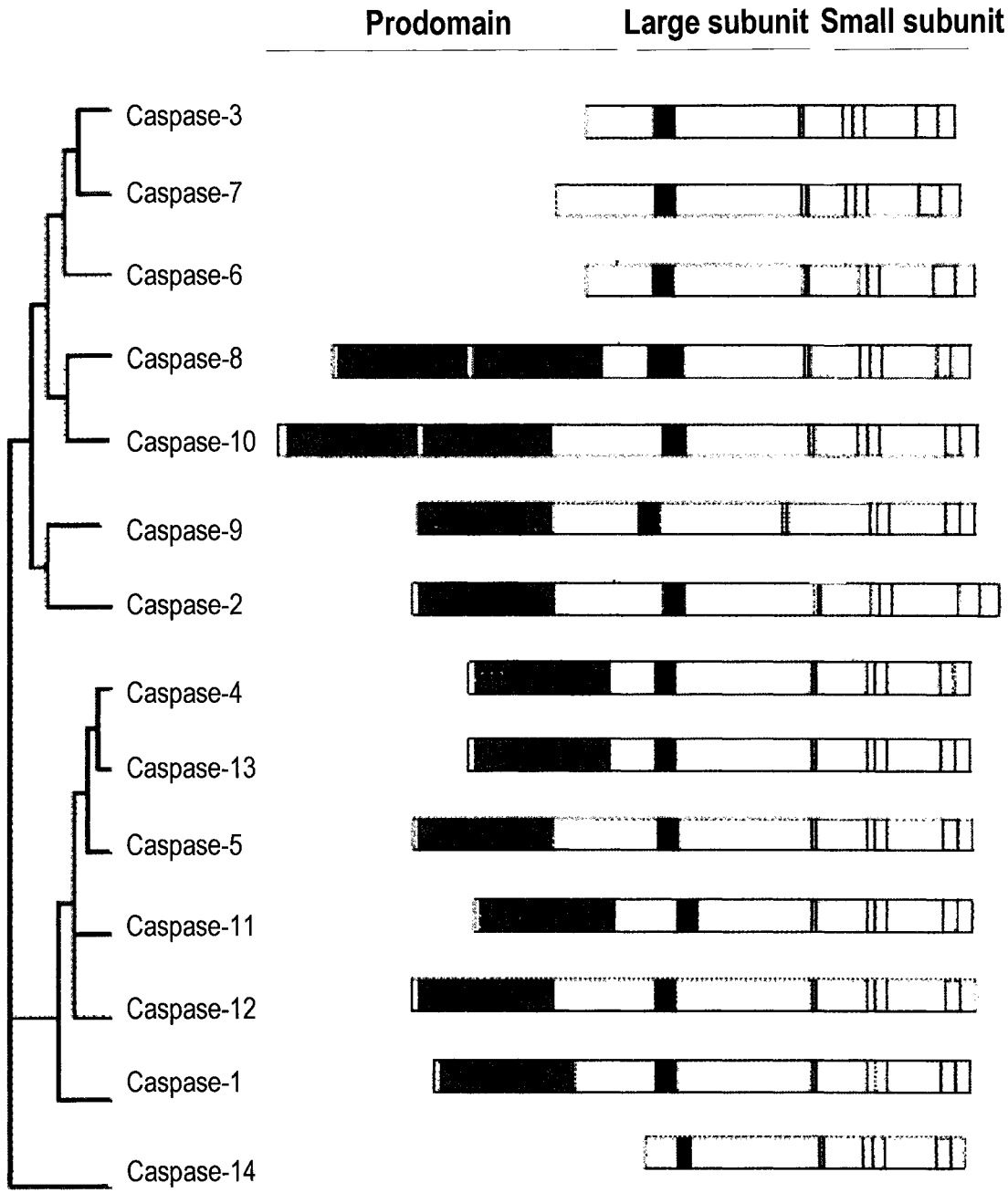
Prodomain
Large subunit
Small subunit
Caspase-3
Caspase-7
Caspase-6
Caspase-8
Caspase-10
Caspase-9
Caspase-2
Caspase-4
Caspase-13
Caspase-5
Caspase-11
Caspase-12
Caspase-1
Caspase-14

Fig. 4

Caspase prodomain ranges in length from 23 amino acids (aa) for caspase-6 and 7 to 219 amino acids for caspase-10. Caspases with large prodomains are thought to be involved in the initiation of the apoptotic response (e.g. caspase-8, and -9) and those with short prodomains (e.g. caspase-3) are so-called effector caspases, apparently activated by the initiator caspases. Although prodomains tend to be much more divergent than the catalytic segments, two related motifs have been found in this region. The death effector domain (DED) (Chinnaiyan et al, 1995) is found in caspase-8 and -10 and appears to be involved in interactions with DEDs of signaling adaptor proteins such as FADD (Chinnaiyan et al, 1995; Boldin et al, 1995) and TRADD (Hsu et al, 1995). The caspase-recruitment domain [CARD (Hofmann et al, 1997)] is found in caspase-1, 2, 4, and 9 and appears to be important in promoting interactions of these caspases with one another and with a range of other regulatory and adapter proteins (Earnshaw et al, 1999).

When alignments of large and small subunits of the 11 human caspases are compared, 29 residues are identical in at least 10 family members. Of these, seven are involved in substrate recognition and catalysis. The other 22 conserved residues are scattered throughout the protein. Many of these residues are hydrophobic and are likely to be involved in maintenance of the overall structure of the native enzyme. Because relatively few of these conserved residues are exposed on the surface of the active enzyme, it is unlikely that they are involved in interactions with other ligands. Instead, they might be important for interactions that occur between procaspase chains during assembly and processing of enzymes (Earnshaw et al, 1999).

8.5.2 Caspase Activation

All caspases are produced in cells as catalytically inactive zymogens and must undergo proteolytic activation during apoptosis. Conversion of each caspase precursor to the mature enzyme requires a minimum of two cleavages, one separating the prodomain from the large subunit and another separating the large and small subunits (Fig. 5). All of these cleavages involve Asp-X bonds and appear to occur in an ordered fashion, with cleavage between the large and small subunits preceding removal of the prodomain (Li et al, 1997; Srinivasula et al, 1998; Martin et al, 1996; Han et al, 1997). Each active caspase is derived from the processing and self-association of two procaspase zymogens. The resulting tetrameric enzymes, which have been described as homodimers of heterodimers, contain two active sites at opposite ends of the molecule (Walker et al, 1994; Mittl et al, 1997). The large and small subunits within each heterodimer interdigitate to form a core composed of a six-stranded β-sheet flanked by α-helices, a quaternary structure that is unique among proteases (Walker et al, 1994; Rotonda et al, 1996; Wilson et al, 1994).

Initiator caspases are activated by a mechanism called scaffold-mediated activation. This process involves assembly of a molecular platform in response to death stimuli followed by recruitment of procaspases. The net result is an increase in the local concentration and/or conformation change in the initiator procaspases, creating a microenvironment in which the zymogens can process each other efficiently to yield fully active caspases (Yamin et al, 1996). It has been demonstrated that forced

Figure 5. Caspase Activation

All caspases, produced in cells as catalytically inactive zymogens, are activated by proteolytic cleavage of two Asp-X bonds, one separating the large and small subdomains (cleavage 1) and another separating the prodomain from the large subunit (cleavage 2). All caspases contain a conserved pentapeptide QACXG in their active (17 kDa, large) subunit. Each active caspase is derived from the processing and self-association of two procaspase zymogens. The tetrameric active enzyme contains two active sites at opposite ends of the molecule.

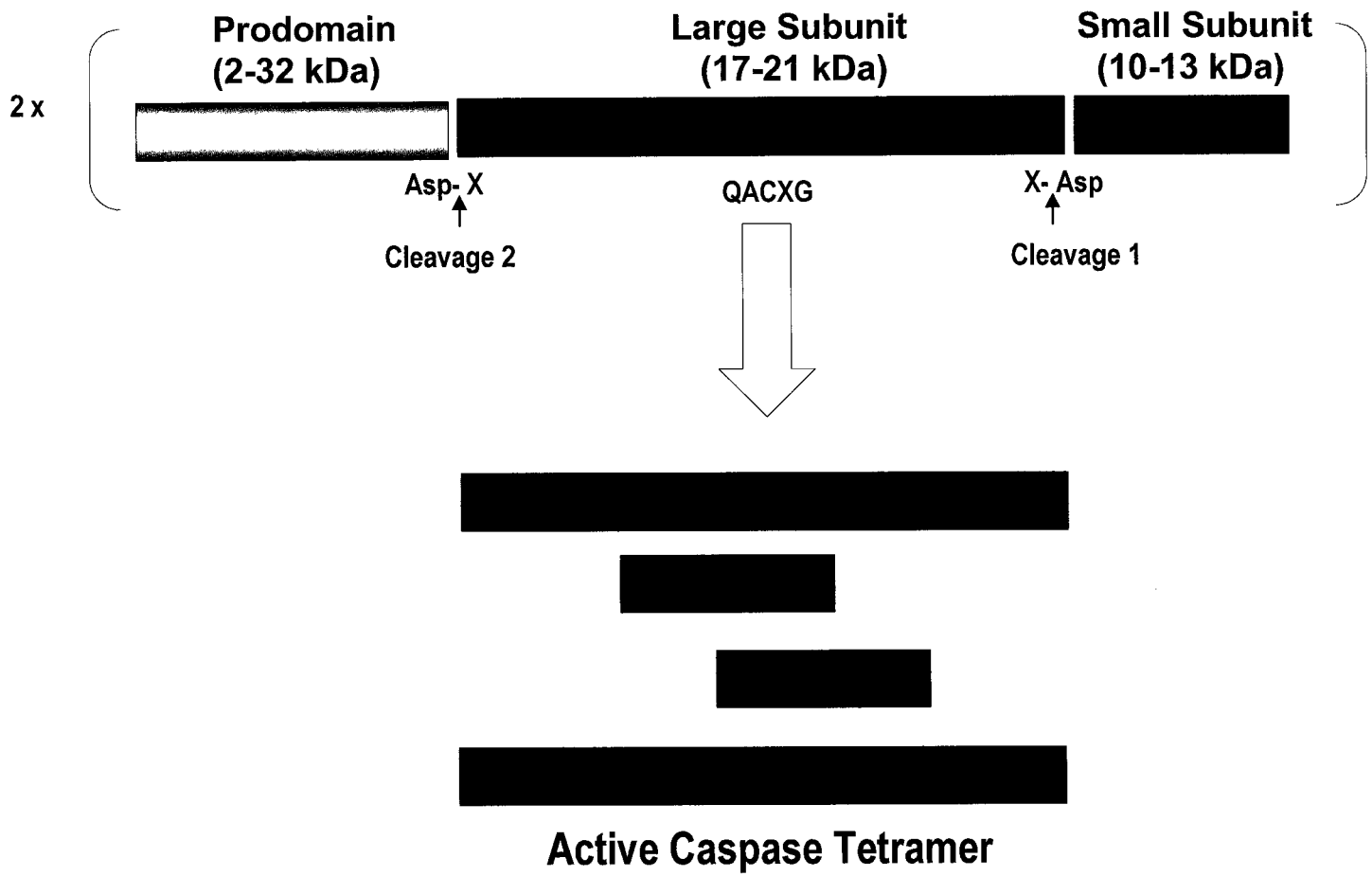
Procaspase Zymogen (32-56 kDa)
2 x
Prodomain
(2-32 kDa)
Large Subunit
(17-21 kDa)
Small Subunit
(10-13 kDa)
Asp- X
QACXG
X- Asp
Cleavage 2
Cleavage 1
Active Caspase Tetramer

Fig. 5

oligomerization of procaspase-8 and -9 by the adaptor proteins FADD and APAF-1, respectively, facilitate zymogen autoactivation and promote apoptosis (Muzio et al, 1998; Martin et al, 1998; Yang et al, 1998). This process may confine the mobility of the zymogen, resulting in increased local enzyme concentration and promoting autoactivation. Caspase-activation by non-caspase proteases (e.g. granzyme B) represents another mechanism for activation (Stennicke et al, 1998; Zhou et al, 1997). It has been demonstrated that initiator caspases are capable of efficient activation of effector caspases (Srinivasula et al, 1998; Deveraux et al, 1998).

8.5.3 Regulation of Caspase Activity

Given the potentially significant effect of caspase activation in the life and death decision of the cell, it is not surprising that caspase activation is tightly regulated. Regulation of caspase activity occurs at several levels: 1) Transcriptional regulation; 2) Regulation of death receptor-induced activation; 3) Regulation of the cytochrome c-Apaf1 pathway by BCL-2 family members; 4) Regulation by IAP proteins and 5) Post-translational modification.

Several observations suggest that transcriptional regulation of pro-caspase gene expression might be important in regulation of apoptosis (Krajewska et al, 1997; Ni et al, 1997; Chen et al, 2001). For example, procaspase-3 is present at high levels in many lymphoid and mature myeloid cells but it is present at low levels in breast epithelium and

normal neurons (Krajewska et al, 1997). One factor that influences pro-caspase gene expression is γ-interferon. Treatment of human U937 leukemia cells with γ-interferon can enhance caspase expression and susceptibility to apoptosis (Tamura et al, 1996). In contrast, cells lacking the interferon-responsive transcription factors display diminished steady-state levels of pro-caspase 1, 2, and 3 mRNA and diminished apoptotic responses to certain signals (Tamura et al, 1996; Kumar et al, 1997).

Activation of caspase zymogens by death receptor-associated scaffolds can be regulated by a polypeptide FLIP/I-FLICE (Inohara et al, 1997). FLIP (Fas-associated death domain-like interleukin-1-beta-converting enzyme-inhibitory protein), which contains DEDs, bind the prodomains of procaspase-8 and 10, thereby inhibiting their recruitment to Fas- and TNFR1-induced activation complexes (Irmler et al, 1997; Srinivasula et al, 1997). In the activation of procaspase-9 by the Apaf1, the cytochrome c scaffold appears to be regulated by anti-apoptotic Bcl-2 family members. Bcl-2 and Bcl-X_L, which are localized predominantly in the outer mitochondrial membranes, can inhibit mitochondrial cytochrome c release (Yang et al, 1997; Kim et al, 1997). In addition Bcl-X_L has been shown to inhibit the formation of Apaf-1-procaspase-9 complexes and subsequent zymogen activation (Hu et al, 1998).

Caspase activity can also be regulated by interactions with IAP proteins. XIAP, cIAP-1 and -2 bind to and inhibit caspase-3 and -7 at subnanomolar (XIAP) to submicromolar (cIAP-1 and -2) concentrations (Deveraux et al, 1997; Roy et al, 1997). They also bind to procaspase-9 and prevent its activation (Deveraux et al, 1998).

Moreover, active caspases also seem to be regulated by post-translational modification (Thome et al, 1998; Li et al, 1997). For example, nitrosylation of the active-site cystein of caspases by nitric oxide (NO) inhibits caspase activation (Kim et al, 1997; Mohr et al, 1997; Li et al, 1997).

8.5.4 Substrate Specificities of Caspases

All caspases recognize at least four contiguous amino acids in their substrates, named P4-P3-P2-P1, and hydrolyze peptide bonds on the carboxyl side of P1 (usually an aspartate). P1 is buried in a deep pocket of caspases, termed the S1 subsite, which is lined by Arg 179, Gln 283, Arg 341 and Ser 347 (Caspase-1 numbering). The S1 subsite is conserved in all human caspases except caspase-8 where Ser 347 is replaced by a Thr (Sleath et al, 1990; Howard et al, 1991). The two residues next to the amino acid of P1 (termed P2 and P3) have a limited effect on substrate cleavage, presumably because their side chains point away from the body of the enzyme (Rotanda et al, 1996; Sleath et al, 1990; Howard et al, 1991). In contrast, the residue P4 (three upstream from the P1 aspartate towards the N-terminus of the protein/peptide) and the S4 subsite to which it binds appear to account for the distinct substrate specificities of caspase-1 and -3 subfamilies. In caspase-1, the S4 subsite is a large, shallow hydrophobic depression that easily accommodates bulky hydrophobic side chains. In caspase-3, this subsite consists of a rather narrow hydrophilic pocket that can accommodate small acidic side chains but excludes bulky side chains (Rotanda et al, 1996). Another structural characteristic that contributes to the differences in the substrate specificity of these enzymes is the presence

or absence of a flap-like loop that projects over the active site (Rotanda et al, 1996). This flap is found in the caspase-3-like enzymes and could explain the failure of the caspases to cleave certain substrates despite the presence of consensus cleavage sites. Certain potential cleavage sites might fail to dock in the catalytic site because of steric hindrance by the flap. The flap is also a potential site for post-translational modifications. For example, phosphorylation could conceivably cause the flap to open or close further, thereby providing a potential regulatory mechanism (Martin et al, 1998).

Although the P1 residue was thought to be exclusively Asp, recent studies indicate that some caspases can also cleave after Glutamate (Glu, E) (Hawkins et al, 2000; Srinivasula et al, 2001). Recently, other amino acid sequences (non-consensus sequences) have been found to be targets of caspases [e.g. CQND and GELE sequences as targets of caspase-3 and -7, respectively (Haussermann et al, 1999; Ethell et al, 2001).

8.5.5 Caspase-3 (CPP32)

Caspase-3 (CPP32) acts as one of the central death executioners and is involved in virtually every model of apoptosis (Porter and Janicke, 1999). Using the DNA sequence encoding the active site of caspase-1 and CED-3 to search an expressed sequence tag (EST) database, a human sequence was identified, cloned, and shown to encode a 32 kDa cystein protease called CPP32 (Fernandes et al, 1994). Two other groups identified caspase-3 independently. One named it Yamma (the Hindu god of death) and the other apopain (Tewari et al, 1995; Nicholson et al, 1995). Using mass spectrometry (M.S.) and

N-terminal sequence analysis, the active enzyme was shown to be composed of two subunits (17 and 12 kDa) derived from the precursor protein by cleavage at Asp-28-Ser-29 and Asp-175-Ser-176 (Nicholson et al, 1995). The enzyme exhibits a large substrate diversity, as it cleaves a variety of proteins involved in cell maintenance or repair at the consensus DXXD, including poly (ADP-ribose) polymerase, p21-activated kinase-2, gelsolin, and DNA-dependent protein kinase (Nicholson et al, 1995; Liu et al, 1997; Enari et al, 1998). Moreover, survival factors like Bcl-2, Bcl-xl, and AKT are known to be cleaved by active caspase-3, leading to apoptosis. Recently non-consensus amino acid sequences (non-DXXD sequences) have been found to be the target of caspase-3 (Haussermann et al, 1999; Ethell et al, 2001). Some of the identified non-consensus sequences and their corresponding substrates are listed in Table 1.

8.6 Phosphorylation of Caspase-3 Substrates Influences Caspase-3-Mediated proteolysis

A few independent studies have shown that phosphorylation of caspase-3 substrates makes them more resistant to caspase-3-mediated proteolysis (Hoon et al, 2003; Barkette et al, 1997; Caulin et al 1997). Caspase-3-mediated cleavage of p130cas and the influence of phosphorylation were investigated in Rat-1 fibroblast cells (Hoon et al, 2003). Lysophosphatidic acid- and fibronectin-induced p130cas phosphorylation resulted in resistance to caspase-3-mediated cleavage. Cleavage of Keratin 18 (K18), another substrate of caspase-3, occurs sequentially following induction of apoptosis, first at the consensus sequence $DALD^{393}$ and then at the non-consensus sequence $VEVD^{234}$.

Table.1. Caspase-3 non consensus sequences identified to date.

The presence of a negative amino acid, either Aspartate (D) or Glutamate (E), is required at the P1 position of all the non-consensus cleavage sites. The residues at P2 and P3 are variable, whereas the P4 position is more specific as it only accommodates small side chain amino acids and excludes amino acids with bulky hydrophobic side chains.

Reported Caspase-3 non-consensus sequences to date	Substrate protein	Reference
TATD	N-terminal cytoplasmic domain of the human erythroid anion exchanger 1	Mandal et al 2003
EQGD	N-terminal cytoplasmic domain of the human erythroid anion exchanger 1	Mandal et al 2003
DFVE	Ventricular essential myosin light chain	Moretti et al 2002
AQVD	Human recombinase HsRad51	Flygare et al 2000
SALD	Scaffold attachment factor A	Kipp et al 2000
EEED	DNA topoisomerase I	Samejima et al 1999
VEVD	Keratin 18	Caulin et al 1997

Table 1

Hyperphosphorylation of K18 protects it from caspase-3-mediated cleavage at $VEVD^{234}$, but not at $DALD^{393}$ *in vitro*. Therefore, hyperphosphorylation, which occurs early in apoptosis, protects K18 from caspase-3-mediated K18 cleavage in a site-specific manner. Chicken and human IκB-α, also substrates of caspase-3, are cleaved at a conserved aspartate residue *in vitro* and *in vivo* (Barkette et al, 1997). Cleavage of IκB-α by this protease is also blocked by serine phosphorylation. On the contrary, it has been reported that caspase-3-mediated cleavage of STE-20-like kinase 2 (MST2), is positively regulated by phosphorylation. In this context, while truncated endogenous MST2 from apoptotic cells were highly phosphorylated, the full length protein from non-apoptotic or proliferating cells was not (Deng et al, 2003).

8.7 Significance of this work

Recent studies have shown that cisplatin induces caspase-3 activation and AKT cleavage in cisplatin-sensitive but not -resistant ovarian cancer cells. Incubation of ovarian cancer cell lysates with active human recombinant caspase-3 resulted in the cleavage of AKT, as observed in cells following cisplatin treatment (Sasaki et al, 2000; Asselin et al, 2001). Importantly, while down-regulation of Xiap expression by adenoviral anti-sense infection also induced caspase-3-mediated AKT cleavage, over-expression of Xiap suppressed AKT cleavage (induced by cisplatin) and increased phospho-AKT content (Asselin et al, 2001). Investigations into caspase-3 cleavage sites of Akt1 and influence of Akt1 phosphorylation status on this processing may provide

further insight into possible mechanism(s) by which chemoresistance may be conferred in human ovarian carcinoma.

9.0 HYPOTHESIS

Phosphorylation of Akt1 decreases its sensitivity to caspase-3-mediated cleavage.

10.0 OBJECTIVE

10.1 Overall Objective

The overall objective of my thesis research was to investigate the influence of Akt1 phosphorylation on caspase-3-mediated Akt1 cleavage.

10.2 Specific Objectives

My specific objectives were:

1. To investigate whether caspase-3 cleaves Akt1 at its consensus motif $DQDD^{456}$;

2. To investigate whether there are other caspase-3 motifs aside from $DQDD^{456}$ in Akt1;

3. To compare caspase-3-mediated cleavage of Akt1 with its phosphorylated counterpart at the potential cleavage sites.

11.0 MATERIALS

Antibodies including anti-Akt1 (sheep polyclonal IgG), anti-Akt (mouse monoclonal IgG), anti-Akt2 (rabbit polyclonal IgG), anti-His (mouse monoclonal IgG), rabbit anti-sheep IgG [horse radish peroxidase (HRP) conjugate], and human recombinant Akt1, Akt2 and Ak3 were purchased from Upstate (Lake Placid, NY). Anti-AKT (rabbit polyclonal IgG) and anti-Akt3 (rabbit polyclonal IgG) were purchased from Cell Signaling Technology®, Inc. (Beverly, MA, USA). Active recombinant human caspase-3 and -7 were purchased from Pharmingen (Mississauga, ON, Canada). The mass plates were purchased from Applied Biosystem (Foster City, Ca, USA). Ammonium persulfate, Tween 20, Trizma base, potassium carbonate, (N-[2-hydroxyethyl]piperazine-N ' -[2-ethane-sulfonic acid]) (HEPES), Imidazole, sodium hydroxide, (2-[N-morpholine]ethane-sulfonic acid) (MES), 3-[(3-Cholamidopropyl) dimethylammonio]-1-propanesulfonate (CHAPS), Piperazine-N,N'-bis(2-ethane-sulfonic acid) (PIPES), silver nitrate, formaldehyde, sodium acetate, N-Ethylmorpholine, benzamide hydrochloride hydrate, 7-amino-4-methylcoumarin (AMC), α-Cyano-4-hydroxycinnamic acid (CHCA), and sinapinic acid were purchased from Sigma Chemical Co (St. Louis Mo., USA). Ac-DEVD-AMC was purchased from BioSource International, Inc., (Camarillo, California, USA). Goat anti-rabbit and anti-mouse IgG HRP conjugate, acrylamide, N,N-methylene, bis-acrylamide, Tris, glycine, Trans-Blot® transfer medium, pure nitrocellulose and Poly (vinylidene flouride) (PVDF) membranes, Sypro® Ruby protein stain and prestained low range molecular weight markers were purchased

from Bio-Rad Laboratories (Mississauga, Ontario, Canada). Also, prestained and unstained protein markers were purchased from MBI Fermentas (Newington, NH, USA). Dithiothreitol (DTT) and Coomassie blue were obtained from Boehringer Mannheim (Montreal, Quebec, Canada). Enhanced chemiluminescence (ECL) kit was purchased from Amersham Life Sciences (Oakville, Ontario, Canada). Glycine was purchased from Roche Diagnostic (Laval, Quebec, Canada). Sodium thiosulfate pentahydrate, sodium dodecyl sulphate, bromophenol blue, sodium chloride, ethanol and sucrose were purchased from BDH (Toronto, Ontario, Canada). Methanol and glacial acetic acid were purchased from EM Sciences (Gibbstown, NJ, USA). TEMED was purchased from Invitrogen (Carlsbad, CA, USA). Zip Tip for desalting protein extracts and the Enzymatic CaroRelease Kit were purchased from Millipore© (Billerica, Massachusetts, U.S.A) and QA Bio (San Mateo, CA, USA), respectively.

12.0 METHODS

12.1 AKT Sequence Analysis and Molecular Mass Estimation of Akt1 Cleavage Fragments

Protein sequences of Human Akt1 (Genebank ®Accession # AAH00479), Akt2 (Genebank ®Accession # AY056465), and Akt3 (Genebank ®Accession NP035915), were obtained from NCBI. The theoretical size of the caspase-3-mediated Akt1 cleavage fragments were estimated using EXPASY (http://ca.expasy.org/sprot/sprot-top.html).

12.2 Caspase-3-Mediated Akt1 Cleavage Assays

12.2.1 Caspase-3 Activity Assay

Ac-DEVD-AMC fluorogenic substrate was incubated in the presence and absence of active human recombinant caspase-3 (200 ng) in a 96-well plate (flat-bottom type). The reactions were carried out at 37°C in PIPES assay buffer (20 mM PIPES, 100 mM NaCl, 2M DTT, 1 mM EDTA, 0.1% W/V CHAPS, and 10% W/V sucrose, pH 7.2). AMC liberated from caspase-3-mediated cleavage of Ac-DEVD-AMC was measured spectrofluorometrically with an excitation wavelength of 380 nm and emission wavelength range of 430-460 nm. The relative AMC fluorescence unit (RFU) was read at 3-seconds intervals over a 30-minute period (Fig. 6.B). Ac-DEVD-AMC in the absence of caspase-3 was used as negative control (Fig. 6.A).

Figure 6. Kinetics for caspase-3 activity

Ac-DEVD-AMC fluorogenic substrate was incubated in the absence (panel A) and presence (panel B) of active human recombinant caspase-3 (1h, 37°C, PIPES). The liberated AMC as a result of caspase-3-mediated cleavage of Ac-DEVD-AMC was measured spectrofluorometrically (excitation wavelength: 380 nm; emission wavelength: 430-460 nm) every three seconds to demonstrate the kinetics curve for activity of caspase-3 (panel B). Ac-DEVD-AMC in the absence of caspase-3 was used as negative control (panel A).

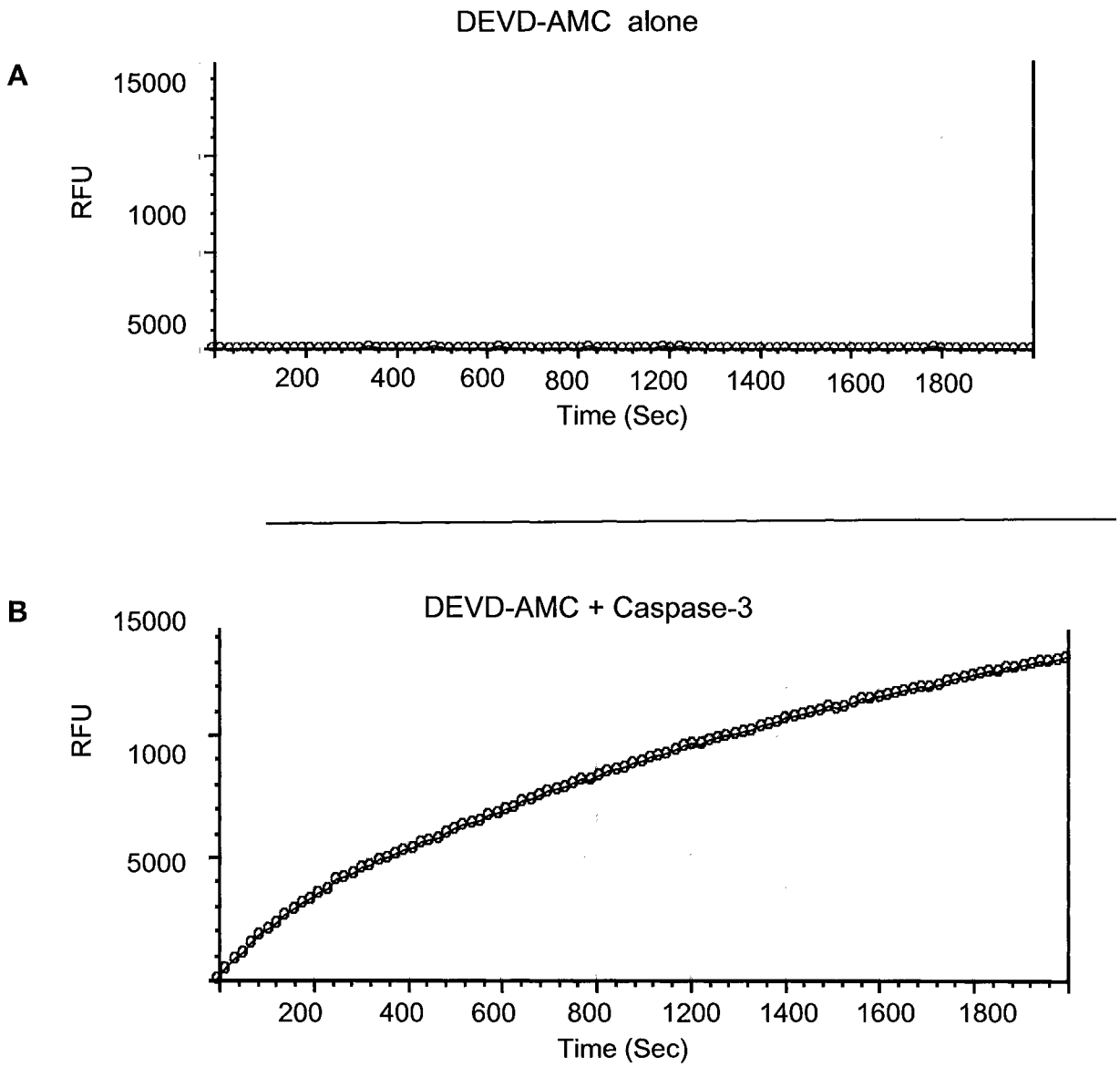
A
DEVD-AMC alone
15000
1000
5000
RFU
200
400
600
800
1200
1400
1600
1800
Time (Sec)
B
DEVD-AMC + Caspase-3
15000
1000
5000
RFU
200
400
600
800
1200
1400
1600
1800
Time (Sec)

Fig.6

12.2.2 AKT Cleavage Assay

Caspase-3-mediated AKT cleavage assay was carried out at 37°C in the absence and presence of the caspase inhibitor DEVD-CHO (20 pM) in PIPES assay buffer in a total reaction volume of 40 µl. The reactions were stopped by boiling for 5 minutes in 4X gel loading buffer (200 mM Tris.Cl, 400 mM DTT, 8% w/v SDS, 0.4% w/v bromophenol blue, 4% w/v Glycerol). In time course studies, human recombinant Akt1 (125 ng) was incubated with active human recombinant caspase-3 (40 ng, PIPES, pH 7.2) for different durations of incubation (0.5 - 4 h). In concentration–response studies, human recombinant Akt1 (125 ng) was incubated with various concentrations of active human recombinant caspase-3 (0 - 320 ng). Caspase-3-mediated Akt1 cleavage was assessed by immunoblotting with N-terminus anti-AKT, anti-His and C-terminus anti-Akt1 antibodies. To assess the pH dependence of the Akt1 cleavage assay, a ternary buffer (30 molar sodium acetate, 30 mM 2-[N-Morpholino] ethane sulfonic acid, 30 mM N-Ethylmorpholine) containing the ingredients required for full caspase-3 activity (100 mM NaCl, 10% sucrose, 10 mM DTT, and 0.1% CHAPS) was prepared. The buffer was adjusted to different pH values of 3, 4, 5, 6, and 7 and used in the Akt cleavage assay described above.

12.2.2.1 Caspase-3-Mediated Cleavage of Akt1, Akt2 and Akt3.

Akt1, Akt2 and Akt3 (125 ng each) were incubated with various concentrations of caspase-3 [0, 20, 40 and 80 ng in a total volume of 40 µl PIPES (pH 7.2); 2 h]. Proteins were resolved by SDS-PAGE and blotted with N-terminus anti-AKT (capable of detecting all the three isoforms, with highest affinity for Akt1), anti-Akt2 and anti-Akt3, and C-terminus anti-Akt1, anti-Akt2 and anti-Akt3 antibodies.

12.2.2.2 Akt1 Cleavage: Caspase-3 versus Caspase-7 and Influence of Phosphorylation

To compare the ability of Akt1 to serve as substrate for caspase-3 and caspase-7, Akt1 (125 ng) was incubated with various concentrations of active human recombinant caspase-3 and -7 [0 - 80 ng in a total volume of 40 µl of PIPES (pH 7); 2h]. Samples were analyzed by Western blotting, using N-terminus anti-AKT and C-terminus anti-Akt1 antibodies. In addition, Akt1 and phospho-Akt1 (125 ng each) were incubated with active human recombinant caspase-3 (0 - 160 ng, 2h, PIPES, pH 7.2). The samples were analyzed by Western blotting, using anti-Akt1 and anti-AKT antibodies that recognized both Akt1 and phospho-Akt1.

12.3 Western Blot Analysis

The reaction mixtures were resolved by SDS-PAGE on either small (7 cm × 9 cm) or large (20 cm × 20 cm) standard Laemmli gels (8 %, 10 %, 12 % or 15 %; Laemmli, 1970) for 2 h and 24 h, respectively. To achieve a better partition of the higher molecular

weight fragments, gels were run for 4 h (110 V; small gels; RT) or 36 – 48 h (90 V; large gels; 4° C). The proteins on the gel were then electrotransferred (30 V, 16 h or 110 V, 2h) onto nitrocellulose membranes which were then blocked (RT, 1 h) with TBS-T containing 5 % (w/v) skim milk powder and incubated (4° C, 16 h) with primary antibody (1: 2000) diluted in TBS-T and 5% (w/v) skim milk powder. The blots were then washed (3 × 5 min) with TBS-T, incubated with HRP-conjugated secondary antibody (1:2000) in TBS-T and 5 % (w/v) skim milk powder (RT, 1 h) and washed again in TBS-T (3 × 10 min) and in TBS (1 × 5 min). Peroxidase activity was visualized with ECL kit, following the manufacturer's instructions.

12.4 Protein Staining

12.4.1 Coommassie Blue Staining

Samples were resolved by SDS-PAGE as described previously. The proteins were electrotransferred (110 v, 1 h) onto PVDF membranes in 3-(cyclohexylamino)-1-propanesulfonic acid (CAPS) buffer. The membranes were rinsed in water, saturated with 100 % methanol for a few seconds and stained with the coomassie blue (0.1 % Coomassie blue 250, 40 % methanol, 1% acetic acid) for 5 minutes. The proteins were de-stained in 50 % methanol with 1 % acetic acid; 3 × 5 min) and washed with distilled water (2 X 5 min).

12.4.2 Silver Staining

Samples were resolved on SDS-PAGE as discussed earlier. The gels were fixed in 5 % acetic acid / 30 % ethanol (2 × 30 min), washed in water (5 × 5 min), sensitized in 0.02% sodium thiosulfate pentahydrate (1 x 1 min) and washed in water (2 × 1 min). The gels were incubated in 0.2 % silver nitrate for 2 h in a glass container, washed with water (2 × 1 min), and developed in a solution containing 4 % potassium carbonate, 0.025 % (v/v) formalin, 0.0125 % sodium thiosulfate pentahydrate (8-20 min). The reactions were stopped by washing the gel first in a 4 % Tris with 2 % acetic acid, and then in water (2 × 1 min). The gels were preserved in 30 % ethanol and 4 % acetic acid (2 × 30 min). All reagents were prepared fresh at room temperature.

12.4.3 Sypro Ruby Staining

Following SDS-PAGE, the gels were fixed in 10 % methanol containing 7 % acetic acid (30 min) in a polypropylene plastic staining container, stained with Sypro Ruby with continuous agitation for 3, 6, 12 or 18 h and washed for 60 min in a fixing solution (10 % methanol, 7 % acetic acid). To minimize background florescence, the gels were further rinsed (30-120 min) in the fixing solution and subsequently with water prior to imaging with a UV transilluminator (300 nm).

12.5 Molecular Mass Estimation of the Novel Fragments

The molecular mass of Akt1 and its caspase-3-mediated cleavage fragments were estimated by comparing their mobility with those of the protein standards on SDS-PAGE. The gels used for these studies were silver-stained as in section 12.4.2. Ratio of fonts (R_f) were measured according to the equation R_f = *distance migrated by protein/ distance migrated by dye*, in which the dye used was that of the sample buffer. Distance of migration of the sample or dye was measured with the AlphaImager (Alpha Innotech, San Leandro, CA, USA). With the R_f values determined, the molecular mass of the unknown peptides were calculated using the Excel Spread Sheets (Invitrogen).

12.6 Mass Spectrometry: Matrix-assisted Laser Desorption Time-of-flight Mass Spectrometry (MALDI-TOF M.S.) and Surface Enhanced Laser Desorption-Ionization Mass Spectrometry (SELDI M.S.)

For Delayed Extraction Matrix-assisted Laser Desorption Time-of-flight Mass Spectrometry (MALDI-M.S.) analysis of the Akt1 cleavage fragments, Akt1 and phospho-Akt1 (1 μg each) were incubated (6 h; 37°C) with active human recombinant caspase-3 (0.5 μg) in 10 μl of PIPES assay buffer. The reactions were stopped by the addition of 1μl of glacial acetic acid. 4 μl of the samples (2 x 2 μl) were spotted on the mass plates, and allowed to dry at room temperature. The matrix (sinapinic acid or CHCA) was added before analyzing the plates. Albumin was used as a calibrant.

Samples were de-salted using ZIP-Tip columns, which were activated with 10 µl of 50% acetonitrile (ACN/CH_3CN; five times) and equilibrated in 10 µl of 0.1 % TFA/H_20 (10 times). 10 µl of samples were loaded and the tips were washed with 10 µl 0.1% TFA/H_2O (10 times). The protein was eluted ten times with 10 µl 80 % acetonitrile (CAN/CH_3CN) and the elutes (100 µl total volume) were lyophilized using a Speed-Vac. The crystal was redissolved in 5 µl 3 % TFA/H_2O and applied onto the M.S. plate.

Samples for Surface Enhanced Laser Desorption-Ionization Mass Spectrometry (SELDI M.S.) were prepared as for MALDI-TOF M.S. but with the following modifications: The plates were washed with distilled water after the protein was crystallized on the plates, in order to remove excess salt and impurities. One advantage of this technique is the binding of a protein of interest to the chemical or biological docking sites on the array surface through an affinity interaction, allowing proteins that bind non-specifically and buffer contaminant to be washed away, and thus eliminating sample noise. Caspase-3-mediated Akt1 digests were applied to a normal phase protein chip, followed by washing with distilled water. Reaction mixtures were subjected to SELDI-M.S. analysis as described in "The ProteinChip ß-Amyloid Multipeptide Kit (CIPHERGEN). The data was analyzed for the molecular mass of the Akt1 fragments generated following proteolysis by caspase-3. Caspase-3-alone was incubated for the same duration to eliminate presence of bands detected in the samples as a result of caspase-3 autocatalysis.

12.7 Deglycosylation assay

Phospho-Akt1 (1 μg) was incubated with active human recombinant caspase-3 (0.8 μg, 16 h, 37°C, PIPES), and subsequently with the deglycosylation reagents (Enzymatic carbo-release kit) according to the manufacturer's instructions (QA Bio, San Mateo, CA, USA). Bovine Fetuin was used as positive control. Samples were resolved by SDS-PAGE. The gels were either silver- or Sypro Ruby-stained. Degree of deglycosylation was determined by a shift in the molecular weight of the fragments on the gel.

13.0 RESULTS

13.1 Sequence Analysis of Akt1

Human Akt1 protein sequence obtained from NCBI (Genebank® Accession # AAH00479) revealed the presence of a caspase-3-consensus sequence $DQDD^{456}$ (Fig. 7.A). Since the molecular mass of the protein is 55.7 kDa, an N-terminus fragment of 53.0 kDa and a C-terminus fragment of 2.7 kDa were expected to result from caspase-3-mediated Akt1 cleavage at this site. The recombinant Akt1 used in these studies was a fusion protein with a His-tagged peptide at its N-terminus (Fig. 7.B); the molecular mass of the recombinant Akt1 was therefore calculated to be 59 kDa, yielding two fragments of 2.7 and 56.3 kDa upon cleavage at $DQDD^{456}$.

13.2 Possibility of Caspase-3-Mediated Akt1 Cleavage at $DQDD^{456}$

To determine the possibility of caspase-3-mediated Akt1 cleavage at the consensus cleavage site $DQDD^{456}$, human recombinant Akt1 was incubated in the presence of different concentrations of active human recombinant caspase-3 and for different durations of incubation (PIPES; pH 7.0; 37° C). The specific activity of the caspase-3 was measured as described in the Materials and Methods section prior to setting the incubations (Fig. 6). Since we first aimed at detecting the smaller C-terminus 2.7 kDa fraction, samples were resolved on high percentage (15 %) SDS-PAGE gels and probed with a C-terminus anti-Akt1 antibody with an epitope residing at amino acid (aa) 464 to 478 (Fig. 7.A). An anticipated band of 2.7 kDa implying

Figure 7. Human Akt1 amino acid (aa) sequence.

Panel A: Human Akt1 sequence. Akt1 is a 55.7 kDa protein, which contains a caspase-3-binding motif at aa 453-456 ($DQDD^{456}$). Theoretically caspase-3-mediated cleavage of Akt1 at this site gives rise to two fragments of 2.7 (aa 457-480) and 53.0 kDa (aa 1-456). The areas highlighted in blue (aa 1-140) and green (aa 466-480) indicate the epitope for the N-terminus AKT and C-terminus Akt1 antibodies, respectively.

Panel B: Recombinant human Akt1 sequence. The recombinant Akt1 used in these studies was a fusion protein having a His-tagged peptide at its N-terminus (aa 1-28), therefore the molecular mass of the recombinant human Akt1 was calculated to be 59 kDa, yielding two fragments of 2.7 and 56.3 kDa upon cleavage at $DQDD^{481}$.

A

1	MSDVAIVKEG	WLHKRGEYIK	TWRPRYFLLK	NDGTFIGY KE	RPQDVDQREA	PLNNFSVAQC
61	QLMKTERPRP	NTFIIRCLQW	TTVIERTFHV	ETPEEREEWT	TAIQTVADGL	KKQEEEEMDF
121	RSGSPSDNSG	AEEMEVSLAK	PKHRVTMNEF	EYLKLLGKGT	FGKVILVKEK	ATGRYYAMKI
181	LKKEVIVAKD	EVAHTLTENR	VLQNSRHPFL	TALKYSFQTH	DRLCFVMEYA	NGGELFFHLS
241	RERVFSEDRA	RFYGAEIVSA	LDYLHSEKNV	VYRDLKLENL	MLDKDGHIKIT	DFGLCKEGI
301	KDGATMKTFC	GTPEYLAPEV	LEDNDYGRAV	DWWGLGVVMY	EMMCGRLPFY	NQDHEKLFEL
361	ILMEEIRFPR	TLGPEAKSLL	SG LLKKDPKQ	RLGGGSEDAK	EIMQHRFFAG	IVWQHVYEKK
421	LSPPFKPQVT	SETDTRYFDE	EFTAQMITIT	PP**DQDD**SMEC	VDSERRPHFP	QFSYSASSTA

▲

B

1	MSFFHHHHHH	DFDIPTTENL	YFQGAMGSMS	DVAIVKEGWL	HKRGEYIKTW	RPRYFLLKND
61	GTFIGY KERP	QDVDQREAPL	NNFSVAQCQL	MKTERPRPNT	FIIRCLQWTT	VIERTFHVET
121	PEEREEWTTA	IQTVADGLKK	QEEEEMDFRS	GSPSDNSGAE	EMEVSLAKPK	HRVTMNEFEY
181	LKLLGKGTFG	KVILVKEKAT	GRYYAMKILK	KEVIVAKDEV	AHTLTENRVL	QNSRHPFLTA
241	LKYSFQTHDR	LCFVMEYANG	GELFFHLSRE	RVFSEDRARF	YGAEIVSALD	YLHSEKNVVY
301	RDLKLENLML	DKDGHIKITD F	GLCKEGIKD	GATMKTFCGT	PEYLAPEVLE	DNDYGRAVDW
361	WGLGVVMYEM	MCGRLPFYNQ	DHEKLFELIL	MEEIRFPRTL	GPEAKSLLSG	LLKKDPKQRL
421	GGGSEDAKEI	MQHRFFAGIV	WQHVYEKKLS	PPFKPQVTSE	TDTRYFDEEF	TAQMITITPP
481	DQDDSMECVD	SERRPHFPQF	SYSASGTA			

Fig. 7

cleavage at $DQDD^{456}$ was not detectable, despite of the detection of a novel band of ~43 kDa (termed band A henceforth) in concentration-response and time course studies (Fig. 8.A & 8.B, respectively, n = 5). In order to gain a better partition of band A from the intact Akt1, the experiments were replicated and resolved on 10% SDS-PAGE gels (Fig. 8.C & 8.D, n = 10).

It has been demonstrated that the optimal pH required for the full activity of recombinant caspase-3 is 7.4 (Thornberry et al 1997). Thornberry and colleagues performed the caspase-3-cleavage assays for a small peptide (Z-DEVD-AFC) at the pH range of 5.5-10. Moreover, they used different buffers for each pH point. Akt1 is a big protein, with a molecular mass of 59 kDa. We investigated influence of pH on caspase-3-mediated Akt1 cleavage for the pH range of 3-7. In order to abolish the possible confounding effects of different salts on caspase activity, a ternary buffer (30 M sodium acetate, 30 mM 2-[N-Morpholino]) ethane sulfonic acid, 30 mM N-Ethylmorpholine) able to accommodate the reaction within a pH of 3-8 was designed. Human recombinant Akt1 was incubated in the absence and presence of active human recombinant caspase-3 at pH 3, 4, 5, 6, and 7. Incubation of Akt1 in the absence of caspase-3 at each pH point was used as negative control to eliminate any bands which may have resulted from pH-dependent degradation. The samples were analyzed by 15 % SDS-PAGE gels using the C-terminus anti-Akt1 antibody. A band of 2.7 kDa (implying cleavage at $DQDD^{456}$) was not detectable at any of the pH points although maximal intensity of band A was detected at pH 6 and 7 in the presence of caspase-3 (Fig. 9).

Figure 8. Concentration-response and time course studies for caspase-3-mediated-Akt1 cleavage: Presence of the first novel band (Band A) was detected in the process of investigating the 2.7 kDa fragment.

Human recombinant Akt1 (125 ng) was incubated with increasing concentrations of active human recombinant caspase-3 (0, 40, 80, and 160 ng, PIPES, 2h, 37°C, panel A & C) and for different durations (0.5, 1, 2 and 4h, PIPES, 37°C, panel B & D). Samples were resolved on 15 % (panels A & B) and 10 % (panels C & D) SDS-PAGE, followed by immunoblotting with a C-terminus anti-Akt1 antibody. Each figure shows a representative membrane of 5-10 experiments.

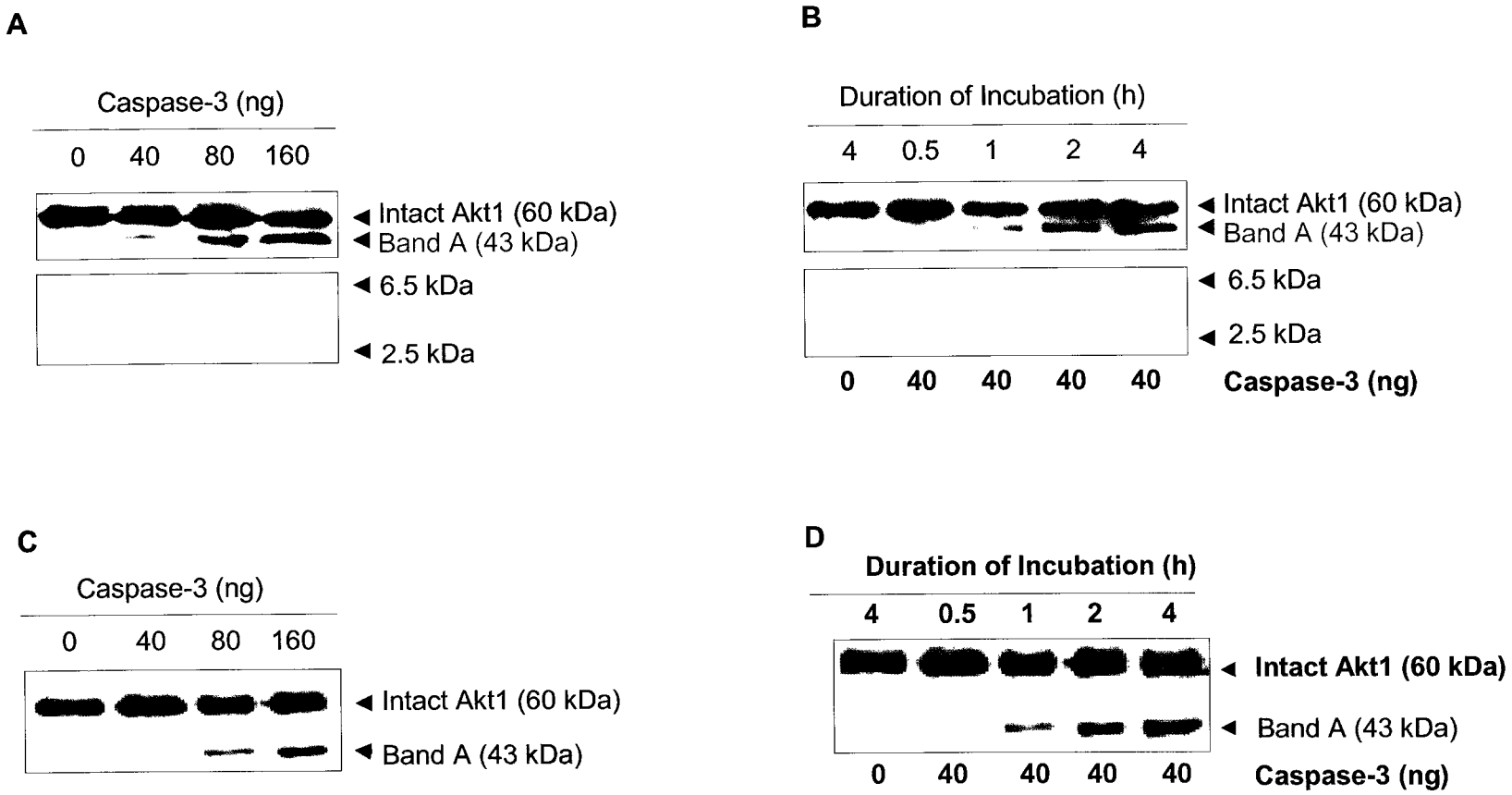
A
Caspase-3 (ng)
0 40 80 160
Intact Akt1 (60 kDa)
Band A (43 kDa)
6.5 kDa
2.5 kDa
B
Duration of Incubation (h)
4 0.5 1 2 4
Intact Akt1 (60 kDa)
Band A (43 kDa)
6.5 kDa
2.5 kDa
0 40 40 40 40
Caspase-3 (ng)
C
Caspase-3 (ng)
0 40 80 160
Intact Akt1 (60 kDa)
Band A (43 kDa)
D
Duration of Incubation (h)
4 0.5 1 2 4
Intact Akt1 (60 kDa)
Band A (43 kDa)
0 40 40 40 40
Caspase-3 (ng)

Fig. 8

Figure 9. pH dependence of caspase-3-mediated Akt1 cleavage.

Human recombinant Akt1 (125 ng) was incubated in the absence and presence of active human recombinant caspase-3 at pH 3, 4, 5, 6 and 7 (4h, 37°C, ternary buffer). Samples were analyzed by Western blot, using a C-terminus anti-Akt1 antibody. This blot is representative of three experiments.

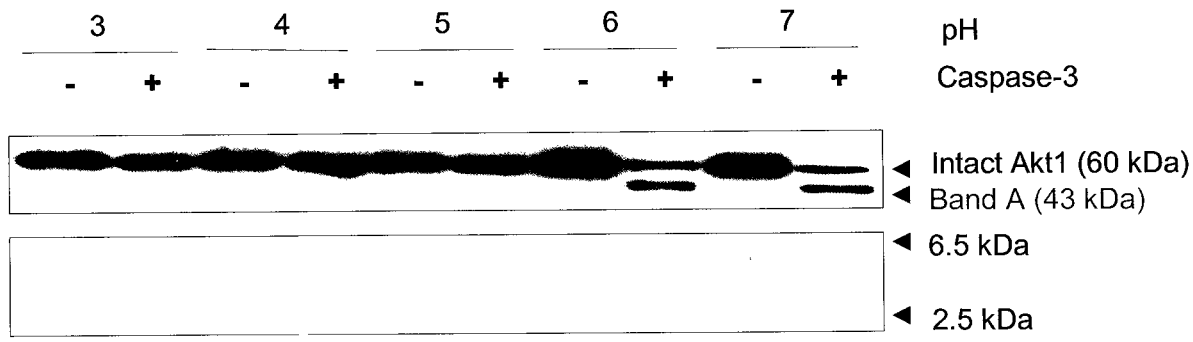
3
4
5
6
7
pH
- + - + - + - + - +
Caspase-3
Intact Akt1 (60 kDa)
Band A (43 kDa)
6.5 kDa
2.5 kDa

Fig. 9

To further assess the possibility of cleavage at $DQDD^{456}$, we aimed at detecting the big 56.3 kDa N-terminus fraction by Western analysis following incubation of human recombinant Akt1 with increasing concentrations of active human recombinant caspase-3 and for different durations of incubation, using N-terminus anti-AKT (epitope at aa 1 to 140, Fig. 7.A) and anti-His (epitope at aa 5-10, Fig. 7. B) antibodies. The presence of a band (hereafter called band C, ~ 57 kDa) was detected with an anti-His antibody, implying cleavage at $DQDD^{456}$ (Fig. 10.B). The intensity of band C increased with increasing concentrations of caspase-3 and was accompanied by a corresponding decrease in the intensity of Akt1. Moreover, a novel band of ~51 kDa (henceforth named band B) was detected with the N-terminus anti-His antibody (Fig. 10.A and 10.B).

Human recombinant Akt1 was incubated with higher concentrations of active human recombinant caspase-3 (0, 40, 80, and 160 ng, Fig.10.C) and for different durations of incubation (0, 0.5, 1, 2 and 4h, 80ng caspase-3, PIPES, 37° C, Fig. 10.D). Samples were subject to Western blot analysis. Due to close proximity of band C (57 kDa) to the intact Akt1 (59 kDa), the gels were over-run at 110V (i.e. 4 h as opposed to 2 h). An N-terminus anti-AKT antibody capable of detecting Akt1 and all the N-terminus Akt1 fragments was used for these blots (Fig.10.C and 10.D). Both experiments were replicated (n = 3) and the results indicated a similar trend for band B and C, as observed in figures 10.A and 10.B. Incubation of human recombinant Akt1 with caspase-3 in the presence of a caspase-3-inhibitor (DEVD-CHO), resulted in the

Figure 10. Concentration-response and time course studies for caspase-3-mediated Akt1 cleavage: Presence of the second novel band (Band B) was detected in the process of investigating the 57 kDa fragment.

Human recombinant Akt1 (125 ng) was incubated with various concentrations of active human recombinant caspase-3 (0, 10, 20, 40 ng, panel A & B; 0, 40, 80, and 160 ng, Panel C; 37˚C , PIPES, 2h) and for different durations of incubation (0.5, 1, 2, and 4 h, 37˚C , PIPES, panel D). Samples were resolved on 10 % SDS-PAGE (110v, 2.5 h, panels A & B; 110 v, 4.5 h, panels C & D), followed by immunoblotting with either an anti-His antibody (panels A & B) or an N-terminus anti-AKT antibody (panels C & D) to analyze the cleavage fragments. Panels A and B reflect the same blot with film exposed for 60 and 5 seconds, respectively. All figures show representative membranes of 3 experiments.

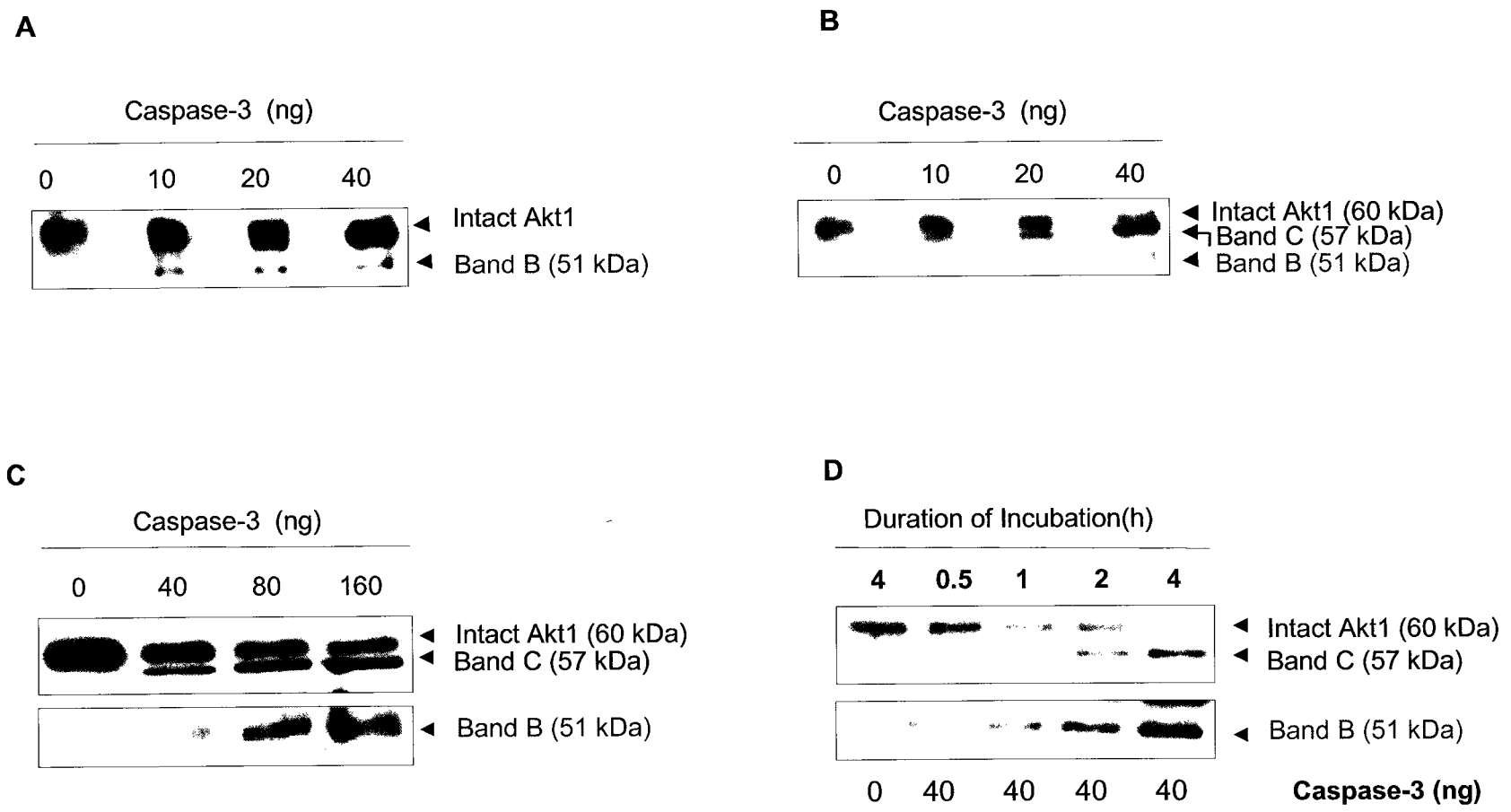
A
Caspase-3 (ng)
0
10
20
40
Intact Akt1
Band B (51 kDa)
B
Caspase-3 (ng)
0
10
20
40
Intact Akt1 (60 kDa)
Band C (57 kDa)
Band B (51 kDa)
C
Caspase-3 (ng)
0
40
80
160
Intact Akt1 (60 kDa)
Band C (57 kDa)
Band B (51 kDa)
D
Duration of Incubation(h)
4
0.5
1
2
4
Intact Akt1 (60 kDa)
Band C (57 kDa)
Band B (51 kDa)
0
40
40
40
40
Caspase-3 (ng)

Fig. 10

complete disappearance of band C (57 kDa) supporting the contention that the 57 kDa fragment is produced by caspase-3-mediated cleavage of Akt1 (Fig. 11).

Moreover, analysis of the caspase-3-mediated Akt1 cleavage assays by the Surface-Enhanced-Laser-Desorption-Ionization (SELDI) mass spectrometry (M.S.) revealed a very strong peak with a molecular mass of 2.7 kDa (Fig. 23; the result is described in section 13.9) This data supports the notion that caspase-3 cleaves Akt1 at the consensus $DQDD^{456}$.

13.3 At least Two Novel Caspase-3-Cleavage Sites are Present in Akt1

In the process of analyzing caspase-3-mediated Akt1 cleavage at $DQDD^{456}$, two additional bands were observed by SDS-PAGE, suggesting the possibility of Akt1 cleavage by caspase-3 at non-consensus (non-DXXD) motives.

The first novel band (band A) was detected in concentration-response and time course studies in which human recombinant Akt1 was incubated with active human recombinant caspase-3 and immunoblotted with a C-terminus anti-Akt1 antibody. The band intensified with increasing concentration of caspase-3 and duration of incubation (Fig. 8) and was completely eliminated in the presence of 20 pM of caspase-3 inhibitor (DEVD-CHO, Fig. 12.A), supporting the notion that band A is a cleaved Akt1 fragment produced by caspase-3 at the non-consensus motif A.

Figure 11. Appearance of Band C (57 kDa) is suppressed when human recombinant Akt1 was incubated with active human recombinant caspase-3 in the presence of a caspase-3 inhibitor.

Human recombinant Akt1 (125 ng) was incubated with active human recombinant caspase-3 (50 ng), in the absence and presence of 20 or 40 pM of the caspase-3 inhibitor DEVD-CHO or 0.09 % DMSO (vehicle control) at 37°C (PIPES, 2 h). Samples were resolved on 10% SDS-PAGE (110 v, 4.5 h) followed by immunoblotting with an N-terminus anti-Akt antibody. Figures show representative membranes of three experiments.

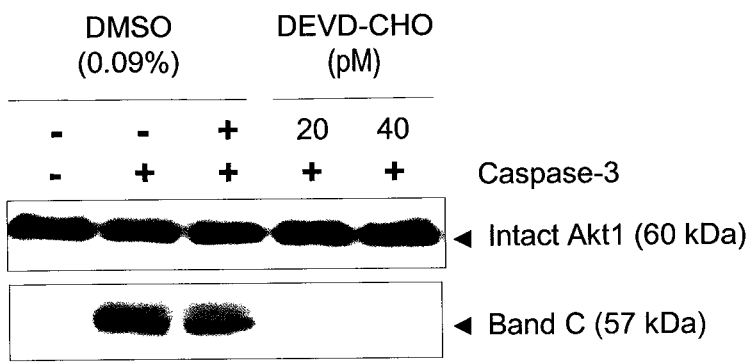
DMSO
(0.09%)
DEVD-CHO
(pM)
- - + 20 40
- + + + +
Caspase-3
Intact Akt1 (60 kDa)
Band C (57 kDa)

Fig. 11

The second novel band (band B) identified earlier with both N-terminus anti-His and anti-AKT antibodies (Fig. 10) was further investigated in the presence of a caspase-3-inhibitor (DEVD-CHO), following human recombinant Akt1 incubation with active human recombinant caspase-3. Band B was entirely blocked in the presence of 20 pM of DEVD-CHO (Fig. 12.B), thus supporting the notion that it is a cleaved Akt1 fragment produced by caspase-3, also at a non-consensus motif B.

13.4 Influence of Akt1 Phosphorylation on its Cleavage by Caspase-3 at the two Novel Cleavage Sites

Evidence suggests that phosphorylation of caspase-3 substrates can modulate its sensitivity to caspase-3-mediated cleavage in a site-specific manner (Ku et al, 2001). Since we demonstrated the presence of two novel caspase-3 cleavage sites in Akt1, we were interested in determining how Akt1 phosphorylation influences its cleavage at each site. This objective was to compare the relative ability of human recombinant Akt1 and its phosphorylated counterpart (p-Akt1) to serve as substrate for active human recombinant caspase-3 in concentration-response (Fig. 13) and time course studies (Fig. 14) by Western blot analysis, using both C-terminus anti-Akt1 and N-terminus anti-AKT antibodies. Our results clearly show that the amount of Akt1 and p-Akt1 cleavage

Figure 12. The novel cleavage bands (A and B) are absent when Akt1 was incubated with active caspase-3 and its inhibitor.

Human recombinant Akt1 (125 ng) was incubated with active human recombinant caspase-3 (50 ng) in the absence and presence of a caspase-3 inhibitor (DEVD-CHO, 20 and 40 pM) or 0.09 % DMSO (vehicle control). Samples were analyzed by Western blot, using a C-terminus anti-Akt1 antibody (panel A) or an N-terminus anti-AKT antibody (panel B). Each figure is a representative of 3 experiments.

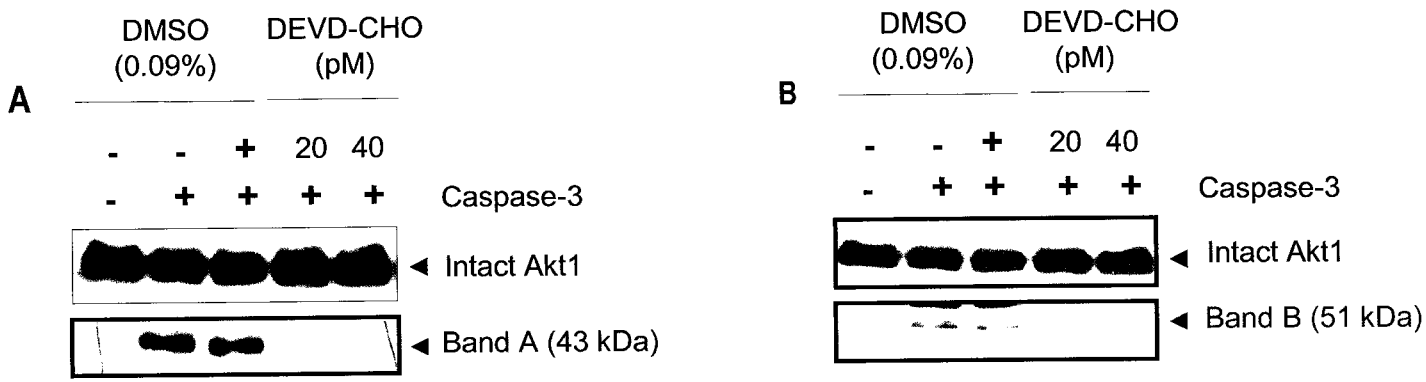
A
DMSO
(0.09%)
DEVD-CHO
(pM)
- - + 20 40
- + + + + Caspase-3
Intact Akt1
Band A (43 kDa)
B
DMSO
(0.09%)
DEVD-CHO
(pM)
- - + 20 40
- + + + + Caspase-3
Intact Akt1
Band B (51 kDa)

Fig. 12

Figure 13. Concentration-response studies on the effect of caspase-3 on cleavage of Akt1 and phospho-Akt1

Human recombinant Akt1 and phospho-Akt1 (125 ng each) were incubated with various concentrations of human recombinant caspase-3 (2 h, 37° C; 0, 10, 20, 40 ng in panel A and 0, 40, 80, 160 ng in panels B and C). Samples were analyzed by Western blot, using a C-terminus anti-Akt1 (panel A) or an N-terminus anti-AKT (panels B & C) antibody capable of detecting Akt1, phospho-Akt1 and their C- and N-terminus cleavage fragments, respectively. Panel B and C represent the same blot with film exposed for 60 and 5 seconds, respectively. Panel A shows representative blots of 5 experiments. Panel B and C is representative of two experiments. P, Phospho-Akt1; A, Akt1.

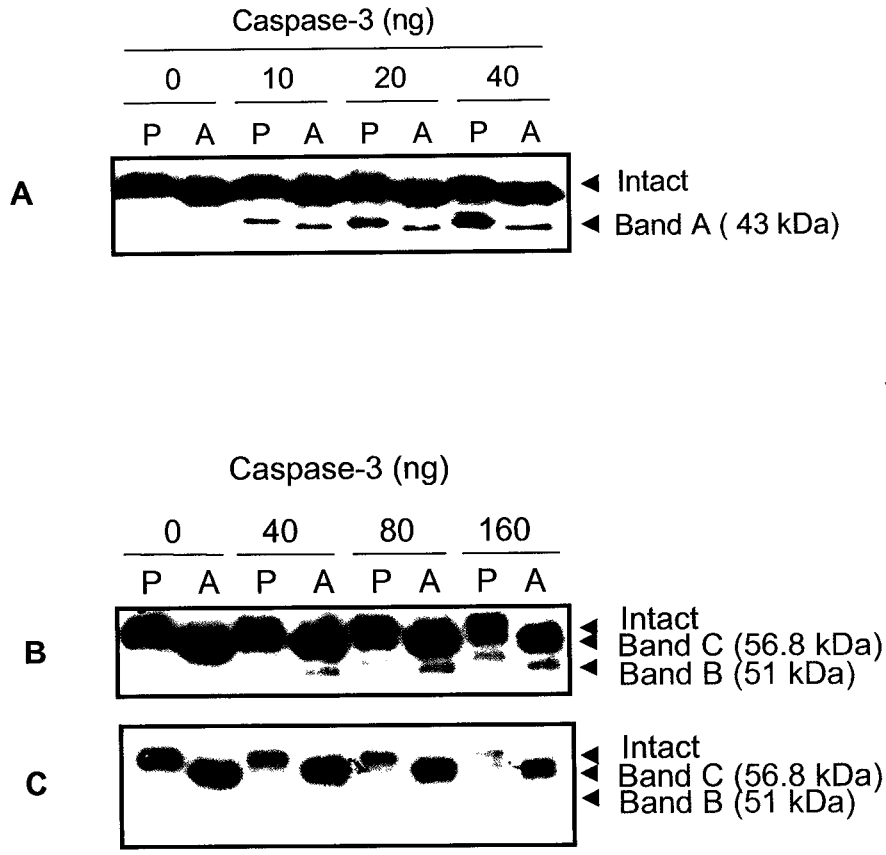
Caspase-3 (ng)
0
10
20
40
P A P A P A P A
A
Intact
Band A (43 kDa)
Caspase-3 (ng)
0
40
80
160
P A P A P A P A
B
Intact
Band C (56.8 kDa)
Band B (51 kDa)
C
Intact
Band C (56.8 kDa)
Band B (51 kDa)

Fig.13

Figure 14. Time course studies on the effect of caspase-3 on Akt1 and phospho-Akt1

Human recombinant Akt1 and phospho-Akt1 (125 ng each) were incubated with active human recombinant caspase-3 (40 ng) for 0.5, 1, 2 and 4 h (37° C, PIPES). Samples were subjected to Western blot analysis, using a mixture of N-terminus anti-AKT and C- terminus anti-Akt1 antibodies. This panel is representative of three experiments.

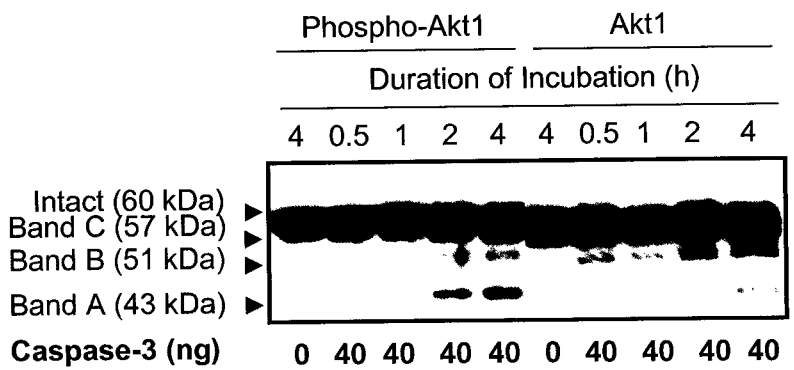
Phospho-Akt1
Akt1
Duration of Incubation (h)
4 0.5 1 2 4 4 0.5 1 2 4
Intact (60 kDa)
Band C (57 kDa)
Band B (51 kDa)
Band A (43 kDa)
Caspase-3 (ng)
0 40 40 40 40 0 40 40 40 40

Fig. 14

increased with increasing concentrations of caspase-3 (Fig. 13) or increasing duration of incubation (Fig. 14) and that Akt1 phosphorylation influenced caspase-3-mediated cleavage in a site-specific manner: Whereas site A (at which Akt1 is cleaved to produce band A) was more susceptible to cleavage in the phosphorylated Akt1, cleavage at site B (at which Akt1 is cleaved to produce band B) was more evident in the non-phosphorylated form (Fig. 13 & 14). In these studies, the phosphorylated form of the protein appeared to have a higher molecular mass on the blots (Fig. 13 & 14). Therefore, we confirmed the molecular mass of the phosphorylated and non-phosphorylated forms of the protein by two different mass spectrometry methods: MALDI-TOF M.S. and SELDI-M.S., as described in the Materials and Methods section. We observed a molecular mass for Akt1 and phospho-Akt1 of 61 and 70 kDa, respectively, by MALDI-TOF (Fig. 15), and of 59 and 73 kDa, respectively by SELDI-M.S. (Fig. 16).

13.5 Band A appears as multiple fragments

In order to attain a better partition of the adjacent fragments on the SDS-PAGE, the gels were further resolved. Upon higher resolution of samples on SDS-PAGE, followed by silver stain analysis (Fig. 17.A) or immunoblotting (Fig. 19.A), band A appeared as a triplet. This triplet was best observed in the silver-stained big gels (20 cm × 20 cm) that were over-run for 48 h (Fig. 17.B). One possible explanation for this observation is the glycosylation status of the recombinant Akt1 protein. This hypothesis was tested by performing a deglycosylation assay on the caspase-3-mediated Akt1 crude digests,

Figure 15. Matrix-Assisted Laser Desorption Ionization Time-of-Flight (MALDI-TOF) Mass Spectrometry (M.S.) analysis of the human recombinant Akt1 and phospho-Akt1 indicates a higher molecular mass for the phosphorylated Akt1.

Human recombinant Akt1 and phospho-Akt1 (1 μg each) were diluted in PIPES assay buffer (total volume:10 μl). The samples were desalted using Zip-Tip columns as mentioned in the Materials and Methods Section. 4 μl of the samples were spotted onto an M.S. plate. The digests were mixed with a saturated solution of an ultra-violet absorbing matrix [e.g. α-cyano-4-hydroxy-cinnamic acid (CHCA)]. The experiment was replicated using 2,3 dihydroxy benzoic acid (DHB) as matrix. The instrument was calibrated with bovine serum albumin (BSA; panel A). MALDI-TOF M.S. analysis of phospho-Akt1 showed presence of two peaks at 70 and 35 kD (panel B), while that of Akt1 revealed two peaks at 62 and 31 kDa (panel C). M^+, single charged ions; $M^+/2$, double charged ions.

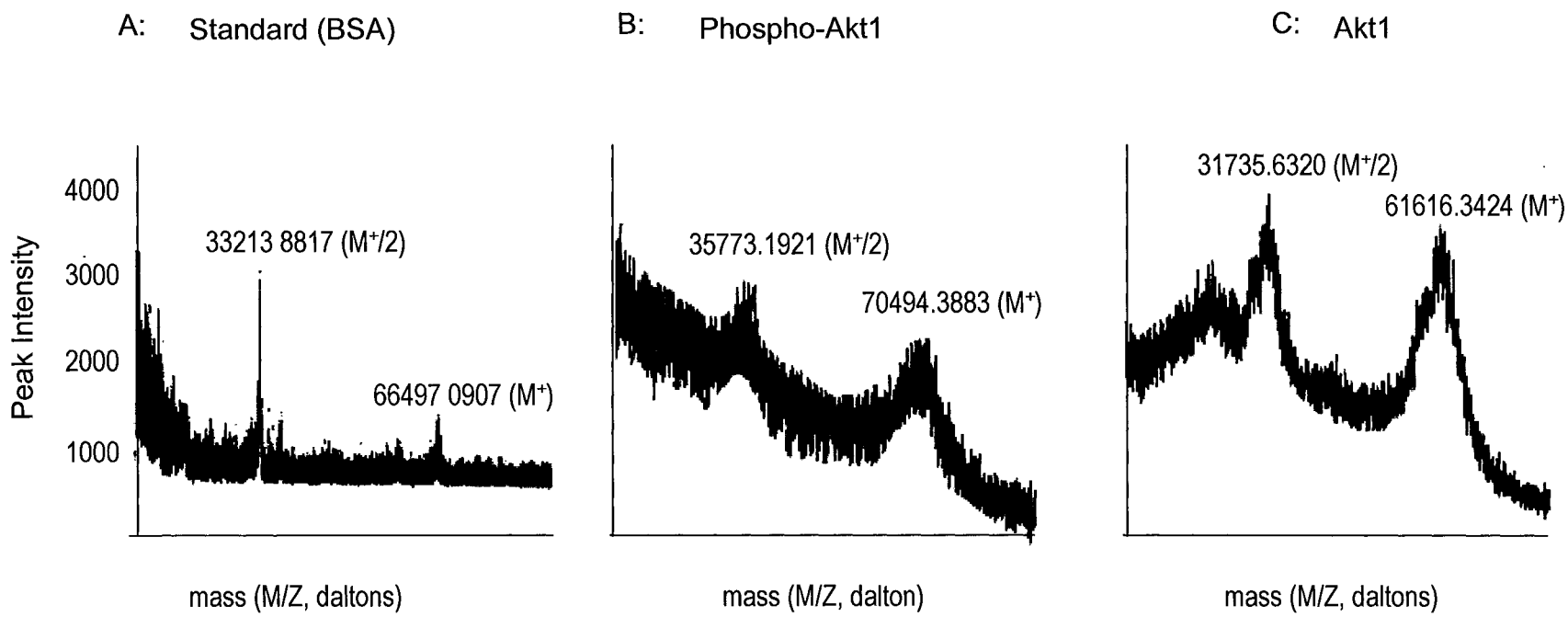
A: Standard (BSA)
B: Phospho-Akt1
C: Akt1
Peak Intensity
4000
3000
2000
1000
33213 8817 (M+/2)
66497 0907 (M+)
35773.1921 (M+/2)
70494.3883 (M+)
31735.6320 (M+/2)
61616.3424 (M+)
mass (M/Z, daltons)
mass (M/Z, dalton)
mass (M/Z, daltons)

Fig. 15

Figure 16. Surface Enhanced Laser Desorption/Ionization M.S. analysis of the human recombinant Akt1 and phospho-Akt1 indicates a higher molecular mass for the phosphorylated Akt1.

Human recombinant Akt1 and phospho-Akt1 (1 μg each) were diluted in PIPES assay buffer (18 μl total volume). 2 μl of the samples were spotted onto a normal phase protein chip. CHCA was used as a matrix. SELDI-M.S. analysis of phospho-Akt1 showed presence of two peaks at 73 and 35 kD, while that of Akt1 revealed three peaks at 59, 29, and 19 kDa. M^+, single charged ions; $M^+/2$, double charged ions; $M^+/3$, triple charged ions.

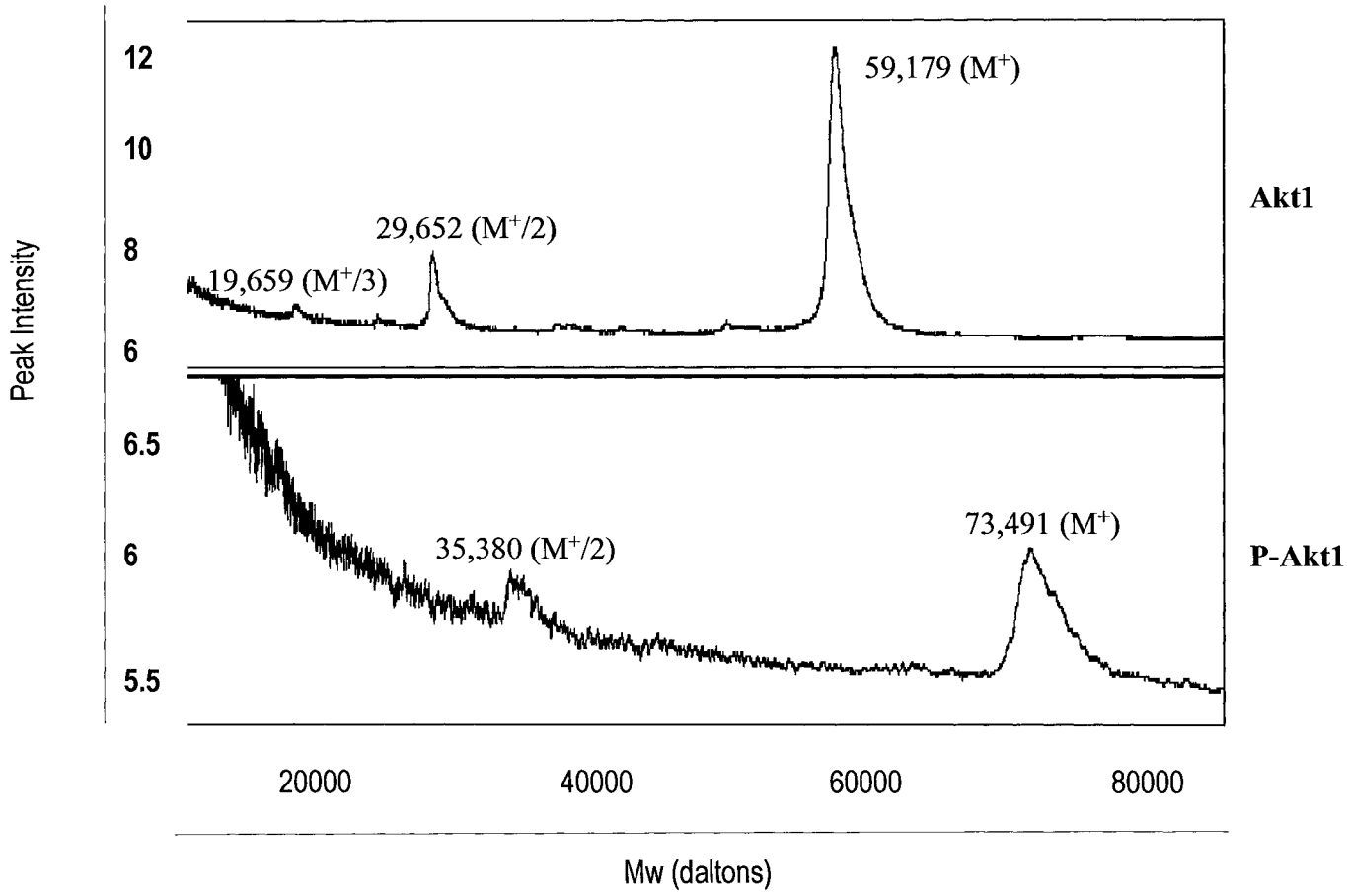
Peak Intensity
12
10
8
6
6.5
6
5.5
59,179 (M+)
29,652 (M+/2)
19,659 (M+/3)
Akt1
35,380 (M+/2)
73,491 (M+)
P-Akt1
20000
40000
60000
80000
Mw (daltons)

Fig. 16

following incubation of the human recombinant Akt1 (1μg) with active human recombinant caspase-3 (800 ng, 16h, 37°C, PIPES). Bovine Fetuin (B.F., 60 kDa) was used as positive control. The deglycosylation of B.F. resulted in a shift in the mobility of the protein from 60kDa to 48 kDa, implying that the assay worked (Fig.18). The observation of an absence of a shift in the mobility of the larger fragment of the triplet (43 kDa) into smaller ones indicates that glycosylation was not involved (Fig. 18, n = 3). The observation that the triplet was detected by immunoblotting (Fig. 19. A) raises the perception that the three fragments may all have been produced by caspase-3 cleavage. Of the triplet in band A, the 42 and 43 kDa fragments were consistently detected and gave equal intensity when analyzed by immunoblotting (Fig. 19.A), whereas the 41 kDa fragment was barely detectable (Fig. 19.A, left panel). Also, the demonstration that both 42 and 43 kDa fragments were abolished in the presence of a caspase-3-inhibitor (DEVD-CHO, Fig. 19.B), and that their pattern of cleavage varied between Akt1 and phospho-Akt1, such that the 43 kDa fragment was more cleaved upon phosphorylation while the 42 kDa fragment became more resistant (Fig. 19.C) implies that both of these fragments were a result of caspase-3-mediated proteolysis of Akt1 at two different sites adjacent to each other.

13.6 Molecular Mass Estimation of the Unknown Novel Bands Using Electrophoresis.

Electrophoresis has been used for years to estimate molecular mass of unknown fragments. Even though the advancement of the new technology and availability of more

precise techniques such as mass spectrometry for mass estimation of peptides and proteins outdates electrophoresis, this method is still used and is convenient for estimation of molecular mass of proteins and peptides. Molecular mass of the unknown bands (A and B) were estimated using silver-stained big gels. The reason for this was the lack of protein-dye conjugates in the non-pre-stained standards (used in staining protocols), which gives a more precise estimate of the molecular mass in contrast to estimation by pre-stained standards in Western blots. Following silver staining of the peptides obtained as a result of human recombinant Akt1 incubation with active human recombinant caspase-3, R_f values were calculated and inserted into an Excel spread sheet (Invitrogen) and corresponding molecular mass of 41, 42, and 43 kDa (for the triplet of band A) and 51 kDa (for band B) were obtained (Fig. 17. B, n = 2).

13.7 Specificity of the Novel Akt1 Cleavage Site to Caspase-3

Since caspase-3 and caspase-7 are similar structurally and functionally, and their specificity profiles are virtually indistinguishable (Thornbery 1997), we aimed to determine whether the novel site A is also a novel cleavage motif for caspase-7. To achieve this objective, human recombinant Akt1 was incubated in the presence of different concentrations of caspase-3 and caspase-7, and the reaction mixtures were analyzed by Western blot. Our data demonstrated that site A was not specific to caspase-3, since caspase-7 cleaved Akt1 at the same site (n = 3, Fig. 20). Furthermore the same

Figure 17. Molecular mass estimation of the novel caspase-3-mediated Akt1 cleavage fragments by SDS-PAGE: Band A appears as a triplet upon further gel resolution.

Human recombinant Akt1 was incubated in the absence and presence of caspase-3 as described previously. Samples were resolved on SDS-PAGE (10 %, 110 v, 3-4 h) and analyzed by silver staining (panel A). Human recombinant Akt1 (1μg) was incubated with active human recombinant caspase-3 (0.8 μg, 16h, PIPES, 37˚C). Samples were resolved on large (20 cm × 20 cm) SDS-PAGE gel (10 %, 100 V, 48 h), which was subsequently silver stained. R_f values were measured by alpha-imager and the molecular mass for each band was calculated using Microsoft Excel worksheets. Fragments of 41, 42, and 43 kDa correspond to the triplet and the 51 kDa band corresponds to band B.

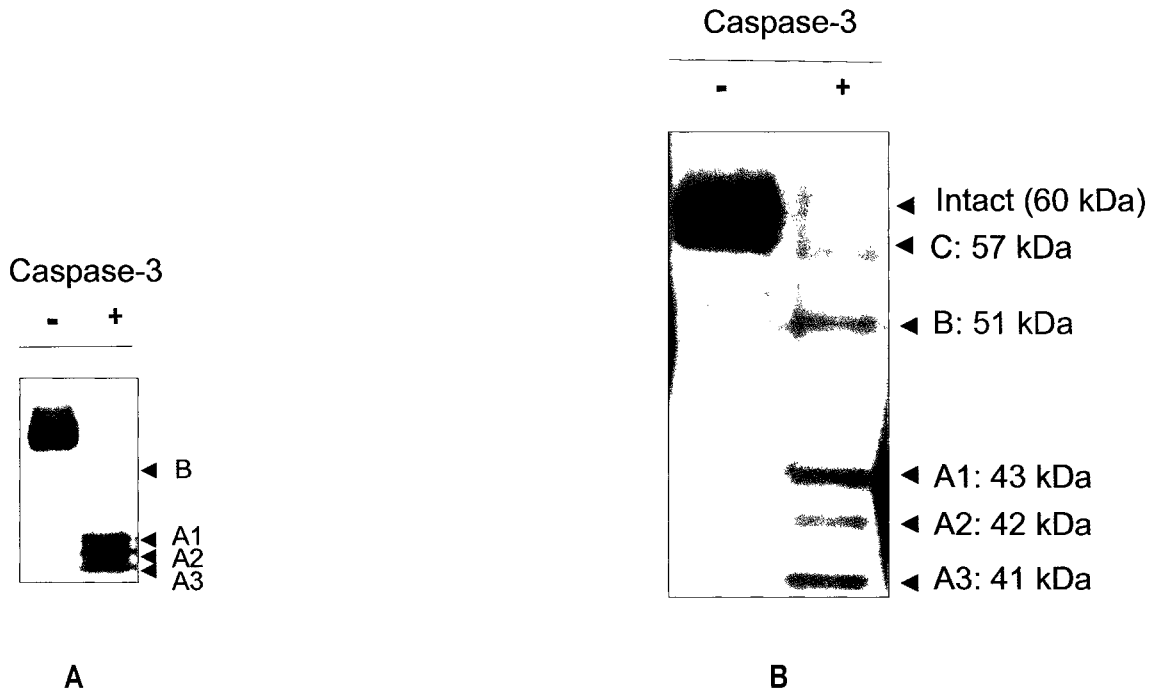
Caspase-3
-
+
B
A1
A2
A3
A
Caspase-3
-
+
Intact (60 kDa)
C: 57 kDa
B: 51 kDa
A1: 43 kDa
A2: 42 kDa
A3: 41 kDa
B

Fig. 17

Figure 18. Human recombinant Akt1 was not glycosylated.

Human recombinant Akt1 (1μg) was incubated in the presence of active human recombinant caspase-3 (0.8 μg, 24 h, 37°C) followed by deglycosylation assay (6 h, 37° C). A lane composed of the deglycosylation reagents but without Akt1 was used as negative control to eliminate presence of any band contributed by the deglycosylation enzymes. Bovine Fetuin (a highly glycosylated protein) was used as a positive control, to ensure that the assay worked. Samples were resolved by SDS-PAGE and silver-stained. The experiment was replicated three times.

Figure 19. Fragments in Band A may be the result of cleavage at three different sites in close proximity of each other.

Panel A: The triplet is detected immunologically by anti-Akt1 antibody. Human recombinant Akt1 (125 ng) was incubated in the presence of increasing concentrations of caspase-3 (0, 80, 160, and 320 ng). Samples were subjected to 10% SDS-PAGE analysis (110v, 4.5 h) followed by Western blotting with a C-terminus anti-Akt1 antibody (n = 5). Left and right panels reflect the same blot with the film exposed for 240 and 30 seconds, respectively.

Panel B: The appearance of the 42 and 43 kDa fragments are blocked in the presence of a caspase-3 inhibitor. Human recombinant Akt1 (125 ng) was incubated with active human recombinant caspase-3 (50 ng) in the absence and presence of 20 and 40 pM of the caspase-3 inhibitor DEVD-CHO or 0.09 % DMSO. Samples were subjected to SDS-PAGE analysis (110 V, 4.5 h) and immunoblotted with a C-terminus anti-Akt1 antibody (n = 3).

Panel C: Phosphorylation increases the appearance of the 43 kDa and decreases that of the 42 kDa fragment. Human recombinant Akt1 and phospho-Akt1 (125 ng each) were incubated with active human recombinant caspase-3 (40 ng) for 0, 0.5, 1, 2, and 4 h (37°C, PIPES). Samples were subjected to Western blot analysis, using a C- terminus anti-Akt1 antibody (n = 3).

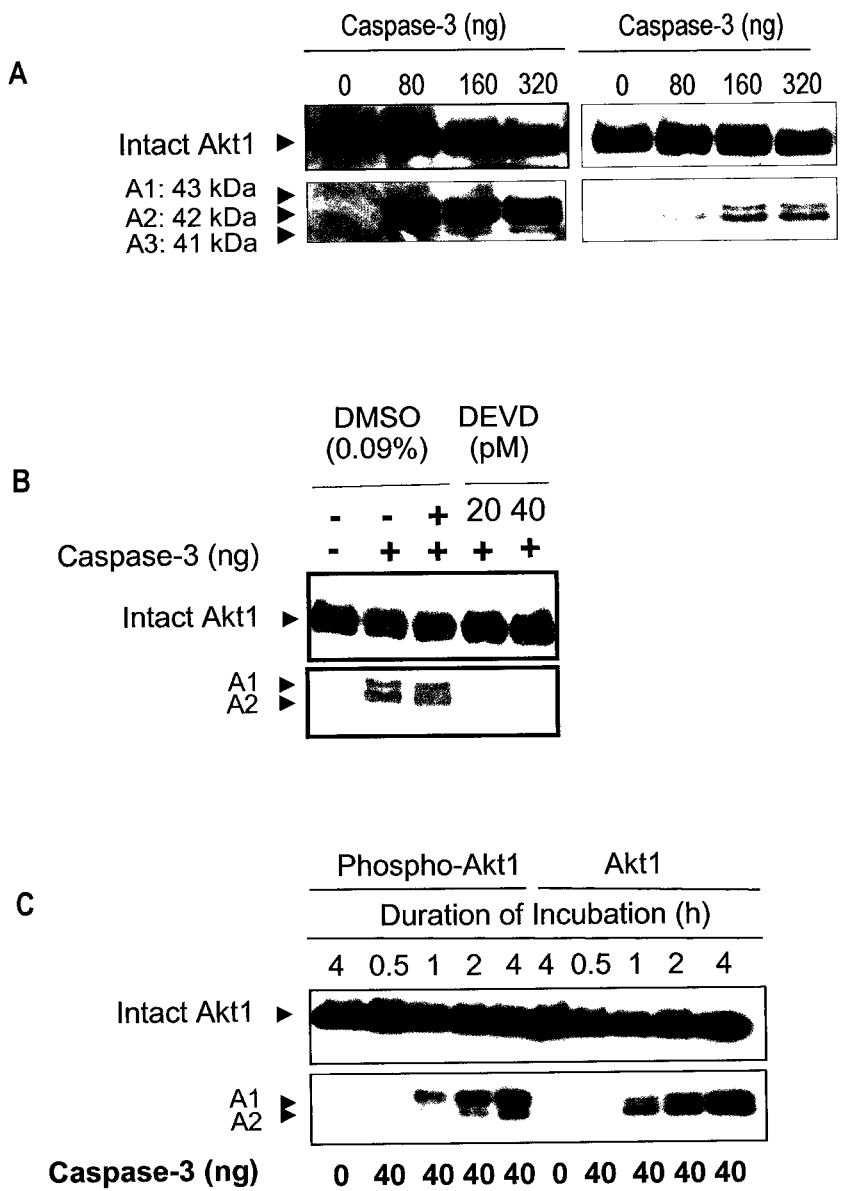
A
Caspase-3 (ng)
Caspase-3 (ng)
0 80 160 320
0 80 160 320
Intact Akt1
A1: 43 kDa
A2: 42 kDa
A3: 41 kDa
B
DMSO (0.09%)
DEVD (pM)
- - + 20 40
Caspase-3 (ng) - + + + +
Intact Akt1
A1
A2
C
Phospho-Akt1
Akt1
Duration of Incubation (h)
4 0.5 1 2 4 4 0.5 1 2 4
Intact Akt1
A1
A2
Caspase-3 (ng)
0 40 40 40 40 0 40 40 40 40

Fig. 19

blots were re-probed with the N-terminus anti-AKT antibody. The results showed that the novel site B was also cleaved when Akt1 was incubated with increasing concentrations of caspase-7 (Fig. 20). However this cleavage was very subtle.

13.8 The Novel Caspase-3 Cleavage Site A is Specific to Akt1

Among AKT isoforms, Akt2 is known to be significantly involved in ovarian cancer chemoresistance while Akt3 is not highly expressed in ovarian cells and a significant role for Akt3 has not been demonstrated to date. We were interested to investigate whether the novel caspase-3 cleavage sites in Akt1 are also potential sites of cleavage in Akt2 and Akt3. To this end, human recombinant Akt1, Akt2 and Akt3 were incubated with various concentrations of caspase-3, followed by Western analysis. Using C-terminus anti-Akt1, anti-Akt2, and anti-Akt3 antibodies, we showed that site A is specific to Akt1, and similar cleavage fragments were not observed for Akt2 (Fig. 21.A, top panel, n = 3) or Akt3 (Fig 21.B top panel). The same blots were stripped and re-probed with N-terminus anti-AKT, -Akt2, and -Akt3 antibodies. A band with a molecular mass of 50 and 52 kDa (very close to band B, 51 kDa) was detected in Akt2 and Akt3, respectively (Fig. 21.A and 21.B, lower panels). It is possible that site B may be present in the latter two isoforms, although more analysis are required to confirm this notion since there was a difference in molecular mass between intact Akt1 (59 kDa), and Akt2 and Akt3 (66 kDa), and different R_f values among the three bands was noted.

Figure 20. Caspase-7-mediated Akt1 cleavage also gave rise to Band A and Band B.

Human recombinant Akt1 (125 ng) was incubated with various concentrations of caspase-3 and caspase-7 (0, 20, 40, 80 ng, PIPES, 2h, 37°C). Samples were analyzed by Western blotting, using a C-terminus anti-Akt1 and an N-terminus anti-AKT antibody capable of detecting Akt1 and its C-and N-terminus cleavage fragments. Figure shows representative membrane of three experiments.

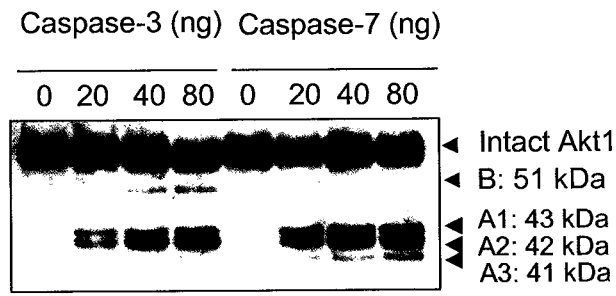
Caspase-3 (ng)
Caspase-7 (ng)
0 20 40 80 0 20 40 80
Intact Akt1
B: 51 kDa
A1: 43 kDa
A2: 42 kDa
A3: 41 kDa

Fig. 20

Figure 21. Novel Band A was not detectable when Akt2 and Akt3 were incubated with caspase-3.

Human Recombinant Akt1, Akt2 and Akt3 were incubated with different concentrations of active human recombinant caspase-3 (0 20, 40, 80 ng; 2h, 37°C). Samples were analyzed by SDS-PAGE, using C-terminus anti-Akt1, -Akt2 and –Akt3 antibodies and N-terminus anti-AKT, -Akt2, and -Akt3 antibodies. Each figure shows representative membranes of three experiments.

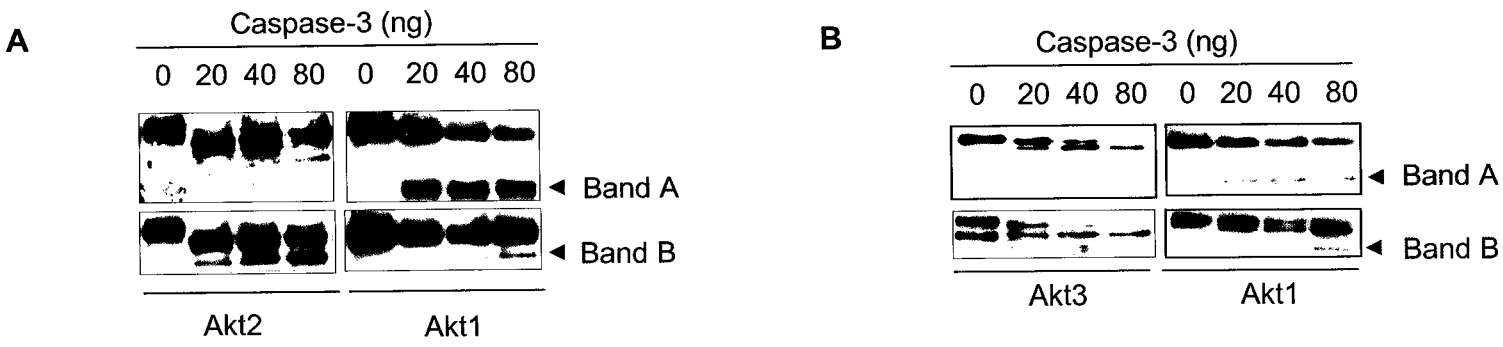
A
Caspase-3 (ng)
0 20 40 80 0 20 40 80
Band A
Band B
Akt2
Akt1
B
Caspase-3 (ng)
0 20 40 80 0 20 40 80
Band A
Band B
Akt3
Akt1

Fig. 21

13.9 Molecular Mass Estimation of the Novel Bands Using SELDI-M.S.

SELDI M.S., a technique based on Protein-Chip technology, was used to measure the peptide mass of the caspase-3-mediated-Akt1 cleavage fragments. SELDI-M.S. analysis of caspase-3-mediated Akt1 digests consistently indicates presence of several peaks within 2.6, 2.7, 3, 6/7, 8, 9, 16 and 57 kDa (Table 2, n = 3). The presence of these peaks in the samples, but absence in the caspase-3 autocatalysis spectra, indicates that all the eight peaks are Akt1 cleavage fragments resulting from the action of caspase-3. We propose that the peaks corresponding to a molecular mass of 2.6 or 2.7 (Fig. 22) and 57 kDa (Fig. 23) are correlated with Akt1 cleavage at $DQDD^{456}$. The remainder of the peaks may be as a result of cleavage at novel caspase-3 cleavage sites. The 16 kDa peak (Fig. 24) may be associated with cleavage at site A, based on the previous observation of presence of a 43 kDa band A (electrophoresis) and presence of a 59 kDa peak for the intact Akt1 (SELDI-M.S., 43 + 16 = 59). The same assumption was made for the 9 kDa peak (Fig. 24) as cleavage at site B, taking into consideration that band B was estimated at about 51 kDa previously. The 8 kDa peak (Fig. 24), half the molecular mass of the 16 kDa peak, is proposed to be the same as the 16 kDa peak based on the principle of charge to mass ratio which states the double charged molecules will give a molecular mass of half of that of the single charged molecules.

Table 2. Summary of SELDI-M.S. analysis of caspase-3-mediated Akt1 cleavage assays.

SELDI-M.S. analysis of caspase-3-mediated Akt1 cleavage assays consistently demonstrated presence of several peaks within 2.6, 2.7, 3, 6-7, 8, 9 and 16 kDa (n = 3).

# of peaks	Replicate 1 (daltons)	Replicate 2 (daltons)	Replicate3 (daltons)
1	2504	2617	2633.8
2	2841	2704	2713.3
3	3294	3535	3453.8
4	6442.8	7219	6948.3
5	8282.3	8830	8096.6
6	9181.2	9165.7	9224.2
7	16598.6	16558.4	16173.5
8	16111.7	16219	16358

Table 2

Figure 22. Detection of two peaks of 2713.3 and 2633.8 daltons by SELDI-M.S analysis of caspase-3-mediated Akt1 digests supports the notion of cleavage at $DQDD^{456}$ consensus sites.

Human recombinant Akt1 (1 μg) was incubated with active human recombinant caspase-3 (0.05 μg) in a total reaction mixture of 18 μl (PIPES, 37 ° C, 24 h). The reactions were stopped by adding 2 μl of glacial acetic acid. Caspase-3 alone was incubated (PIPES, 37 ° C, 24 h) as a negative control. Samples were spotted onto the protein chip and were thoroughly washed with distilled water after the proteins were crystalized. Reaction mixtures were subjected to M.S. analysis. Panel A shows (from top to bottom) the spectra (range of 1000 to 4000 Daltons) for the standards (used for calibration of the instrument), caspase-3 alone, p-Akt1 + caspase-3, and Akt1 + caspase-3, respectively. Panels B and C is the magnified version of the peaks within the 2600 to 2800 daltons range for caspase-3 autocatalysis and caspase-3-mediated Akt1 cleavage digests.

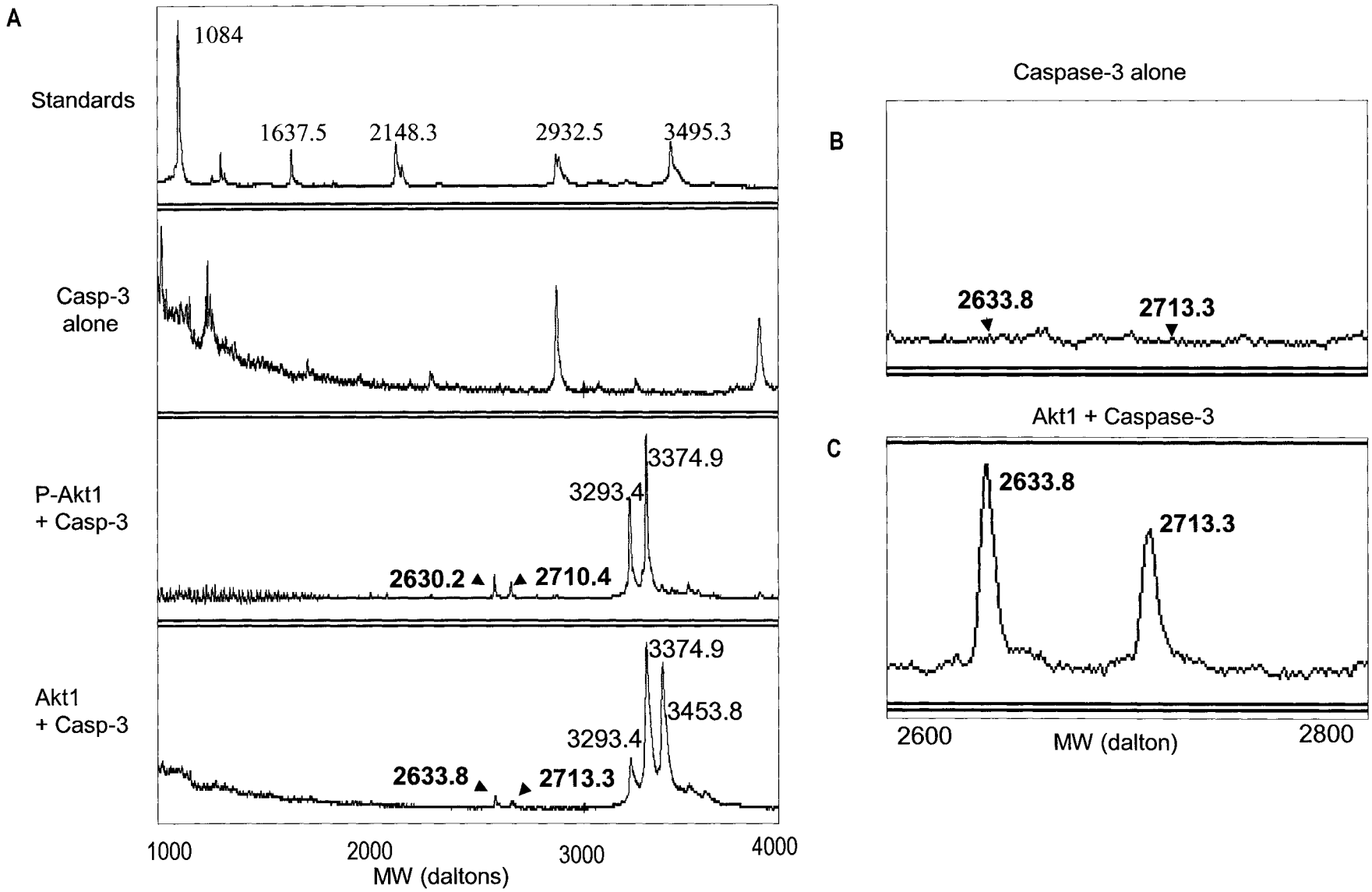
A
Standards
1084
1637.5
2148.3
2932.5
3495.3
Casp-3
alone
P-Akt1
+ Casp-3
3374.9
3293.4
2630.2
2710.4
Akt1
+ Casp-3
3374.9
3453.8
3293.4
2633.8
2713.3
1000
2000
3000
4000
MW (daltons)
B
Caspase-3 alone
2633.8
2713.3
C
Akt1 + Caspase-3
2633.8
2713.3
2600
MW (dalton)
2800

Fig. 22

Figure 23. The presence of a peak of 57 kDa, as detected by SELDI-M.S. analysis of caspase-3-mediated Akt1 digest, confirms caspase-3-mediated Akt1 cleavage at the consensus DQDD sequence.

The reactions were set up and spotted onto the protein chips as mentioned in Fig. 22. Samples were subjected to M.S. analysis. Figure demonstrates the analysis at the range of 40,000 to 80,000 daltons. From top to bottom are the spectra for: standards, caspase-3 autocatalysis, p-Akt1 + caspase-3, and Akt1 + caspase-3.

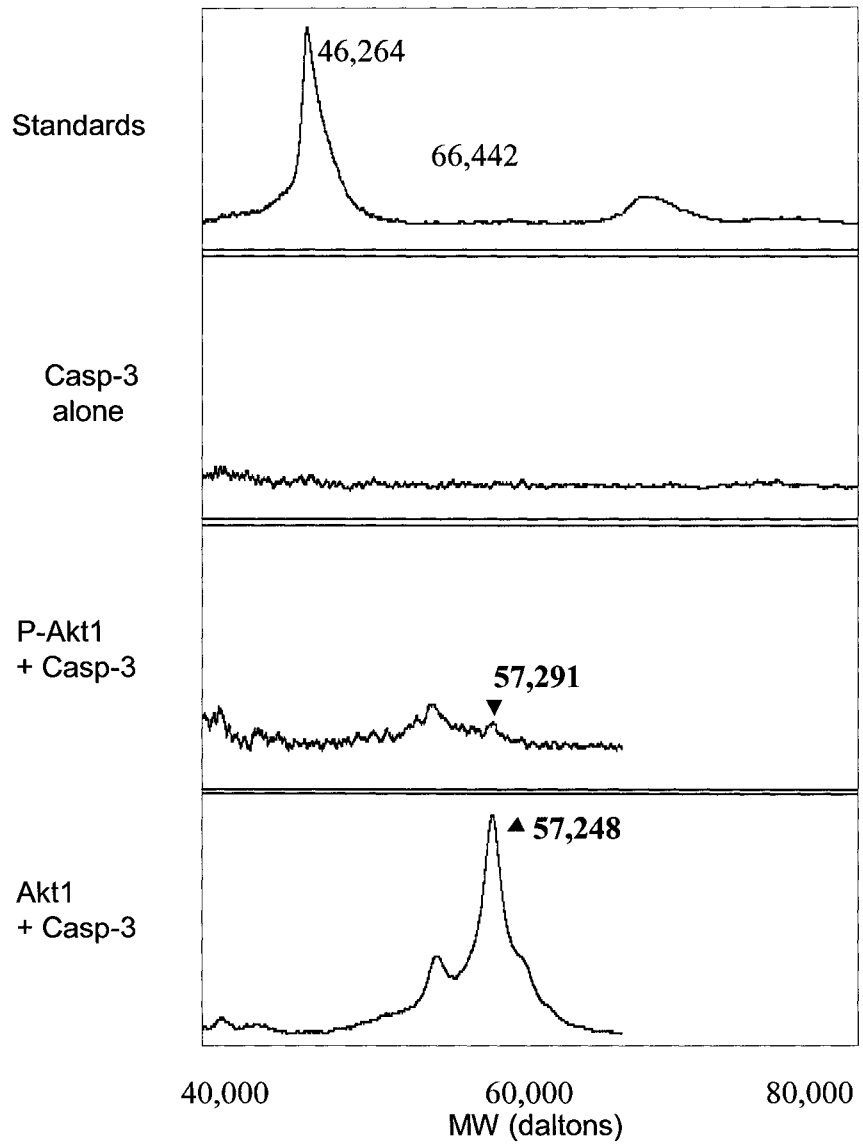
Standards
46,264
66,442
Casp-3
alone
P-Akt1
+ Casp-3
57,291
Akt1
+ Casp-3
57,248
40,000
60,000
80,000
MW (daltons)

Fig. 23

Figure 24. The presence of two peaks at 16.1/16.3 and 9.2 kDa as detected by SELDI-M.S analysis of caspase-3-mediated Akt1 digest, may be a result of cleavage at sites A and B, respectively.

The digest reactions were set up and spotted onto the protein chips as mentioned in Fig.22. Samples were subjected to M.S. analysis. Panel A shows (from top to bottom) the spectra (range of 7,500 to 20,000 daltons) for the standards, caspase-3 alone, p-Akt1 + caspase-3 and Akt1 + caspase-3, respectively. Panel B and C is the magnified version of the 9.2 and 16.1/16.3 kDa peaks for Akt1 at 8,000 to 10,000 and 1600 to 1700 daltons, respectively. Caspase-3 autocatalysis is included in the top panels of each figure.

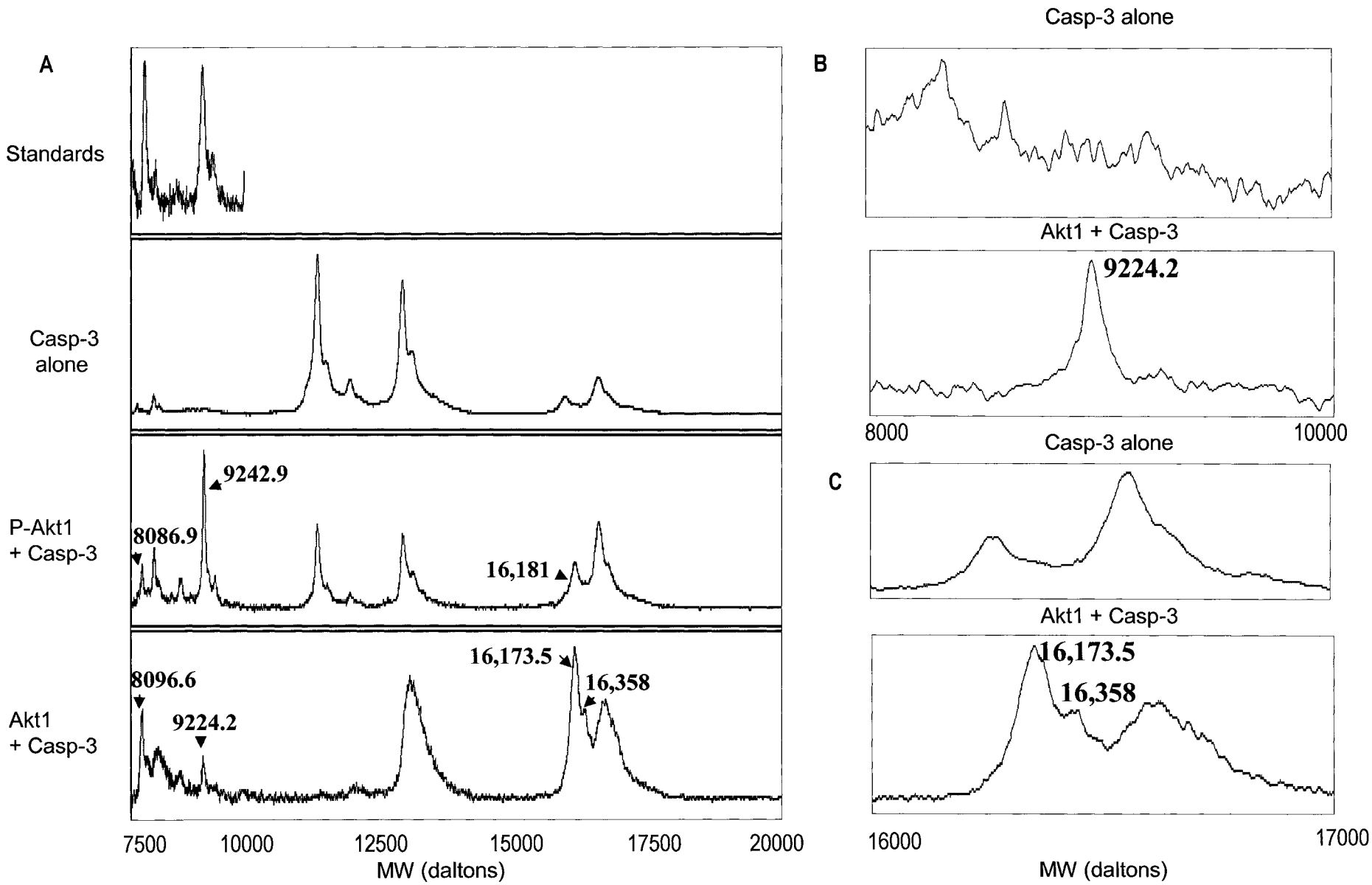
A
Standards
Casp-3 alone
P-Akt1 + Casp-3
Akt1 + Casp-3
9242.9
8086.9
16,181
8096.6
9224.2
16,173.5
16,358
7500
10000
12500
15000
17500
20000
MW (daltons)
B
Casp-3 alone
Akt1 + Casp-3
9224.2
8000
10000
C
Casp-3 alone
Akt1 + Casp-3
16,173.5
16,358
16000
17000
MW (daltons)

Fig. 24

13.10 Estimation of Novel Caspase-3 Cleavage Sites

Thornberry et al (1997) investigated the substrate specificities of caspases for caspase-1, 2, 3, 4, 5, 6, 7, 8, and 9. Their data demonstrated that based on the substrate specificity, these proteases can be divided into three major categories. Caspase-3 (DEVD), and 7 (DEVD) were categorized under the same group in terms of having the same optimal sequence. However, other sequences aside from these consensus sequences have been identified for different caspases (Table. 1). Aspartate (D) at P1 position is preferred in order for caspase-3 to bind the substrate, with Glutamate (E) as the next likely candidate. Therefore all the D and E residues in the Akt1 sequence were presumed as possible P1 position for cleavage (Fig. 25) and a table was prepared containing the theoretical size of all the cleavage fragments corresponding to these P1 positions in Akt1 (Table. 3). Based on the molecular mass estimation of the larger unknown bands by SDS-PAGE and the smaller unknown peaks by SELDI-M.S data, as well as the presence of D/E residues at P1 position, we proposed three sites of EEEE^{117} and EEMD^{119} and DAKE^{398} to be the novel cleavage sites giving rise to fragments of band A and band B, respectively. These sites were calculated to be at EEEE^{145} and EEMD^{147} and DAKE^{426} in the His-tagged fusion recombinant Akt1 protein. The presence of three novel sites present in Akt1 as well as the consensus sequence DQDD^{456} might have given rise to a combination of different size fragments, which were not detected by Western blot (due to limitation within the antibody) but were observed by SELDI-analysis. For instance the size of the fragment from DAKE^{426} to DQDD^{456} is calculated to be within 6.5 kDa

theoretically, and we observed presence of 6-7 kDa peaks in the SELDI-M.S. analysis (Table 2, Fig. 26).

Figure 25 Aspartate (D) and Glutamate (E) residues in the recombinant human Akt1 sequence.

The recombinant human Akt1 sequence reveals presence of 85 negative amino acids, aspartate or glutamate (highlighted in red). All these residues were hypothesized to be possible P1 positions for cleavage by caspase-3.

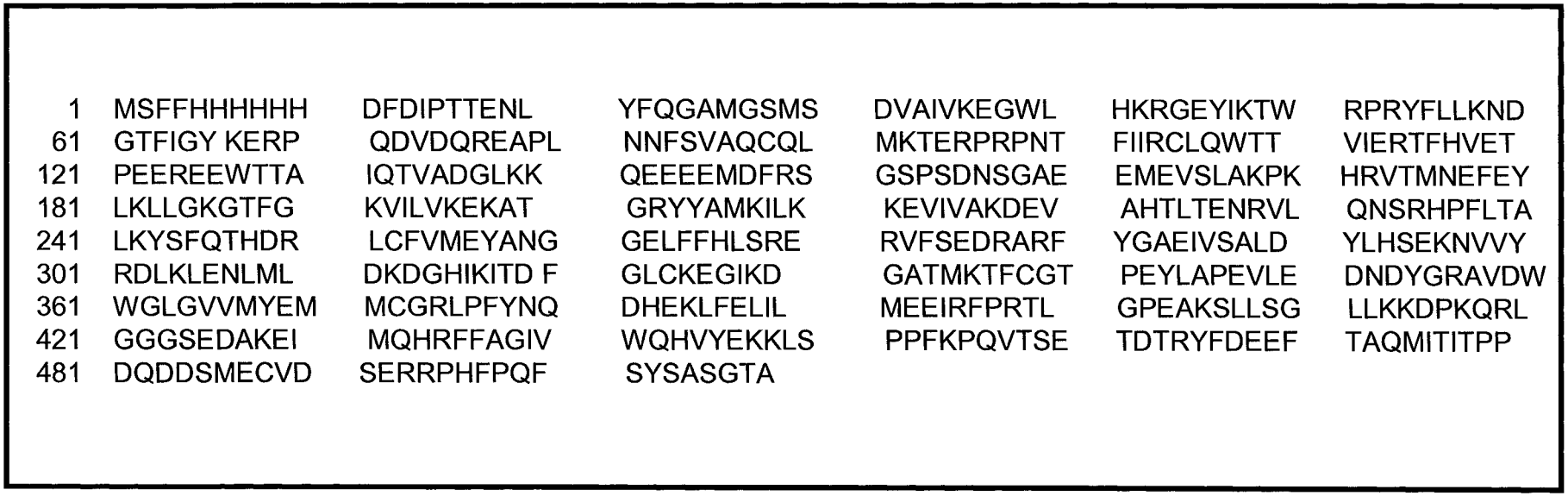
1 MSFFHHHHHH DFDIPTTENL YFQGAMGSMS DVAIVKEGWL HKRGEYIKTW RPRYFLLKND
61 GTFIGY KERP QDVDQREAPL NNFSVAQCQL MKTERPRPNT FIIRCLQWTT VIERTFHVET
121 PEEREEWTTA IQTVADGLKK QEEEEMDFRS GSPSDNSGAE EMEVSLAKPK HRVTMNEFEY
181 LKLLGKGTFG KVILVKEKAT GRYYAMKILK KEVIVAKDEV AHTLTENRVL QNSRHPFLTA
241 LKYSFQTHDR LCFVMEYANG GELFFHLSRE RVFSEDRARF YGAEIVSALD YLHSEKNVVY
301 RDLKLENLML DKDGHIKITD F GLCKEGIKD GATMKTFCGT PEYLAPEVLE DNDYGRAVDW
361 WGLGVVMYEM MCGRLPFYNQ DHEKLFELIL MEEIRFPRTL GPEAKSLLSG LLKKDPKQRL
421 GGGSEDAKEI MQHRFFAGIV WQHVYEKKLS PPFKPQVTSE TDTRYFDEEF TAQMITITPP
481 DQDDSMECVD SERRPHFPQF SYSASGTA

Fig. 25

Table. 3. All the theoretical caspase-3-mediated cleavage fragments of Akt1 at aspartate (D) and glutamate (E) residues.

This table indicates theoretical C- and N- terminus fragments that can be generated when His-tagged recombinant Akt1 is cleaved at all the aspartate and glutamate residues. The abbreviations used in the table are: aa#, the position number of the amino acid residue after which caspase-3 will cleave; aaP1, amino acid at P1 position, whether a glutamate or an aspartate; C frag: the C-terminus fragment as a result of cleavage at the specified site; N frag, the N-terminus fragment as a result of cleavage at the specified site; SITE, the four contagious amino acids (P1-P4) where the caspase-3 is proposed to bind. The calculations are based on the molecular mass of the recombinant Akt1 protein.

aa #	aa P1	C frag	N frag	Akt1-His	SITE
11	D	57541.47	1468.57	59010.04	HHHD
13	D	57279.2	1730.84	59010.04	HDFD
18	E	56737.6	2272.44	59010.04	PTTE
31	D	55335.04	3675	59010.04	SMSD
37	E	54695.25	4314.79	59010.04	IVKE
45	E	53731.15	5278.89	59010.04	KRGE
60	D	51735.79	7274.25	59010.04	LKND
68	E	50839.78	8170.26	59010.04	GYKE
72	D	50343.26	8666.78	59010.04	RPQD
74	D	50129.04	8881	59010.04	QDVD
77	E	49715.61	9294.43	59010.04	DQRE
94	E	47839.43	11170.61	59010.04	MKTE
113	E	45513.67	13496.37	59010.04	TVIE
119	E	44743.81	14266.23	59010.04	FHVE
122	E	44416.47	14593.57	59010.04	ETPE
123	E	44287.36	14722.68	59010.04	TPEE
125	E	44002.06	15007.98	59010.04	EERE
126	E	43872.94	15137.1	59010.04	EREE
136	D	42785.74	16224.3	59010.04	TVAD

aa #	aa P1	C frag	N frag	Akt1-His	SITE
142	E	42101.94	16908.1	59010.04	KKQE
143	E	41972.82	17037.22	59010.04	KQEE
144	E	41843.71	17166.33	59010.04	QEEE
155	D	40634.45	18375.59	59010.04	SPSD
160	E	40176.03	18834.01	59010.04	SGAE
161	E	40046.91	18963.13	59010.04	GAEE
163	E	39786.6	19223.44	59010.04	EEME
177	E	38194.71	20815.33	59010.04	TMNE
179	E	37918.42	21091.62	59010.04	NEFE
196	E	35929.93	23080.11	59010.04	LVKE
212	E	34147.75	24862.29	59010.04	LKKE
218	D	33521.99	25488.05	59010.04	VAKD
219	E	33392.87	25617.17	59010.04	AKDE
226	E	-203359	262369	59010.04	TLTE
249	D	29885.94	29124.1	59010.04	QTHD
256	E	29006.84	30003.2	59010.04	FVME
262	E	28415.26	30594.78	59010.04	NGGE
270	E	27385.07	31624.97	59010.04	LSRE

Table 3

aa #	aa P1	C frag	N frag	Akt1-His	SITE
275	E	26766.38	32243.66	59010.04	VFSE
276	D	26651.54	32358.5	59010.04	FSED
284	E	25700.24	33309.8	59010.04	YGAE
290	D	25101.54	33908.5	59010.04	SALD
295	E	24471.87	34538.17	59010.04	LHSE
302	D	23596.87	35413.17	59010.04	VYRD
306	E	23113.26	35896.78	59010.04	LKLE
311	D	22526.56	36483.48	59010.04	LMLD
313	D	22283.7	36726.34	59010.04	LDKD
320	D	21518.42	37491.62	59010.04	KITD
326	E	20840.6	38169.44	59010.04	LCKE
330	D	20427.13	38582.91	59010.04	GIKD
342	E	19202.72	39807.32	59010.04	GTPE
347	E	18629.07	40380.97	59010.04	LAPE
350	E	18287.66	40722.38	59010.04	EVLE
351	D	18172.57	40837.47	59010.04	VLED
353	D	17943.38	41066.66	59010.04	EDND
359	D	17281.67	41728.37	59010.04	RAVD
369	E	16060.23	42949.81	59010.04	VMYE
381	D	14603.51	44406.53	59010.04	YNQD

aa #	aa P1	C frag	N frag	Akt1-His	SITE
383	E	14337.26	44672.78	59010.04	QDHE
386	E	13819.63	45190.41	59010.04	KLFE
392	E	13219.84	45790.2	59010.04	ILME
393	E	13090.73	45919.31	59010.04	LMEE
403	E	11923.35	47086.69	59010.04	LGPE
415	D	10668.82	48341.22	59010.04	LKKD
425	E	9658.7	49351.34	59010.04	GGSE
426	D	9543.61	49466.43	59010.04	GSED
429	**E**	**9215.24**	**49794.8**	**59010.04**	**DAKE**
446	E	7071.74	51938.3	59010.04	HVYE
460	E	5503.9	53506.14	59010.04	VTSE
462	D	5287.7	53722.34	59010.04	SETD
467	D	4604.97	54405.07	59010.04	RYFD
468	E	4475.85	54534.19	59010.04	YFDE
469	E	4346.74	54663.3	59010.04	FDEE
481	D	3030.2	55979.84	59010.04	TPDD
483	D	2786.98	56223.06	59010.04	PDQD
484	D	2671.89	56338.15	59010.04	DQDD
487	E	2324.51	56685.53	59010.04	DSME
490	D	2007.15	57002.89	59010.04	ECVD
492	E	1790.95	57219.09	59010.04	VDSE

Table 3 continued

Figure 26. A peak of 6.9 kDa detected in SELDI-M.S analysis of caspase-3-mediated Akt1 digests may represent a fragment between the two cleavage sites $DQDD^{456}$ and $DAKE^{396}$.

The digest reactions were set up and spotted onto the protein chips as mentioned in Fig.22. Samples were subjected to M.S. analysis. From top to bottom are the spectra (range of 6,000 to 8,000 daltons) for the standards, caspase-3 alone, p-Akt1 + caspase-3 and Akt1 + caspase-3, respectively.

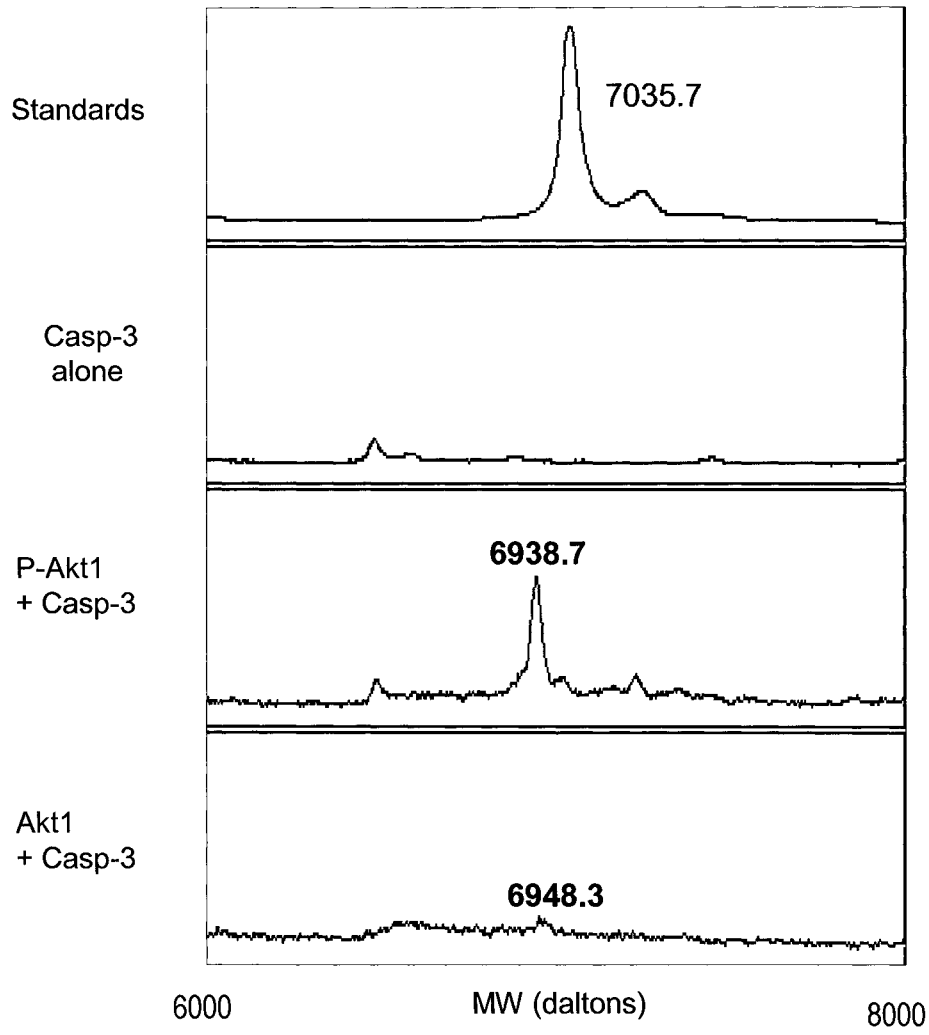
Standards
7035.7
Casp-3
alone
P-Akt1
+ Casp-3
6938.7
Akt1
+ Casp-3
6948.3
6000
MW (daltons)
8000

Fig. 26

14.0 Discussion

14.1 Significance of Caspase-3-Mediated Akt1 Cleavage

Increased resistance to apoptosis via deregulation of key pro- and anti-apoptotic pathways is a key factor in the onset and maintenance of chemoresistance. Recent evidence suggests that chemoresistance in ovarian cancer results in part from a defective apoptotic machinery in which survival factors such as Xiap, PI3-K, and AKT are over-expressed or maintained at high levels despite treatment with chemotherapeutic agents (Cheng et al, 2002).

Caspase-3, also referred to as the main executioner of cell death, acts via specific limited proteolysis and inactivation of proteins that are necessary for cell viability (Thornberry and Lazebnik, 1998). Activation of caspase-3 within pre-apoptotic cells has been demonstrated to lead to the proteolytic cleavage and inactivation of AKT (Asselin et al 2001), instigating the hypothesis that deregulation of the interaction between caspase-3 and AKT may be a major determinant of chemoresistance and that an understanding of caspase-3-mediated regulation of AKT is essential in order to improve cancer therapy and overcome chemoresistance via manipulating apoptotic pathways.

The work that initially documented AKT as a potential human oncogene detected amplification of Akt1 in a single gastric carcinoma (Staal et al 1987). Akt1 regulates the activity of FKHRL1, a member of the forkhead family of transcription factors, leading to

the association of FKHRL1 with 14-3-3 proteins and its retention in the cytoplasm (Brunet et al, 1999). Akt1 also phosphorylates and impairs the nuclear import of p27, and opposes cytokine-mediated G1 arrest (Liang et al, 2002). By targeted disruption of the Akt1 gene, Chen et al (2001) created an Akt1 null mouse model in which homozygous mice which were viable but smaller than wild type littermates exhibited the following physiological and cellular characteristics: 1) shorter life span upon exposure to genotoxic stress, 2) increased spontaneous apoptosis in the cells of testes and thymi, 3) increased sensitivity to gamma irradiation and dexamethasone-induced apoptosis, and 4) higher susceptibility of the cells to apoptosis induced by TNF, agonistic anti-Fas antibody, ultraviolet irradiation, and serum withdrawal. Another group of researchers detected increased Akt1 kinase activity in primary carcinomas of prostate, breast and ovary (Sun et al 2001). They also showed that stable transfection of a constitutively active Akt1 resulted in a malignant phenotype in NIH3T3 cells.

Although a role for the Akt1 isoform has been demonstrated in carcinogenesis by many researchers, its possible involvement in ovarian cancer and chemoresistance in ovarian carcinoma requires further investigation. The previous findings documenting a relationship between AKT cleavage and caspase-3 (Asselin et al 2001) in conjunction with the current analysis of the Akt1 sequence (Genebank® Accession # AAH00479) demonstrating the presence of one caspase-3 consensus (DXXD, Thornberry et al 1997) and fifteen non-consensus cleavage sites previously reported for other peptides/proteins (Table 1), puts forward the proposal that the interaction between caspase-3 and Akt1 may

be a determinant of the cell fate and that the regulation of this interaction may play a significant role in overcoming chemoresistance in ovarian malignancies.

14.2 Caspase-3 Consensus Sequence in Akt1 (DQDD)

Caspases have been grouped into subfamilies according to their preferred cleavage sites, with caspase-3 as the prototype of DEXD-dependent proteases. Known substrates of caspase-3 usually contain aspartic acid at P1 and P4, and maybe glutamate at P3 positions [N-terminus-(P4) *Asp-Glu-X-Asp* (P1)-C-terminus (Nicholson et al 1995)]. Caspase-3 catalyzes the cleavage of numerous protein substrates with this motif, including poly (ADP-ribose) polymerase (DEVD), the Huntington's disease gene product (DEED), the catalytic subunit of DNA-dependent protein kinase (DEVD), Ca^{2+} ATPase isoform (DEID), the large subunit of replication factor C (DEVD), protein lipase C theta (DEVD), the 70-kDa subunit of the U1 small ribonucleoprotein (DGPD), BRCA1 (DLLD), DNA topoisomerase I (DDVD), actin-capping protein α adducin (DDSD), and focal adhesion kinase (DQTD) (Nicholson et al 1995, Go et al 1995, Tewari et al 1995, Goldberg et al, 1996, Zhan et al 2002, Crouch et al 1996, and Samejima et al 1999). Although AKT has been reported to be a new substrate for caspase-3 (Asselin et al 2000), the site(s) of cleavage has not yet been defined. Since a caspase-3 consensus sequence ($DQDD^{456}$) is present in the Akt1 sequence, our first objective was to demonstrate caspase-3-mediated Akt1 cleavage at this site. Treatment of Akt1 with caspase-3 resulted in the appearance of a band of approximately 57 kDa (band C) on Western blot analysis. The intensity of band C increased with increasing concentrations of caspase-3 and

duration of incubation, and was decreased by the presence of the caspase-3-inhibitor DEVD-CHO. Moreover, two peaks at 2.7 and 57 kDa were observed by SELDI-M.S. analysis of the Akt1 digests. These findings are in agreement with the possibility of cleavage at $DQDD^{456}$ motif, although a 2.7 kDa fragment (detected by SELDI-M.S. analysis) was not detectable by immunoblotting. Although the reason for this was not clear, we speculated a few possibilities. Since the internal cell environment can support reactions at a pH other than 7, we tested the nature of caspase-3-mediated Akt1 cleavage at pH 3, 4, 5, 6, and 7 and showed that a 2.7 kDa fragment was not detectable at all pH levels tested. By examining the effect of pH on this cleavage, we demonstrated that other caspase-3-mediated cleavage fragments were best detected at pH levels of 6 and 7 which were slightly lower than the optimal pH for activity of caspase-3 (pH 7.2) reported by Thornberry and colleagues (1997). We then exploited smaller pore nitrocellulose membrane (0.2 μm) in the immunoblotting studies to eliminate the possible escaping of the smaller fragments through the membrane pores during electro-transfer. The result did not reveal a 2.7 kDa fragment, despite the observed 2.5 kDa band in the pre-stained protein standards. Moreover, whether the content of the pre-stained protein standards (e.g. the intensity of the loading buffer, or presence of tagged molecules bound to the standard proteins) was different from our sample preparation, is not known. Whether the small size cleavage fragments had diffused throughout the gel in the process of running the SDS-PAGE, lacked affinity for the antibody, or was lost by further proteolysis, remains to be determined.

14.3 Unexpected Novel Bands as a Result of Caspase-3-Mediated Akt1 Proteolysis: Caspase-3 Non-Consensus Sequences

In the process of investigating caspase-3-mediated Akt1 proteolysis at the $DQDD^{456}$ site by Western blot analysis, we detected two unexpected novel bands (Bands A and B), the former being C-terminus and the latter an N-terminus fragment. The observation that both novel bands increased in response to increasing concentrations of caspase-3 and duration of incubation, and diminished in the presence of the caspase-3 inhibitor DEVD-CHO, conveys the notion that the bands are the product of caspase-3-mediated proteolysis of Akt1. Using electrophoresis technique and R_f measurements (Sadeghi et al 2003), an approximate molecular mass of 43 and 51 kDa was assigned to bands A and B, respectively, signifying that these two fragments are cleaved at the non-$DQDD^{456}$ site.

Upon higher resolution of the SDS-PAGE, band A appeared to be a triplet (A1, A2, and A3). By electrophoresis, a molecular mass of 43, 42, and 41 kDa was assigned to the triplet A1, A2 and A3, respectively. The triplet was best observed following SDS-PAGE (over-run gels) and silver-staining. Silver-staining is one of the most sensitive techniques for detection of the actual amount of the proteins/peptides without involving any band pertaining to artifacts of ECL or antibody. Whether the triplet was the result of caspase-3-mediated cleavage of Akt1 at three novel sites in close proximity of each other, remains to be determined. The fact that the triplet was detected immunologically by Western blot analysis does not support the idea that these fragments might have been due

to the presence of impurities. The possibility that the triplet represents different extents of protein glycosylation was tested by performing a deglycosylation assay on the caspase-3-mediated Akt1 crude digests. The observation of an absence of a shift of the larger fragment [A1 (43 kDa)] into smaller ones indicates that glycosylation was not involved. Within the triplet in band A, the A1 (43 kDa) and A2 (42 kDa) fragments were consistently detected and produced equal intensity when analyzed by immunoblotting, whereas the A3 (41 kDa) fragment was often barely detectable. Also, the demonstration that both A1 and A2 fragments were abolished in the presence of a caspase-3-inhibitor (DEVD-CHO) implies that both of these fragments were a result of caspase-3-mediated proteolysis of Akt1.

In summary, it is proposed that the presence of at least three non-consensus caspase-3 cleavage sites in Akt1 gives rise to three fragments of 51 kDa (Band B) and 43 and 42 kDa (fragments A1 and A2). However, since the 41 kDa fragment (A3) was not detectable consistently, the possibility that it comes from a fourth novel cleavage site, remains unclear. Further proteolysis of A1 or A2 may be a possibility for the observation of this third fragment.

The first approach on which we embarked to identify the novel cleavage sites was SELDI M.S.. This technique, among the most powerful tools in proteomics, is based on Protein-Chip technology. One of the advantages of this technique is its high precision, such that the molecular mass of the peptides can be precisely measured with variations within Dalton range (compared to the kilodalton range by electrophoresis). Through

analysis by SELDI-M.S., we consistently demonstrated presence of eight peaks of 2.6/2.7, 3, 6/7, 8, 9, 16, and 57 kDa. Aside from the 2.6/2.7 and 57 kDa peaks, which were recognized as the cleavage fragments at the consensus sequence $DQDD^{456}$, all other peaks seemed to reflect Akt1 cleavage at non-consensus motifs.

Among the caspase family of proteases, cleavage sites for caspase-3 and -7 are believed to be less conserved than previously anticipated by Thornberry et al (1997). Recently non-conventional sequences, where aspartate is not present at P1 or P4 position, have been reported to be targets of caspase-3 and -7. As depicted in Table.1, all non-conventional sites discovered to date have a negative amino acid (glutamate, D or aspartate, E) at their P1 position. Based on this survey, all the D and E residues in the Akt1 sequence were assigned a theoretical P1 position and two N-terminus and C-terminus fragments were calculated for potential cleavage at each P1 position. Interestingly, fifteen caspase-3 and -7 non-consensus sites reported previously were present in Akt1, four of which shared more than two amino acids with the previously demonstrated non-conventional sites (P2 or P3 position in addition to P1 and P4). Moreover, we found a non-conventional site of SALD in Akt1, which has been previously reported to be cleaved by caspase-3 in scaffold attachment factor A (Kipp et al 2000).

We considered the following observations in arriving at our conclusions on the novel cleavage sites described in this thesis: 1) Observation of peaks at 59 and 61 kDa for the intact Akt1 by SELDI-M.S. and MALDI-TOF M.S., respectively; 2) Detection of

fragments A with molecular mass of 41, 42, and 43 kDa by SDS-PAGE; 3) Detection of band B with molecular mass of 51 kDa by SDS-PAGE; 4) Detection of two 16 kDa peaks by SELDI-M.S.; 5) Detection of a 9 kDa peak by SELDI-M.S.; and 6) The presence of a negatively charged amino-acid (D or E) at P1 position of caspase-3 cleavage sites. Considering the size of the intact Akt1 (~59 kDa), the small 16-16.5 kDa peaks, detected by SELDI-M.S. and the large 42-43 kDa fragments detected by electrophoresis complement each other to be the fragments generated from cleavage at the same sites (site A1 and A2), since the sum of their masses is approximately 59 kDa. The same deduction applies to the 9 kDa peak and 51kDa band, which provides a combined mass of about 60 kDa. Six sites of TVAD[108], KKQE[114], KQEE[115], QEEE[116], EEEE[117], and EEMD[119], with a D/E at P1 positions were found in Akt1 (Fig. 7.A) which could result in the production of N-terminus fragments of 16-17 and C-terminus fragments of 41 - 43 kDa. Of these, EEEE[117], and EEMD[119] are proposed to be cleavage sites A1 and A2 for two reasons: 1) In addition to P1 position, they both have a negative amino acid at P4 positions and a glutamate at P3 position, 2) EXXD has been previously shown to be cleaved by caspase-3 in DNA topoisomerase I (Kumiko et al, 1999; Samejima et al 1999). Moreover, the presence of these two sites in close proximity of each other may account for our consistent detection of the 42 and 43 kDa fragments and 16.1 and 16.3 peaks by Western and SELDI-M.S. analysis, respectively.

The site of DAKE[398] was the only site with E/D at both P1 and P4 position which gives rise to two N- and C-terminus fragments of 50 and 9.2 kDa, respectively. Therefore

this site was proposed to be the second novel cleavage giving rise to the 51 kDa band (Band B), and the 9.2 kDa peak.

Due to the presence of multiple cleavage sites in Akt1 (one consensus and three non consensus), a combination of middle fragments (i.e. fragments located between two cleavage sites), may be obtained upon its cleavage by caspase-3 (Table 2). The 6/7 kDa peak observed in the spectra by SELDI-M.S analysis corresponds to a middle cleavage fragment starting from $DAKE^{429}$ to $DQDD^{456}$. The 8 kDa peak is proposed to be the double charged version of the single charged 16 kDa fragment, based on the principle of mass to charge ratio in M.S. analysis.

14.4 Comparative Studies on the Presence of Novel Sites in AKT Isoforms

The overall homology of the three isoforms of AKT (Akt1, Akt2, and Akt3) is greater than 85%. They share a very similar structure, which contains an N-terminal PH domain, a central kinase domain, and a serine/threonine-rich C-terminal region. In addition, all of the three isoforms share a caspase-3-motif (DXXD) in their C-terminal tail. We performed a comparative study between the three AKT isoforms and demonstrated that the proposed novel cleavage sites A1 and A2 were absent in Akt2 and Akt3. Moreover, comparison of the protein sequence of Akt1 with those of Akt2 and Akt3 (gene bank) and the absence of the $EEEE^{117}$, and $EEMD^{119}$ sites in Akt2 and Akt3 sequence (in agreement with Western blot data), provides further support for the proposed sites of cleavage.

Since caspase-7 shares striking substrate sequence similarities to caspase-3 and is a target of Xiap, and thus equally significant in the regulation of chemoresistance, we investigated whether the proposed novel sites were a target for caspase-7. We found that the novel bands could also be produced by incubation of Akt1 with caspase-7.

14.5 Influence of Akt phosphorylation status on its cleavage by caspase-3

It is now well-established that post-translational modifications of proteins, such as glycosylation, methylation, phosphorylation and ubiquitylation influence the physiological behavior of the proteins. A few independent studies have shown that phosphorylation of caspase-3 substrates make them more resistant to caspase-3-mediated proteolysis (Hoon et al. 2003, Barkette et al 1997). Caspase-3-mediated cleavage of p130cas and the influence of phosphorylation was investigated in Rat-1 fibroblast cells (Hoon et al 2003). Lysophosphatidic acid- and fibronectin-induced p130cas phosphorylation resulted in its resistance to caspase-3-mediated cleavage. Cleavage of Keratin 18 (K18), another substrate of caspase-3, occurs sequentially following induction of apoptosis, first at the consensus sequence $DALD^{393}$ and then at the non-consensus sequence $VEVD^{234}$. Hyperphosphorylation of K18 protects it from caspase-3-mediated cleavage at $VEVD^{234}$, but not at $DALD^{393}$ *in vitro*. Therefore hyperphosphorylation, which occurs early in apoptosis, protects K18 from caspase-3-mediated K18 cleavage in a site-specific manner. Chicken and human IκB-α, also substrates of caspase-3, are cleaved at a conserved aspartate residue *in vitro* and *in vivo* (Barkette et al 1997).

Cleavage of IκB-α by this protease is also blocked by serine phosphorylation. On the contrary, it has been reported that caspase-3-mediated cleavage of STE-20-like kinase 2 (MST2), is positively regulated by phosphorylation. In this context, while truncated endogenous MST2 from apoptotic cells were highly phosphorylated, the full length protein from non-apoptotic or proliferating cells was mainly not phosphorylated (Deng et al, 2003).

Asselin and colleagues (2001) demonstrated that while down-regulation of Xiap expression via adenoviral anti-sense infection induced caspase-3 mediated AKT cleavage, Xiap over-expression suppressed AKT cleavage induced by cisplatin and increased phospho-Akt content. Whether AKT phosphorylation negatively regulates the efficiency of caspase-3-mediated AKT processing, remained to be elucidated. We tested the notion that attenuation of caspase-3-mediated Akt1 cleavage mediated by phosphorylation represents a mechanism by which chemoresistance is conferred in human ovarian carcinoma by comparing the extent of cleavage between Akt1 and phospho-Akt1 at the consensus site $DQDD^{456}$ and three novel non-consensus sites. We showed that phosphorylation influenced cleavage of Akt1, similar to keratin 18, in a site-specific manner, in which the cleavage at the non-consensus sites A2, and B were negatively influenced by phosphorylation whereas that at site A1 was enhanced by phosphorylation. Cleavage at the consensus site C seems to be negatively regulated by phosphorylation, however further replicates with fine separation of band C (57 kDa) from the intact (60 kDa) on the SDS-PAGE is required to confirm this observation.

14.6 Possible physiological significance of findings: The importance of the novel cleavage sites and influence of phosphorylation.

The presence of multiple caspase-3 cleavage sites in Akt1, as depicted by this work, raises a few remarkable questions as follow: 1) Are all the identified sites cleaved in vivo upon inducing caspase-3 activation? 2) What is the basal concentration of caspase-3 and what concentrations of caspase-3 are required for induction of Akt1 cleavage in vivo? 3) Are these sites get cleaved preferentially at different concentrations of caspase-3 (i.e. Is there a priority in the order of cleavage)? 4) If all the sites are equally cleaved in the cell in response to caspase-3 activation, which of the sites are functionally significant (i.e. Does cleavage at each site specifically induces Akt1 activation or inactivation)? Theses questions seem to be complex and require further research, as there is no information as to whether and how cleavage at each site may affect the three-dimensional structure and functionality of the protein. For example, the consensus sequence $DQDD^{456}$ is located at the C-terminus end of the protein and cleavage at this site yields a novel Akt1 fragment with only a 2.7 kDa difference in mass from intact Akt1. Since the cleavage fragment (2.7 kDa) is small and located away from the functional domain of the protein, it may have minimal influence on the activity and function of the protein whereas the opposite may be true for the novel cleavage sites considering their positions within the Akt1 sequence. For instance, site B is located in the middle of the two Akt1 activation/phosphorylation sites (Thr 308 and Ser 473) within the kinase domain of the protein. It is possible that the functionality of Akt1 may be

compromised upon cleavage at this site. These possibilities can be investigated using different approaches, as proposed in the Future Studies Section.

Based on the present findings and the discovery of multiple caspase-3 cleavage sites in Akt1, the initial hypothesis that phosphorylation of Akt1 makes the protein more resistant to caspase-3 mediated cleavage, should be restated as: Phosphorylation of Akt1 alters its ability to be cleaved by caspase-3 in a site-specific manner. Whether phosphorylation influences the overall structure of Akt1 in a way that some sites become more accessible to caspase-3 subsites while it creates significant steric hindrance to negatively influence Akt1 cleavage at other sites, remains unclear and should be further investigated following confirmation of the proposed cleavage sites.

14.7 Conclusion

14.7.1 Proposed Model for the Cleavage sites and the Influence of Phosphorylation

In the present studies, four bands (A1, A2, B, and C) were detected on Western blots following incubation of Akt1 with caspase-3. Band C, with a molecular mass of 57 kDa, was proposed to be a product of cleavage at the $DQDD^{456}$ consensus site. The next three bands were a result of caspase-3-cleavage of Akt1 at the non-consensus sites. One of the novel bands (band B, 51 kDa) was detected with an N-terminus antibody, while the

next two bands (A1, 42 kDa and A2, 43 kDa,) were detected using a C-terminus antibody, indicating that they are N- and C-terminus fragments, respectively.

Based on the identification of non-conventional caspase-3 sites in Akt1, together with the presence of the Western blot and SELDI-M.S data, the three motifs $EEEE^{117}$, $EEMD^{119}$, and $DAKE^{398}$ are proposed to be novel sites of cleavage which result in bands A1, A2, and B, respectively (Figure 27). Moreover, the comparative studies between Akt1 and other Akt isoforms (Akt2 and Akt3) in Western analysis for identical motives, lends support for the proposed model.

Figure 27. The proposed model for the caspase-3 cleavage sites in Akt1

In addition to the presence of a caspase-3 consensus sequence $DQDD^{456}$ in Akt1, the three motifs $EEEE^{117}$, $EEMD^{119}$, and $DAKE^{398}$ are proposed to be non-consensus novel sites of cleavage for bands A1, A2, and B, respectively. The pair fragments of 2.7 and 53; 41.7 and 13.9; 41.4 and 14.1; and 9.2 and 46.4 kDa are expected as as result of cleavage at each site of $DQDD^{456}$, $EEEE^{117}$, $EEMD^{119}$, and $DAKE^{398}$, respectively in the human cellular Akt1.

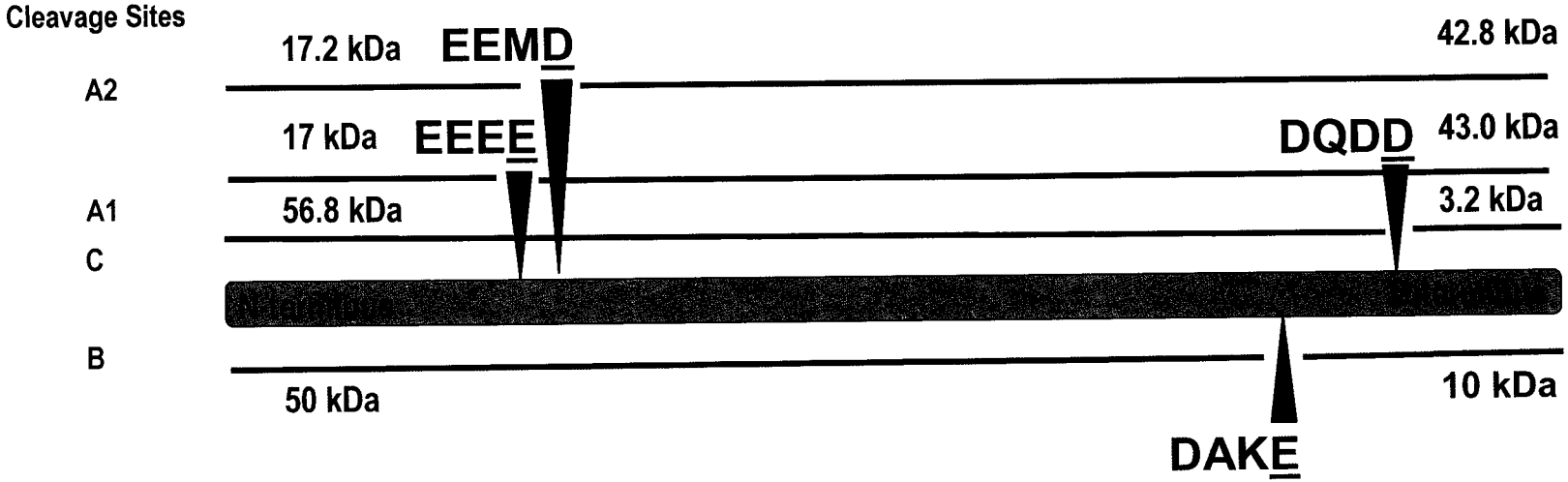
Cleavage Sites
17.2 kDa
EEMD
42.8 kDa
A2
17 kDa
EEEE
DQDD
43.0 kDa
A1
56.8 kDa
3.2 kDa
C
B
50 kDa
10 kDa
DAKE

Fig. 27

In the present studies we have demonstrated that sites B and A2 were more resistant to caspase-3-mediated cleavage in the phosphorylated Akt1 than Akt1. These findings are consistent with our hypothesis that phosphorylation decreases the sensitivity of Akt1 to caspase-3-mediated cleavage. Based on these findings, it is possible that sites B and A2 may be significant in that their cleavage may result in inactivation of the protein. The complexity imposed by phosphorylation on three dimensional structure of the protein and the localization of amino acids within the proposed sequences requires further investigation.

14.8 Future Studies

14.8.1 Confirmation of the proposed cleavage site

In order to confirm the identification of cleavage sites for caspase-3, small peptides containing the proposed non-consensus sequences can be designed. Custom peptide synthesis is a well-established technology and is commercially available to serve different applications, including non-quantitative enzyme-substrate studies and phosphorylation reactions. Peptides are arbitrarily considered as sequences of amino acids of up to about 100 residues and it is now feasible to produce peptides of greater than 98% purities (http://www.celtek-peptides.com). The small peptides can be incubated with active human recombinant caspase-3 and the by-products of the proteolysis can be analyzed using mass spectrometry as described previously. This is a very fast and reliable method to investigate the cleavage of the proposed non-consensus sites for caspase-3. However, cleavage at these sites by caspase-3 does not guarantee that the same sites on Akt1 are accessible and cleaved by casapase-3 in vivo.

In order to confirm whether the caspase-3 non-consensus sites located within Akt1 are accessible to caspase-3, cleavage of the Akt1 molecule must be examined. This is required since depending on the specific conformation of the Akt1, a cleavage site, however present, may or may not be accessible by caspase-3. One of the most common approaches to assess novel cleavage sites in a protein of interest is by site-directed mutagenesis (Mandal et al 2003). This method is suitable for identifying of Band A or B. Edman sequencing is another prevalent method for confirming the sites of cleavage (Kipp et al 2000) although this approach can only be used for identification of fragments that are cleaved at the N-terminus, such as Band B.

14.8.2 Physiological studies on Akt cleavage at specific site and the influence of phosphorylation

In order to investigate whether all the novel caspase-3 cleavage sites (EEEE^{117}, EEMD^{119}, and DAKE^{398}) identified in the recombinant Akt1 are authentic Akt1 sites of cleavage in the cells, aliquots of the whole cell lysates from sensitive ovarian cancer cell lines (e.g. A2780s) following treatment with a high concentrations of cisplatin (e.g. 10 μM) or active recombinant caspase-3 (e.g. 10 μg) can be immuno-blotted with the same AKT antibodies used in this study. If all the sites in the endogenous Akt1 are cleaved, concentration-response studies (2.5-10 μM cisplatin, or 1-10 μg active recombinant caspase-3) can be carried out to examine if the order of cleavage at these sites is concentration-dependent. To examine the significance of the identified novel sites and their role in apoptosis, constructs of Akt1 with and without mutation at the cleavage sites

will be expressed in the ovarian cancer cells and the apoptotic response between the two groups will be compared following cisplatin treatment in vitro.

To investigate the influence of phosphorylation on caspase-3-mediated Akt1 cleavage in the cells, two groups of cells will be required, with one having higher phospho-Akt1 content. One way to accomplish this goal is to increase Xiap content in the cells with adenoviral Xiap sense cDNA expression (LacZ as control). Our laboratory has previously shown that Xiap over-expression results in elevated phospho-Akt1 content in ovarian cancer cells (Asselin et al 2001). An alternative approach in increasing phospho-Akt content is use of growth stimulation with platelet-derived growth factor (PDGF) and epidermal growth factor (EGF). These growth factors have been shown to increase phospho-Akt content in ovarian cancer cells. The Akt1 content of each pair of cells in the described groups can be immunoprecipitated with the anti-Akt1 antibody used in these studies, and incubated in the presence and absence of an exogenous phosphatase, with or without human recombinant caspase-3. The abundance of the Akt1 and phospho-Akt1 cleavage fragments from the two different groups of cell lines can then be compared by Western blot analysis. Furthermore, expression of phosphomimetics at different phosphorylation sites, followed by cisplatin induced apoptosis (caspase-3 activation), will provide the opportunity to examine the influence of different phosphorylation sites on caspase-3-mediated Akt1 cleavages at different novel cleavage sites.

15.0 REFERENCES

Alessi, D. R., Andjelkovic, M., Caudwell, B., Cron, P., Morrice, N., Cohen, P., & Hemmings, B. A. (1996). Mechanism of activation of protein kinase B by insulin and IGF-1. *EMBO J.* **15**, 6541-6551.

Alessi, D. R. & Cohen, P. (1998). Mechanism of activation and function of protein kinase B. *Curr.Opin.Genet.Dev.* **8**, 55-62.

Alnemri, E. S. (1997). Mammalian cell death proteases: a family of highly conserved aspartate specific cysteine proteases. *J.Cell Biochem.* **64**, 33-42.

Alnemri, E. S., Livingston, D. J., Nicholson, D. W., Salvesen, G., Thornberry, N. A., Wong, W. W., & Yuan, J. (1996). Human ICE/CED-3 protease nomenclature. *Cell* **87**, 171.

Ambrosini, G., Adida, C., & Altieri, D. C. (1997). A novel anti-apoptosis gene, survivin, expressed in cancer and lymphoma. *Nat.Med.* **3**, 917-921.

Aoki, M., Batista, O., Bellacosa, A., Tsichlis, P., & Vogt, P. K. (1998). The akt kinase: molecular determinants of oncogenicity. *Proc.Natl.Acad.Sci.U.S.A* **95**, 14950-14955.

Aoki, M., Schetter, C., Himly, M., Batista, O., Chang, H. W., & Vogt, P. K. (2000). The catalytic subunit of phosphoinositide 3-kinase: requirements for oncogenicity. *J.Biol.Chem.* **275**, 6267-6275.

Arends, M. J. & Wyllie, A. H. (1991). Apoptosis: mechanisms and roles in pathology. *Int.Rev.Exp.Pathol.* **32**, 223-254.

Ashkenazi, A. & Dixit, V. M. (1998). Death receptors: signaling and modulation. *Science* **281**, 1305-1308.

Asselin, E., Mills, G. B., & Tsang, B. K. (2001). XIAP regulates Akt activity and caspase-3-dependent cleavage during cisplatin-induced apoptosis in human ovarian epithelial cancer cells. *Cancer Res.* **61**, 1862-1868.

Auersperg, N., Wong, A. S., Choi, K. C., Kang, S. K., & Leung, P. C. (2001). Ovarian surface epithelium: biology, endocrinology, and pathology. *Endocr.Rev.* **22**, 255-288.

Barkett, M., Xue, D., Horvitz, H. R., & Gilmore, T. D. (1997). Phosphorylation of IkappaB-alpha inhibits its cleavage by caspase CPP32 in vitro. *J.Biol.Chem.* **272**, 29419-29422.

Bellacosa, A., Chan, T. O., Ahmed, N. N., Datta, K., Malstrom, S., Stokoe, D., McCormick, F., Feng, J., & Tsichlis, P. (1998). Akt activation by growth factors is a multiple-step process: the role of the PH domain. *Oncogene* **17**, 313-325.

Bellacosa, A., de Feo, D., Godwin, A. K., Bell, D. W., Cheng, J. Q., Altomare, D. A., Wan, M., Dubeau, L., Scambia, G., & Masciullo, V. (1995). Molecular alterations of the AKT2 oncogene in ovarian and breast carcinomas. *Int.J.Cancer* **64**, 280-285.

Bellacosa, A., Testa, J. R., Staal, S. P., & Tsichlis, P. N. (1991). A retroviral oncogene, akt, encoding a serine-threonine kinase containing an SH2-like region. *Science* **254**, 274-277.

Berchuck, A., Kohler, M. F., Boente, M. P., Rodriguez, G. C., Whitaker, R. S., & Bast, R. C., Jr. (1993). Growth regulation and transformation of ovarian epithelium. *Cancer* **71**, 545-551.

Boldin, M. P., Goncharov, T. M., Goltsev, Y. V., & Wallach, D. (1996). Involvement of MACH, a novel MORT1/FADD-interacting protease, in Fas/APO-1- and TNF receptor-induced cell death. *Cell* **85**, 803-815.

Boldin, M. P., Varfolomeev, E. E., Pancer, Z., Mett, I. L., Camonis, J. H., & Wallach, D. (1995). A novel protein that interacts with the death domain of Fas/APO1 contains a sequence motif related to the death domain. *J.Biol.Chem.* **270**, 7795-7798.

Brodbeck, D., Cron, P., & Hemmings, B. A. (1999). A human protein kinase Bgamma with regulatory phosphorylation sites in the activation loop and in the C-terminal hydrophobic domain. *J.Biol.Chem.* **274**, 9133-9136.

Brodbeck, D., Hill, M. M., & Hemmings, B. A. (2001). Two splice variants of protein kinase B gamma have different regulatory capacity depending on the presence or absence of the regulatory phosphorylation site serine 472 in the carboxyl-terminal hydrophobic domain. *J.Biol.Chem.* **276**, 29550-29558.

Brunet, A., Bonni, A., Zigmond, M. J., Lin, M. Z., Juo, P., Hu, L. S., Anderson, M. J., Arden, K. C., Blenis, J., & Greenberg, M. E. (1999). Akt promotes cell survival by phosphorylating and inhibiting a Forkhead transcription factor. *Cell* **96**, 857-868.

Cain, K., Bratton, S. B., Langlais, C., Walker, G., Brown, D. G., Sun, X. M., & Cohen, G. M. (2000). Apaf-1 oligomerizes into biologically active approximately 700-kDa and inactive approximately 1.4-MDa apoptosome complexes. *J.Biol.Chem.* **275**, 6067-6070.

Cantley, L. C. (2002). The phosphoinositide 3-kinase pathway. *Science* **296**, 1655-1657.

Cardone, M. H., Roy, N., Stennicke, H. R., Salvesen, G. S., Franke, T. F., Stanbridge, E., Frisch, S., & Reed, J. C. (1998). Regulation of cell death protease caspase-9 by phosphorylation. *Science* **282**, 1318-1321.

Caulin, C., Salvesen, G. S., & Oshima, R. G. (1997). Caspase cleavage of keratin 18 and reorganization of intermediate filaments during epithelial cell apoptosis. *J.Cell Biol.* **138**, 1379-1394.

Cerretti, D. P., Kozlosky, C. J., Mosley, B., Nelson, N., Van Ness, K., Greenstreet, T. A., March, C. J., Kronheim, S. R., Druck, T., & Cannizzaro, L. A. (1992). Molecular cloning of the interleukin-1 beta converting enzyme. *Science* **256**, 97-100.

Chan, T. O., Rittenhouse, S. E., & Tsichlis, P. N. (1999). AKT/PKB and other D3 phosphoinositide-regulated kinases: kinase activation by phosphoinositide-dependent phosphorylation. *Annu.Rev.Biochem.* **68**, 965-1014.

Chang, H. W., Aoki, M., Fruman, D., Auger, K. R., Bellacosa, A., Tsichlis, P. N., Cantley, L. C., Roberts, T. M., & Vogt, P. K. (1997). Transformation of chicken cells by the gene encoding the catalytic subunit of PI 3-kinase. *Science* **276**, 1848-1850.

Chen, W. S., Xu, P. Z., Gottlob, K., Chen, M. L., Sokol, K., Shiyanova, T., Roninson, I., Weng, W., Suzuki, R., Tobe, K., Kadowaki, T., & Hay, N. (2001). Growth retardation and increased apoptosis in mice with homozygous disruption of the Akt1 gene. *Genes Dev.* **15**, 2203-2208.

Cheng, J. Q., Altomare, D. A., Klein, M. A., Lee, W. C., Kruh, G. D., Lissy, N. A., & Testa, J. R. (1997). Transforming activity and mitosis-related expression of the AKT2 oncogene: evidence suggesting a link between cell cycle regulation and oncogenesis. *Oncogene* **14**, 2793-2801.

Cheng, J. Q., Godwin, A. K., Bellacosa, A., Taguchi, T., Franke, T. F., Hamilton, T. C., Tsichlis, P. N., & Testa, J. R. (1992). AKT2, a putative oncogene encoding a member of

a subfamily of protein-serine/threonine kinases, is amplified in human ovarian carcinomas. *Proc.Natl.Acad.Sci.U.S.A* **89**, 9267-9271.

Cheng, J. Q., Jiang, X., Fraser, M., Li, M., Dan, H. C., Sun, M., & Tsang, B. K. (2002). Role of X-linked inhibitor of apoptosis protein in chemoresistance in ovarian cancer: possible involvement of the phosphoinositide-3 kinase/Akt pathway. *Drug Resist.Updat.* **5**, 131-146.

Cheng, J. Q., Ruggeri, B., Klein, W. M., Sonoda, G., Altomare, D. A., Watson, D. K., & Testa, J. R. (1996). Amplification of AKT2 in human pancreatic cells and inhibition of AKT2 expression and tumorigenicity by antisense RNA. *Proc.Natl.Acad.Sci.U.S.A* **93**, 3636-3641.

Chinnaiyan, A. M., O'Rourke, K., Tewari, M., & Dixit, V. M. (1995). FADD, a novel death domain-containing protein, interacts with the death domain of Fas and initiates apoptosis. *Cell* **81**, 505-512.

Cho, H., Mu, J., Kim, J. K., Thorvaldsen, J. L., Chu, Q., Crenshaw, E. B., III, Kaestner, K. H., Bartolomei, M. S., Shulman, G. I., & Birnbaum, M. J. (2001a). Insulin resistance and a diabetes mellitus-like syndrome in mice lacking the protein kinase Akt2 (PKB beta). *Science* **292**, 1728-1731.

Cho, H., Thorvaldsen, J. L., Chu, Q., Feng, F., & Birnbaum, M. J. (2001b). Akt1/PKBalpha is required for normal growth but dispensable for maintenance of glucose homeostasis in mice. *J.Biol.Chem.* **276**, 38349-38352.

Cianti, C. (2002). [Treatment of ovarian cancer]. *Clin.Ter.* **153**, 135-144.

Coffer, P. J., Jin, J., & Woodgett, J. R. (1998). Protein kinase B (c-Akt): a multifunctional mediator of phosphatidylinositol 3-kinase activation. *Biochem.J.* **335 (Pt 1)**, 1-13.

Cohen, J. J., Duke, R. C., Fadok, V. A., & Sellins, K. S. (1992). Apoptosis and programmed cell death in immunity. *Annu.Rev.Immunol.* **10**, 267-293.

Cramer, D. W. & Welch, W. R. (1983). Determinants of ovarian cancer risk. II. Inferences regarding pathogenesis. *J.Natl.Cancer Inst.* **71**, 717-721.

Crouch, D. H., Gallagher, R., Goding, C. R., Neil, J. C., & Fulton, R. (1996). Multiple phenotypes associated with Myc-induced transformation of chick embryo fibroblasts can be dissociated by a basic region mutation. *Nucleic Acids Res.* **24**, 3216-3221.

Dan, H. C., Sun, M., Kaneko, S., Feldman, R. I., Nicosia, S. V., Wang, H. G., Tsang, B. K., & Cheng, J. Q. (2004). Akt phosphorylation and stabilization of X-linked inhibitor of apoptosis protein (XIAP). *J.Biol.Chem.* **279**, 5405-5412.

Datta, K., Bellacosa, A., Chan, T. O., & Tsichlis, P. N. (1996). Akt is a direct target of the phosphatidylinositol 3-kinase. Activation by growth factors, v-src and v-Ha-ras, in Sf9 and mammalian cells. *J.Biol.Chem.* **271**, 30835-30839.

Datta, S. R., Dudek, H., Tao, X., Masters, S., Fu, H., Gotoh, Y., & Greenberg, M. E. (1997). Akt phosphorylation of BAD couples survival signals to the cell-intrinsic death machinery. *Cell* **91**, 231-241.

del Peso, L., Gonzalez-Garcia, M., Page, C., Herrera, R., & Nunez, G. (1997). Interleukin-3-induced phosphorylation of BAD through the protein kinase Akt. *Science* **278**, 687-689.

Deng, Y., Pang, A., & Wang, J. H. (2003). Regulation of mammalian STE20-like kinase 2 (MST2) by protein phosphorylation/dephosphorylation and proteolysis. *J.Biol.Chem.* **278**, 11760-11767.

Deveraux, Q. L., Roy, N., Stennicke, H. R., Van Arsdale, T., Zhou, Q., Srinivasula, S. M., Alnemri, E. S., Salvesen, G. S., & Reed, J. C. (1998). IAPs block apoptotic events induced by caspase-8 and cytochrome c by direct inhibition of distinct caspases. *EMBO J.* **17**, 2215-2223.

Deveraux, Q. L., Takahashi, R., Salvesen, G. S., & Reed, J. C. (1997). X-linked IAP is a direct inhibitor of cell-death proteases. *Nature* **388**, 300-304.

Dudek, H., Datta, S. R., Franke, T. F., Birnbaum, M. J., Yao, R., Cooper, G. M., Segal, R. A., Kaplan, D. R., & Greenberg, M. E. (1997). Regulation of neuronal survival by the serine-threonine protein kinase Akt. *Science* **275**, 661-665.

Earnshaw, W. C., Martins, L. M., & Kaufmann, S. H. (1999). Mammalian caspases: structure, activation, substrates, and functions during apoptosis. *Annu.Rev.Biochem.* **68**, 383-424.

Eeles, R. A. & Powles, T. J. (2000). Chemoprevention options for BRCA1 and BRCA2 mutation carriers. *J.Clin.Oncol.* **18**, 93S-99S.

Ellis, H. M. & Horvitz, H. R. (1986). Genetic control of programmed cell death in the nematode C. elegans. *Cell* **44**, 817-829.

Ellis, R. E., Yuan, J. Y., & Horvitz, H. R. (1991). Mechanisms and functions of cell death. *Annu.Rev.Cell Biol.* **7**, 663-698.

Eltabbakh, G. H. & Awtrey, C. S. (2001). Current treatment for ovarian cancer. *Expert.Opin.Pharmacother.* **2**, 109-124.

Enari, M., Sakahira, H., Yokoyama, H., Okawa, K., Iwamatsu, A., & Nagata, S. (1998). A caspase-activated DNase that degrades DNA during apoptosis, and its inhibitor ICAD. *Nature* **391**, 43-50.

Ethell, D. W., Bossy-Wetzel, E., & Bredesen, D. E. (2001). Caspase 7 can cleave tumor necrosis factor receptor-I (p60) at a non-consensus motif, in vitro. *Biochim.Biophys.Acta* **1541**, 231-238.

Feeley, K. M. & Wells, M. (2001). Precursor lesions of ovarian epithelial malignancy. *Histopathology* **38**, 87-95.

Ferguson, K. M., Lemmon, M. A., Sigler, P. B., & Schlessinger, J. (1995). Scratching the surface with the PH domain. *Nat.Struct.Biol.* **2**, 715-718.

Fernandes-Alnemri, T., Litwack, G., & Alnemri, E. S. (1994). CPP32, a novel human apoptotic protein with homology to Caenorhabditis elegans cell death protein Ced-3 and mammalian interleukin-1 beta-converting enzyme. *J.Biol.Chem.* **269**, 30761-30764.

Franke, T. F. & Cantley, L. C. (1997). Apoptosis. A Bad kinase makes good. *Nature* **390**, 116-117.

Fruman, D. A., Meyers, R. E., & Cantley, L. C. (1998). Phosphoinositide kinases. *Annu.Rev.Biochem.* **67**, 481-507.

Godwin, A. K., Vanderveer, L., Schultz, D. C., Lynch, H. T., Altomare, D. A., Buetow, K. H., Daly, M., Getts, L. A., Masny, A., & Rosenblum, N. (1994). A common region of deletion on chromosome 17q in both sporadic and familial epithelial ovarian tumors distal to BRCA1. *Am.J.Hum.Genet.* **55**, 666-677.

Green, D. R. (1998). Apoptotic pathways: the roads to ruin. *Cell* **94**, 695-698.

Green, D. R. (2000). Apoptotic pathways: paper wraps stone blunts scissors. *Cell* **102**, 1-4.

Han, Z., Hendrickson, E. A., Bremner, T. A., & Wyche, J. H. (1997). A sequential two-step mechanism for the production of the mature p17:p12 form of caspase-3 in vitro. *J.Biol.Chem.* **272**, 13432-13436.

Hanahan, D. & Weinberg, R. A. (2000). The hallmarks of cancer. *Cell* **100**, 57-70.

Harries, M. & Kaye, S. B. (2001). Recent advances in the treatment of epithelial ovarian cancer. *Expert.Opin.Investig.Drugs* **10**, 1715-1724.

Haussermann, S., Kittstein, W., Rincke, G., Johannes, F. J., Marks, F., & Gschwendt, M. (1999). Proteolytic cleavage of protein kinase Cmu upon induction of apoptosis in U937 cells. *FEBS Lett.* **462**, 442-446.

Hawkin, R. A., Arends, M. J., Ritchie, A. A., Langdon, S., & Miller, W. R. (2000). Tamoxifen increases apoptosis but does not influence markers of proliferation in an MCF-7 xenograft model of breast cancer. *Breast* **9**, 96-106.

Hawkins, P. T., Eguinoa, A., Qiu, R. G., Stokoe, D., Cooke, F. T., Walters, R., Wennstrom, S., Claesson-Welsh, L., Evans, T., & Symons, M. (1995). PDGF stimulates

an increase in GTP-Rac via activation of phosphoinositide 3-kinase. *Curr.Biol.* **5**, 393-403.

Hawkins, P. T., Welch, H., McGregor, A., Eguinoa, A., Gobert, S., Krugmann, S., Anderson, K., Stokoe, D., & Stephens, L. (1997). Signalling via phosphoinositide 3OH kinases. *Biochem.Soc.Trans.* **25**, 1147-1151.

Hemmings, B. A. (1997). Akt signaling: linking membrane events to life and death decisions. *Science* **275**, 628-630.

Herrin, V. E. & Thigpen, J. T. (1999). Chemotherapy for ovarian cancer: current concepts. *Semin.Surg.Oncol.* **17**, 181-188.

Hofmann, K., Bucher, P., & Tschopp, J. (1997). The CARD domain: a new apoptotic signalling motif. *Trends Biochem.Sci.* **22**, 155-156.

Hoon, K. D., Jeon, C. S., Kook, S., Kim, W., & Keun, S. W. (2003). Phosphorylation-dependent cleavage of p130cas in apoptotic rat-1 cells. *Biochem.Biophys.Res.Commun.* **300**, 141-148.

Howard, A. D., Kostura, M. J., Thornberry, N., Ding, G. J., Limjuco, G., Weidner, J., Salley, J. P., Hogquist, K. A., Chaplin, D. D., & Mumford, R. A. (1991). IL-1-converting enzyme requires aspartic acid residues for processing of the IL-1 beta precursor at two distinct sites and does not cleave 31-kDa IL-1 alpha. *J.Immunol.* **147**, 2964-2969.

Hsu, H., Xiong, J., & Goeddel, D. V. (1995). The TNF receptor 1-associated protein TRADD signals cell death and NF-kappa B activation. *Cell* **81**, 495-504.

Hu, L., Hofmann, J., Lu, Y., Mills, G. B., & Jaffe, R. B. (2002). Inhibition of phosphatidylinositol 3'-kinase increases efficacy of paclitaxel in in vitro and in vivo ovarian cancer models. *Cancer Res.* **62**, 1087-1092.

Hu, L., Zaloudek, C., Mills, G. B., Gray, J., & Jaffe, R. B. (2000). In vivo and in vitro ovarian carcinoma growth inhibition by a phosphatidylinositol 3-kinase inhibitor (LY294002). *Clin.Cancer Res.* **6**, 880-886.

Hu, Q., Klippel, A., Muslin, A. J., Fantl, W. J., & Williams, L. T. (1995). Ras-dependent induction of cellular responses by constitutively active phosphatidylinositol-3 kinase. *Science* **268**, 100-102.

Hu, Y., Benedict, M. A., Wu, D., Inohara, N., & Nunez, G. (1998). Bcl-XL interacts with Apaf-1 and inhibits Apaf-1-dependent caspase-9 activation. *Proc.Natl.Acad.Sci.U.S.A* **95**, 4386-4391.

Inohara, N., Ding, L., Chen, S., & Nunez, G. (1997). harakiri, a novel regulator of cell death, encodes a protein that activates apoptosis and interacts selectively with survival-promoting proteins Bcl-2 and Bcl-X(L). *EMBO J.* **16**, 1686-1694.

Inukai, K., Funaki, M., Ogihara, T., Katagiri, H., Kanda, A., Anai, M., Fukushima, Y., Hosaka, T., Suzuki, M., Shin, B. C., Takata, K., Yazaki, Y., Kikuchi, M., Oka, Y., & Asano, T. (1997). p85alpha gene generates three isoforms of regulatory subunit for phosphatidylinositol 3-kinase (PI 3-Kinase), p50alpha, p55alpha, and p85alpha, with different PI 3-kinase activity elevating responses to insulin. *J.Biol.Chem.* **272** , 7873-7882.

Irmler, M., Thome, M., Hahne, M., Schneider, P., Hofmann, K., Steiner, V., Bodmer, J. L., Schroter, M., Burns, K., Mattmann, C., Rimoldi, D., French, L. E., & Tschopp, J. (1997). Inhibition of death receptor signals by cellular FLIP. *Nature* **388**, 190-195.

Jacobson, M.D., Weil, M., Raff, M.C. (1997). Programmed cell death in animal development. *Cell* **88**, 347-354

Jiang, K., Coppola, D., Crespo, N. C., Nicosia, S. V., Hamilton, A. D., Sebti, S. M., & Cheng, J. Q. (2000). The phosphoinositide 3-OH kinase/AKT2 pathway as a critical target for farnesyltransferase inhibitor-induced apoptosis. *Mol.Cell Biol.* **20**, 139-148.

Kane, L. P., Mollenauer, M. N., Xu, Z., Turck, C. W., & Weiss, A. (2002). Akt-dependent phosphorylation specifically regulates Cot induction of NF-kappa B-dependent transcription. *Mol.Cell Biol.* **22**, 5962-5974.

Kane, L. P., Shapiro, V. S., Stokoe, D., & Weiss, A. (1999). Induction of NF-kappaB by the Akt/PKB kinase. *Curr.Biol.* **9**, 601-604.

Kang, J. Q., Chong, Z. Z., & Maiese, K. (2003). Critical role for Akt1 in the modulation of apoptotic phosphatidylserine exposure and microglial activation. *Mol.Pharmacol.* **64**, 557-569.

Kato, S., Yamaguchi, M., Fujii, T., Miyagi, N., Terasaki, M., Hamada, T., & Sugita, Y. (1999). Overexpression of p21Waf-1 in vascular smooth muscle cells: regulation of proliferation, differentiation, and cell size. *Exp.Mol.Pathol.* **66**, 39-52.

Kayalar, C., Ord, T., Testa, M. P., Zhong, L. T., & Bredesen, D. E. (1996). Cleavage of actin by interleukin 1 beta-converting enzyme to reverse DNase I inhibition. *Proc.Natl.Acad.Sci.U.S.A* **93**, 2234-2238.

Kaye, S. B. (2001). Future directions for the management of ovarian cancer. *Eur.J.Cancer* **37 Suppl 9**, S19-S23.

Kennedy, S. G., Wagner, A. J., Conzen, S. D., Jordan, J., Bellacosa, A., Tsichlis, P. N., & Hay, N. (1997). The PI 3-kinase/Akt signaling pathway delivers an anti-apoptotic signal. *Genes Dev.* **11**, 701-713.

Kerr, J.F.R., Wyllie, A.H., Currie, A.R. (1972). Apoptosis: a basic biological phenonmenon with wide ranging implications in tissue kinetics. *British J Cancer* **26**, 239-257

Kharbanda, S., Pandey, P., Schofield, L., Israels, S., Roncinske, R., Yoshida, K., Bharti, A., Yuan, Z. M., Saxena, S., Weichselbaum, R., Nalin, C., & Kufe, D. (1997). Role for Bcl-xL as an inhibitor of cytosolic cytochrome C accumulation in DNA damage-induced apoptosis. *Proc.Natl.Acad.Sci.U.S.A* **94**, 6939-6942.

Kim, C. N., Wang, X., Huang, Y., Ibrado, A. M., Liu, L., Fang, G., & Bhalla, K. (1997). Overexpression of Bcl-X(L) inhibits Ara-C-induced mitochondrial loss of cytochrome c and other perturbations that activate the molecular cascade of apoptosis. *Cancer Res.* **57**, 3115-3120.

Kipp, M., Schwab, B. L., Przybylski, M., Nicotera, P., & Fackelmayer, F. O. (2000). Apoptotic cleavage of scaffold attachment factor A (SAF-A) by caspase-3 occurs at a noncanonical cleavage site. *J.Biol.Chem.* **275**, 5031-5036.

Kodaki, T., Woscholski, R., Hallberg, B., Rodriguez-Viciana, P., Downward, J., & Parker, P. J. (1994). The activation of phosphatidylinositol 3-kinase by Ras. *Curr.Biol.* **4**, 798-806.

Kohn, A. D., Kovacina, K. S., & Roth, R. A. (1995). Insulin stimulates the kinase activity of RAC-PK, a pleckstrin homology domain containing ser/thr kinase. *EMBO J.* **14**, 4288-4295.

Konishi, I., Kuroda, H., & Mandai, M. (1999). Review: gonadotropins and development of ovarian cancer. *Oncology* **57 Suppl 2**, 45-48.

Krajewska, M., Wang, H. G., Krajewski, S., Zapata, J. M., Shabaik, A., Gascoyne, R., & Reed, J. C. (1997). Immunohistochemical analysis of in vivo patterns of expression of CPP32 (Caspase-3), a cell death protease. *Cancer Res.* **57**, 1605-1613.

Ku, N. O., Liao, J., & Omary, M. B. (1997). Apoptosis generates stable fragments of human type I keratins. *J.Biol.Chem.* **272**, 33197-33203.

Ku, N. O. & Omary, M. B. (2001). Effect of mutation and phosphorylation of type I keratins on their caspase-mediated degradation. *J.Biol.Chem.* **276**, 26792-26798.

Kuhn, W. C. (2003). Therapy for recurrent ovarian cancer. *Curr.Womens Health Rep.* **3**, 33-38.

Laemmli U. (1970). Cleavage of structural proteins during the assembley of the head of bacteriophage T4. *Nature* **227**, 680-685

Lazebnik, Y. A., Kaufmann, S. H., Desnoyers, S., Poirier, G. G., & Earnshaw, W. C. (1994). Cleavage of poly(ADP-ribose) polymerase by a proteinase with properties like ICE. *Nature* **371**, 346-347.

Li, H., Bergeron, L., Cryns, V., Pasternack, M. S., Zhu, H., Shi, L., Greenberg, A., & Yuan, J. (1997a). Activation of caspase-2 in apoptosis. *J.Biol.Chem.* **272**, 21010-21017.

Li, J., Billiar, T. R., Talanian, R. V., & Kim, Y. M. (1997b). Nitric oxide reversibly inhibits seven members of the caspase family via S-nitrosylation. *Biochem.Biophys.Res.Commun.* **240**, 419-424.

Li, J., Feng, Q., Kim, J. M., Schneiderman, D., Liston, P., Li, M., Vanderhyden, B., Faught, W., Fung, M. F., Senterman, M., Korneluk, R. G., & Tsang, B. K. (2001). Human ovarian cancer and cisplatin resistance: possible role of inhibitor of apoptosis proteins. *Endocrinology* **142**, 370-380.

Li, J., Sasaki, H., Sheng, Y. L., Schneiderman, D., Xiao, C. W., Kotsuji, F., & Tsang, B. K. (2000). Apoptosis and chemoresistance in human ovarian cancer: is Xiap a determinant? *Biol.Signals Recept.* **9**, 122-130.

Li, P., Nijhawan, D., Budihardjo, I., Srinivasula, S. M., Ahmad, M., Alnemri, E. S., & Wang, X. (1997). Cytochrome c and dATP-dependent formation of Apaf-1/caspase-9 complex initiates an apoptotic protease cascade. *Cell* **91**, 479-489.

Liang, J., Zubovitz, J., Petrocelli, T., Kotchetkov, R., Connor, M. K., Han, K., Lee, J. H., Ciarallo, S., Catzavelos, C., Beniston, R., Franssen, E., & Slingerland, J. M. (2002). PKB/Akt phosphorylates p27, impairs nuclear import of p27 and opposes p27-mediated G1 arrest. *Nat.Med.* **8**, 1153-1160.

Lin, J. H., Deng, G., Huang, Q., & Morser, J. (2000). KIAP, a novel member of the inhibitor of apoptosis protein family. *Biochem.Biophys.Res.Commun.* **279**, 820-831.

Liston, P., Roy, N., Tamai, K., Lefebvre, C., Baird, S., Cherton-Horvat, G., Farahani, R., McLean, M., Ikeda, J. E., Mackenzie, A., & Korneluk, R. G. (1996). Suppression of apoptosis in mammalian cells by NAIP and a related family of IAP genes. *Nature* **379**, 349-353.

Liu, X., Ou, H., Slaughter, C., Wang, X. (1997). DEF, a heterodimeric protein that functions downstream of caspase-3 to trigger DNA fragmentation during apoptosis. *Cell* **89**, 175-184

Mandal, D., Baudin-Creuza, V., Bhattacharyya, A., Pathak, S., Delaunay, J., Kundu, M., & Basu, J. (2003). Caspase 3-mediated proteolysis of the N-terminal cytoplasmic domain of the human erythroid anion exchanger 1 (band 3). *J.Biol.Chem.* **278**, 52551-52558.

Mansouri, A., Zhang, Q., Ridgway, L. D., Tian, L., & Claret, F. X. (2003). Cisplatin resistance in an ovarian carcinoma is associated with a defect in programmed cell death control through XIAP regulation. *Oncol.Res.* **13**, 399-404.

Markman, M., Kennedy, A., Webster, K., Kulp, B., Peterson, G., & Belinson, J. (1998). Low-dose oral granisetron (1 mg) plus intravenous dexamethasone: efficacy in gynecologic cancer patients receiving carboplatin-based chemotherapy. *Gynecol.Oncol.* **71**, 113-115.

Martin, D. A., Siegel, R. M., Zheng, L., & Lenardo, M. J. (1998). Membrane oligomerization and cleavage activates the caspase-8 (FLICE/MACHalpha1) death signal. *J.Biol.Chem.* **273**, 4345-4349.

Martin, S. J., Amarante-Mendes, G. P., Shi, L., Chuang, T. H., Casiano, C. A., O'Brien, G. A., Fitzgerald, P., Tan, E. M., Bokoch, G. M., Greenberg, A. H., & Green, D. R. (1996). The cytotoxic cell protease granzyme B initiates apoptosis in a cell-free system by proteolytic processing and activation of the ICE/CED-3 family protease, CPP32, via a novel two-step mechanism. *EMBO J.* **15**, 2407-2416.

Mashima, T., Naito, M., Noguchi, K., Miller, D. K., Nicholson, D. W., & Tsuruo, T. (1997). Actin cleavage by CPP-32/apopain during the development of apoptosis. *Oncogene* **14**, 1007-1012.

Mayo, L. D. & Donner, D. B. (2001). A phosphatidylinositol 3-kinase/Akt pathway promotes translocation of Mdm2 from the cytoplasm to the nucleus. *Proc.Natl.Acad.Sci.U.S.A* **98**, 11598-11603.

Meier, R. & Hemmings, B. A. (1999). Regulation of protein kinase B. *J.Recept.Signal.Transduct.Res.* **19**, 121-128.

Mittl, P. R., Di Marco, S., Krebs, J. F., Bai, X., Karanewsky, D. S., Priestle, J. P., Tomaselli, K. J., & Grutter, M. G. (1997). Structure of recombinant human CPP32 in

complex with the tetrapeptide acetyl-Asp-Val-Ala-Asp fluoromethyl ketone. *J.Biol.Chem.* **272**, 6539-6547.

Mohr, S., Zech, B., Lapetina, E. G., & Brune, B. (1997). Inhibition of caspase-3 by S-nitrosation and oxidation caused by nitric oxide. *Biochem.Biophys.Res.Commun.* **238**, 387-391.

Muggia, F. M., Braly, P. S., Brady, M. F., Sutton, G., Niemann, T. H., Lentz, S. L., Alvarez, R. D., Kucera, P. R., & Small, J. M. (2000). Phase III randomized study of cisplatin versus paclitaxel versus cisplatin and paclitaxel in patients with suboptimal stage III or IV ovarian cancer: a gynecologic oncology group study. *J.Clin.Oncol.* **18**, 106-115.

Muzio, M., Stockwell, B. R., Stennicke, H. R., Salvesen, G. S., & Dixit, V. M. (1998). An induced proximity model for caspase-8 activation. *J.Biol.Chem.* **273**, 2926-2930.

Nagata, S. & Golstein, P. (1995). The Fas death factor. *Science* **267**, 1449-1456.

Nakatani, K., Thompson, D. A., Barthel, A., Sakaue, H., Liu, W., Weigel, R. J., & Roth, R. A. (1999). Up-regulation of Akt3 in estrogen receptor-deficient breast cancers and androgen-independent prostate cancer lines. *J.Biol.Chem.* **274**, 21528-21532.

Ng, S. S. W., Tsao, M. S., Chow, S., & Hedley, D. W. (2000). Inhibition of phosphatidylinositide 3-kinase enhances gemcitabine-induced apoptosis in human pancreatic cancer cells. *Cancer Res.* **60**, 5451-5455.

Ni, B., Wu, X., Du, Y., Su, Y., Hamilton-Byrd, E., Rockey, P. K., Rosteck, P., Jr., Poirier, G. G., & Paul, S. M. (1997). Cloning and expression of a rat brain interleukin-1beta-converting enzyme (ICE)-related protease (IRP) and its possible role in apoptosis of cultured cerebellar granule neurons. *J.Neurosci.* **17**, 1561-1569.

Nicholson, D. W. (1999). Caspase structure, proteolytic substrates, and function during apoptotic cell death. *Cell Death.Differ.* **6**, 1028-1042.

Nicholson, D. W., Ali, A., Thornberry, N. A., Vaillancourt, J. P., Ding, C. K., Gallant, M., Gareau, Y., Griffin, P. R., Labelle, M., & Lazebnik, Y. A. (1995). Identification and inhibition of the ICE/CED-3 protease necessary for mammalian apoptosis. *Nature* **376**, 37-43.

Nicholson, D. W. & Thornberry, N. A. (1997). Caspases: killer proteases. *Trends Biochem.Sci.* **22**, 299-306.

Okano, J., Gaslightwala, I., Birnbaum, M. J., Rustgi, A. K., & Nakagawa, H. (2000). Akt/protein kinase B isoforms are differentially regulated by epidermal growth factor stimulation. *J.Biol.Chem.* **275**, 30934-30942.

Pekarsky, Y., Koval, A., Hallas, C., Bichi, R., Tresini, M., Malstrom, S., Russo, G., Tsichlis, P., & Croce, C. M. (2000). Tcl1 enhances Akt kinase activity and mediates its nuclear translocation. *Proc.Natl.Acad.Sci.U.S.A* **97**, 3028-3033.

Perego, P., Gatti, L., Righetti, S. C., Beretta, G. L., Carenini, N., Corna, E., Dal Bo, L., Tinelli, S., Colangelo, D., Leone, R., Apostoli, P., Lombardi, L., Beggiolin, G., Piazzoni, L., & Zunino, F. (2003). Development of resistance to a trinuclear platinum complex in ovarian carcinoma cells. *Int.J.Cancer* **105**, 617-624.

Porter, A. G. & Janicke, R. U. (1999). Emerging roles of caspase-3 in apoptosis. *Cell Death.Differ.* **6**, 99-104.

Radisavljevic, S. V. (1977). The pathogenesis of ovarian inclusion cysts and cystomas. *Obstet.Gynecol.* **49**, 424-429.

Rodriguez-Viciana, P., Marte, B. M., Warne, P. H., & Downward, J. (1996). Phosphatidylinositol 3'kinase: one of the effectors of Ras. *Philos.Trans.R.Soc.Lond B Biol.Sci.* **351**, 225-231.

Rodriguez-Viciana, P., Warne, P. H., Dhand, R., Vanhaesebroeck, B., Gout, I., Fry, M. J., Waterfield, M. D., & Downward, J. (1994). Phosphatidylinositol-3-OH kinase as a direct target of Ras. *Nature* **370**, 527-532.

Romashkova, J. A. & Makarov, S. S. (1999). NF-kappaB is a target of AKT in anti-apoptotic PDGF signalling. *Nature* **401**, 86-90.

Rotonda, J., Nicholson, D. W., Fazil, K. M., Gallant, M., Gareau, Y., Labelle, M., Peterson, E. P., Rasper, D. M., Ruel, R., Vaillancourt, J. P., Thornberry, N. A., & Becker, J. W. (1996). The three-dimensional structure of apopain/CPP32, a key mediator of apoptosis. *Nat.Struct.Biol.* **3**, 619-625.

Roy, N., Deveraux, Q. L., Takahashi, R., Salvesen, G. S., & Reed, J. C. (1997). The c-IAP-1 and c-IAP-2 proteins are direct inhibitors of specific caspases. *EMBO J.* **16**, 6914-6925.

Roymans, D. & Slegers, H. (2001). Phosphatidylinositol 3-kinases in tumor progression. *Eur.J.Biochem.* **268**, 487-498.

Ruggeri, B. A., Huang, L., Wood, M., Cheng, J. Q., & Testa, J. R. (1998). Amplification and overexpression of the AKT2 oncogene in a subset of human pancreatic ductal adenocarcinomas. *Mol.Carcinog.* **21**, 81-86.

Sadeghi, M., Hajivandi, M., Bogoev, R., and Amshey, J. (2003) Molecular weight estimation of proteins by gel electropjoresis. *Electrophoresis* 25.3, 36

Salvesen, G. S. & Dixit, V. M. (1997). Caspases: intracellular signaling by proteolysis. *Cell* **91**, 443-446.

Samejima, K., Svingen, P. A., Basi, G. S., Kottke, T., Mesner, P. W., Jr., Stewart, L., Durrieu, F., Poirier, G. G., Alnemri, E. S., Champoux, J. J., Kaufmann, S. H., & Earnshaw, W. C. (1999). Caspase-mediated cleavage of DNA topoisomerase I at unconventional sites during apoptosis. *J.Biol.Chem.* **274**, 4335-4340.

Sasaki, H., Sheng, Y., Kotsuji, F., & Tsang, B. K. (2000). Down-regulation of X-linked inhibitor of apoptosis protein induces apoptosis in chemoresistant human ovarian cancer cells. *Cancer Res.* **60**, 5659-5666.

Shayesteh, L., Lu, Y., Kuo, W. L., Baldocchi, R., Godfrey, T., Collins, C., Pinkel, D., Powell, B., Mills, G. B., & Gray, J. W. (1999). PIK3CA is implicated as an oncogene in ovarian cancer. *Nat.Genet.* **21**, 99-102.

Shi, Y. (2002). Mechanisms of caspase activation and inhibition during apoptosis. *Mol.Cell* **9**, 459-470.

Sleath, P. R., Hendrickson, R. C., Kronheim, S. R., March, C. J., & Black, R. A. (1990). Substrate specificity of the protease that processes human interleukin-1 beta. *J.Biol.Chem.* **265**, 14526-14528.

Slee, E. A., Harte, M. T., Kluck, R. M., Wolf, B. B., Casiano, C. A., Newmeyer, D. D., Wang, H. G., Reed, J. C., Nicholson, D. W., Alnemri, E. S., Green, D. R., & Martin, S. J. (1999). Ordering the cytochrome c-initiated caspase cascade: hierarchical activation of caspases-2, -3, -6, -7, -8, and -10 in a caspase-9-dependent manner. *J.Cell Biol.* **144**, 281-292.

Song, Z., McCall, K., & Steller, H. (1997). DCP-1, a Drosophila cell death protease essential for development. *Science* **275**, 536-540.

Song, Z. & Steller, H. (1999). Death by design: mechanism and control of apoptosis. *Trends Cell Biol.* **9**, M49-M52.

Srinivasula, S. M., Ahmad, M., Fernandes-Alnemri, T., & Alnemri, E. S. (1998). Autoactivation of procaspase-9 by Apaf-1-mediated oligomerization. *Mol.Cell* **1**, 949-957.

Srinivasula, S. M., Saleh, A., Ahmad, M., Fernandes-Alnemri, T., & Alnemri, E. S. (2001). Isolation and assay of caspases. *Methods Cell Biol.* **66**, 1-27.

Staal, S. P. (1987). Molecular cloning of the akt oncogene and its human homologues AKT1 and AKT2: amplification of AKT1 in a primary human gastric adenocarcinoma. *Proc.Natl.Acad.Sci.U.S.A* **84**, 5034-5037.

Stahl, J. M., Sharma, A., Cheung, M., Zimmerman, M., Cheng, J. Q., Bosenberg, M. W., Kester, M., Sandirasegarane, L., & Robertson, G. P. (2004). Deregulated Akt3 activity promotes development of malignant melanoma. *Cancer Res.* **64**, 7002-7010.

Stennicke, H. R., Jurgensmeier, J. M., Shin, H., Deveraux, Q., Wolf, B. B., Yang, X., Zhou, Q., Ellerby, H. M., Ellerby, L. M., Bredesen, D., Green, D. R., Reed, J. C., Froelich, C. J., & Salvesen, G. S. (1998). Pro-caspase-3 is a major physiologic target of caspase-8. *J.Biol.Chem.* **273**, 27084-27090.

Stephens, L., Anderson, K., Stokoe, D., Erdjument-Bromage, H., Painter, G. F., Holmes, A. B., Gaffney, P. R., Reese, C. B., McCormick, F., Tempst, P., Coadwell, J., & Hawkins, P. T. (1998). Protein kinase B kinases that mediate phosphatidylinositol 3,4,5-trisphosphate-dependent activation of protein kinase B. *Science* **279**, 710-714.

Stokoe, D., Stephens, L. R., Copeland, T., Gaffney, P. R., Reese, C. B., Painter, G. F., Holmes, A. B., McCormick, F., & Hawkins, P. T. (1997). Dual role of phosphatidylinositol-3,4,5-trisphosphate in the activation of protein kinase B. *Science* **277**, 567-570.

Sun, M., Wang, G., Paciga, J. E., Feldman, R. I., Yuan, Z. Q., Ma, X. L., Shelley, S. A., Jove, R., Tsichlis, P. N., Nicosia, S. V., & Cheng, J. Q. (2001). AKT1/PKBalpha kinase is frequently elevated in human cancers and its constitutive activation is required for oncogenic transformation in NIH3T3 cells. *Am.J.Pathol.* **159**, 431-437.

Suzuki, Y., Nakabayashi, Y., Nakata, K., Reed, J. C., & Takahashi, R. (2001). X-linked inhibitor of apoptosis protein (XIAP) inhibits caspase-3 and -7 in distinct modes. *J.Biol.Chem.* **276**, 27058-27063.

Takahashi, A. & Earnshaw, W. C. (1996). ICE-related proteases in apoptosis. *Curr.Opin.Genet.Dev.* **6** , 50-55.

Takahashi, R., Deveraux, Q., Tamm, I., Welsh, K., Assa-Munt, N., Salvesen, G. S., & Reed, J. C. (1998). A single BIR domain of XIAP sufficient for inhibiting caspases. *J.Biol.Chem.* **273**, 7787-7790.

Tamura, T., Ueda, S., Yoshida, M., Matsuzaki, M., Mohri, H., & Okubo, T. (1996). Interferon-gamma induces Ice gene expression and enhances cellular susceptibility to apoptosis in the U937 leukemia cell line. *Biochem.Biophys.Res.Commun.* **229**, 21-26.

Tewari, M., Quan, L. T., O'Rourke, K., Desnoyers, S., Zeng, Z., Beidler, D. R., Poirier, G. G., Salvesen, G. S., & Dixit, V. M. (1995). Yama/CPP32 beta, a mammalian homolog of CED-3, is a CrmA-inhibitable protease that cleaves the death substrate poly(ADP-ribose) polymerase. *Cell* **81**, 801-809.

Thome, M., Hofmann, K., Burns, K., Martinon, F., Bodmer, J. L., Mattmann, C., & Tschopp, J. (1998). Identification of CARDIAK, a RIP-like kinase that associates with caspase-1. *Curr.Biol.* **8**, 885-888.

Thompson, C.B. (1995). Apoptosis in the pathogenesis and treatment of disease. *Science* **267**, 1456-1462

Thornberry, N. A., Bull, H. G., Calaycay, J. R., Chapman, K. T., Howard, A. D., Kostura, M. J., Miller, D. K., Molineaux, S. M., Weidner, J. R., & Aunins, J. (1992). A novel heterodimeric cysteine protease is required for interleukin-1 beta processing in monocytes. *Nature* **356**, 768-774.

Thornberry, N. A., Rano, T. A., Peterson, E. P., Rasper, D. M., Timkey, T., Garcia-Calvo, M., Houtzager, V. M., Nordstrom, P. A., Roy, S., Vaillancourt, J. P., Chapman, K. T., & Nicholson, D. W. (1997). A combinatorial approach defines specificities of members of the caspase family and granzyme B. Functional relationships established for key mediators of apoptosis. *J.Biol.Chem.* **272**, 17907-17911.

Toker, A. (2000). Protein kinases as mediators of phosphoinositide 3-kinase signaling. *Mol.Pharmacol.* **57**, 652-658.

Vanhaesebroeck, B., Leevers, S. J., Ahmadi, K., Timms, J., Katso, R., Driscoll, P. C., Woscholski, R., Parker, P. J., & Waterfield, M. D. (2001). Synthesis and function of 3-phosphorylated inositol lipids. *Annu.Rev.Biochem.* **70**, 535-602.

Varfolomeev, E. E., Schuchmann, M., Luria, V., Chiannilkulchai, N., Beckmann, J. S., Mett, I. L., Rebrikov, D., Brodianski, V. M., Kemper, O. C., Kollet, O., Lapidot, T., Soffer, D., Sobe, T., Avraham, K. B., Goncharov, T., Holtmann, H., Lonai, P., & Wallach, D. (1998). Targeted disruption of the mouse Caspase 8 gene ablates cell death induction by the TNF receptors, Fas/Apo1, and DR3 and is lethal prenatally. *Immunity.* **9**, 267-276.

Varticovski, L., Harrison-Findik, D., Keeler, M. L., & Susa, M. (1994). Role of PI 3-kinase in mitogenesis. *Biochim.Biophys.Acta* **1226**, 1-11.

Vivanco, I. & Sawyers, C. L. (2002). The phosphatidylinositol 3-Kinase AKT pathway in human cancer. *Nat.Rev.Cancer* **2**, 489-501.

Walker, N. P., Talanian, R. V., Brady, K. D., Dang, L. C., Bump, N. J., Ferenz, C. R., Franklin, S., Ghayur, T., Hackett, M. C., & Hammill, L. D. (1994). Crystal structure of the cysteine protease interleukin-1 beta-converting enzyme: a (p20/p10)2 homodimer. *Cell* **78**, 343-352.

Wang, H. G., Rapp, U. R., & Reed, J. C. (1996). Bcl-2 targets the protein kinase Raf-1 to mitochondria. *Cell* **87**, 629-638.

Wilson, K. P., Black, J. A., Thomson, J. A., Kim, E. E., Griffith, J. P., Navia, M. A., Murcko, M. A., Chambers, S. P., Aldape, R. A., & Raybuck, S. A. (1994). Structure and mechanism of interleukin-1 beta converting enzyme. *Nature* **370**, 270-275.

Wolf, B. B. & Green, D. R. (1999). Suicidal tendencies: apoptotic cell death by caspase family proteinases. *J.Biol.Chem.* **274**, 20049-20052.

Wyllie, A.H., Kerr, F.R., Currie, A.R. (1980). Cell death: the significance of apoptosis. *Inter Re Cytology* **68**, 251-306

Xue, D. & Horvitz, H. R. (1995). Inhibition of the Caenorhabditis elegans cell-death protease CED-3 by a CED-3 cleavage site in baculovirus p35 protein. *Nature* **377**, 248-251.

Xue, D., Shaham, S., & Horvitz, H. R. (1996). The Caenorhabditis elegans cell-death protein CED-3 is a cysteine protease with substrate specificities similar to those of the human CPP32 protease. *Genes Dev.* **10**, 1073-1083.

Yamin, T. T., Ayala, J. M., & Miller, D. K. (1996). Activation of the native 45-kDa precursor form of interleukin-1-converting enzyme. *J.Biol.Chem.* **271**, 13273-13282.

Yang, J., Liu, X., Bhalla, K., Kim, C. N., Ibrado, A. M., Cai, J., Peng, T. I., Jones, D. P., & Wang, X. (1997). Prevention of apoptosis by Bcl-2: release of cytochrome c from mitochondria blocked. *Science* **275**, 1129-1132.

Yang, X., Chang, H. Y., & Baltimore, D. (1998). Essential role of CED-4 oligomerization in CED-3 activation and apoptosis. *Science* **281**, 1355-1357.

Yasui, K., Mihara, S., Zhao, C., Okamoto, H., Saito-Ohara, F., Tomida, A., Funato, T., Yokomizo, A., Naito, S., Imoto, I., Tsuruo, T., & Inazawa, J. (2004). Alteration in copy numbers of genes as a mechanism for acquired drug resistance. *Cancer Res.* **64**, 1403-1410.

Yu, J., Zhang, Y., McIlroy, J., Rordorf-Nikolic, T., Orr, G. A., & Backer, J. M. (1998). Regulation of the p85/p110 phosphatidylinositol 3'-kinase: stabilization and inhibition of the p110alpha catalytic subunit by the p85 regulatory subunit. *Mol.Cell Biol.* **18**, 1379-1387.

Yuan, J. (1996). Evolutionary conservation of a genetic pathway of programmed cell death. *J.Cell Biochem.* **60**, 4-11.

Yuan, J., Shaham, S., Ledoux, S., Ellis, H. M., & Horvitz, H. R. (1993). The C. elegans cell death gene ced-3 encodes a protein similar to mammalian interleukin-1 beta-converting enzyme. *Cell* **75**, 641-652.

Yuan, Z. Q., Feldman, R. I., Sussman, G. E., Coppola, D., Nicosia, S. V., & Cheng, J. Q. (2003). AKT2 inhibition of cisplatin-induced JNK/p38 and Bax activation by phosphorylation of ASK1: implication of AKT2 in chemoresistance. *J.Biol.Chem.* **278**, 23432-23440.

Yuan, Z. Q., Sun, M., Feldman, R. I., Wang, G., Ma, X., Jiang, C., Coppola, D., Nicosia, S. V., & Cheng, J. Q. (2000). Frequent activation of AKT2 and induction of apoptosis by

inhibition of phosphoinositide-3-OH kinase/Akt pathway in human ovarian cancer. *Oncogene* **19**, 2324-2330.

Zhan, Q., Jin, S., Ng, B., Plisket, J., Shangary, S., Rathi, A., Brown, K. D., & Baskaran, R. (2002). Caspase-3 mediated cleavage of BRCA1 during UV-induced apoptosis. *Oncogene* **21**, 5335-5345.

Zhou, B. P., Liao, Y., Xia, W., Zou, Y., Spohn, B., & Hung, M. C. (2001). HER-2/neu induces p53 ubiquitination via Akt-mediated MDM2 phosphorylation. *Nat.Cell Biol.* **3**, 973-982.

Zhou, Q. & Salvesen, G. S. (1997). Activation of pro-caspase-7 by serine proteases includes a non-canonical specificity. *Biochem.J.* **324 (Pt 2)**, 361-364.

Zou, H., Henzel, W. J., Liu, X., Lutschg, A., & Wang, X. (1997). Apaf-1, a human protein homologous to C. elegans CED-4, participates in cytochrome c-dependent activation of caspase-3. *Cell* **90**, 405-413.

Zou, H., Li, Y., Liu, X., & Wang, X. (1999). An APAF-1.cytochrome c multimeric complex is a functional apoptosome that activates procaspase-9. *J.Biol.Chem.* **274**, 11549-11556.

17. CURRICULUM VITAE

Arezu Jahani-asl

EDUCATIONAL BACKGROUND

Sep. 2002 – Dec. 2004	M.Sc. Cellular and Molecular Medicine, University of Ottawa, Canada
May 2001 – Apr. 2002	B.Sc. Hon. Biotechnology, University of Ottawa, Canada
Sep.1996 – Apr. 2000	B.Sc. Human Biology (with distinction), University of Toronto, Canada

SCHOLARSHIP AND AWARDS

May. 2004	Second Canadian Conference on Ovarian Cancer Research, Best Trainee Award for Poster Presentation (MSc category)
Sep. 1998	University of Toronto, Dean's Honor List, In recognition of academic excellence
Sep. 1997	University of Toronto, membership in the Golden Key National Honor Society at the University of Toronto in recognition of scholastic achievements.

WORK EXPERIENCE

May 2002- present	Ottawa Health Research Institute. Studied caspase-3 consensus and non-consensus cleavage motives in Akt1. Investigated influence of Akt phosphorylation on its cleavage by caspase-3.
Apr. 2001 – May 2001	Agriculture and Agri-food Canada, Research branch, volunteer, performed various PCR-based methods for cultivar identification of barely *(Hordeum vulgare L.)*
May 2001- May 2002	University of Ottawa, Department of Biology, Honor's student, studied the molecular mechanisms of senescence in soybean. Isolated, cloned, sequenced and characterized a candidate gene.

Sep. 2001- May 2002	Ottawa – Carleton District School Board, Science tutor in the classroom. Introduced grade-school students to the world of science and research. Leading Scientific projects for the grades 2 to 6.
Sep.1999 – Sep. 2002	University of Toronto, Department of Chemistry, demonstrating laboratory skills in chemistry for high school Chemistry Olympiad students
1996- 1998	University of Toronto, Department of continuing education, teaching assistant.

LABORATORY SKILLS

Cell culture, Protein extraction and quantifying, Western Blots, apoptosis assay, cell transformation, protein-staining (Silver, Sypro Rubby, Coommassie blue), protein desalting using Zip-Tips, MALDI-TOF mass spectrometry, SELDI mass spectrometry, DNA and RNA extraction, quantification, and separation by gel electrophoresis, restriction digest and mapping, PCR analysis, cloning, bacterial transformation, dark room skills, greenhouse plant care, WHIMS training. Post secondary courses in molecular biology, cellular biology, pharmacology, toxicology, human physiology, cancer, and biochemistry.

COMPUTER SKILLS

Scion Image, Prism 3, ExPacy, NCBI programs, MS Excel, WordPerfect, MS PowerPoint, MS Word.

PUBLICATIONS

Jahani-asl A. Basak A, Tsang B.K. Novel caspase-3-cleavage sites in Akt1: Influence of phosphorylation (In preparation)

Fraser M., Leung B., **Jahani-asl A.**, Yan X, Thompson W.E., Tsang B.K. (2003) Chemoresistance in human ovarian cancer: the role of apoptotic regulators. Reproductive Biology and Endocrinology 2003, 1:66

RESEARCH PRESENTATIONS

Jahani-asl A, Basak A, Tsang BK. Novel Caspase-3 Cleavage Sites in AKT: Influence of Phosphorylation. XVth Ovarian Workshop, Vancouver, Canada July 29-31, 2004

Jahani-asl A, Basak A, Tsang BK. Novel Caspase-3 Cleavage Sites in Akt1: Influence of Phosphorylation. Second Canadian Conference on Ovarian Cancer Research, Ottawa, Ontario, May 16-18, 2004.

Jahani-asl A, Basak A, Tsang BK. Novel Caspase-3 Cleavage Sites in Akt: Influence of Phosphorylation. Canadian Symposium on Human Reproduction and Reproductive Biology, May 3-4, 2004.

Jahani-asl A, Basak A, Tsang BK. Influence of Phosphorylation on Caspase-3-mediated Akt Cleavage. 21st Ottawa Reproductive Biology Workshop, May 3-4, 2003